

UC San Diego

UC San Diego Electronic Theses and Dissertations

Title

Germination and Inhibitory Activity of Spore-Forming Microbes on Surface Materials Used in Healthcare Settings

Permalink

<https://escholarship.org/uc/item/4vd9z686>

Author

Gottel, Neil Robert

Publication Date

2024

Peer reviewed|Thesis/dissertation

UNIVERSITY OF CALIFORNIA SAN DIEGO

Germination and Inhibitory Activity of Spore-Forming Microbes on Surface Materials Used in
Healthcare Settings

A Dissertation submitted in partial satisfaction of the requirements
for the degree Doctor of Philosophy

in

Marine Biology

by

Neil Gottel

Committee in charge:

Professor Jack Gilbert, Chair
Professor Eric Allen
Professor Gürol Süel
Professor Karsten Zengler

2024

Copyright

Neil Gottel, 2024

All rights reserved.

The Dissertation of Neil Gattel is approved, and it is acceptable in quality and form for publication on microfilm and electronically.

University of California San Diego

2024

DEDICATION

To Mom, Dad, and Becky. Your love and support made this possible.

TABLE OF CONTENTS

| | |
|---|-----|
| DISSERTATION APPROVAL PAGE | iii |
| DEDICATION | iv |
| TABLE OF CONTENTS..... | v |
| LIST OF FIGURES | vi |
| LIST OF TABLES | ix |
| ACKNOWLEDGEMENTS..... | x |
| VITA..... | xi |
| ABSTRACT OF THE DISSERTATION | xii |
| INTRODUCTION | 1 |
| Chapter 1 GERMINATION OF BACILLUS AND PRIESTIA SPORES ON HEALTHCARE-ASSOCIATED SURFACE MATERIALS..... | 25 |
| Chapter 2 INHIBITION OF STAPHYLOCOCCUS AUREUS BY BACILLUS AND PRIESTIA SPORES ON HEALTHCARE RELEVANT SURFACES | 45 |
| Chapter 3 GERMINATION AND PATHOGEN INHIBITION BY 3D PRINTED STRUCTURES CONTAINING <i>BACILLUS SUBTILIS</i> SPORES | 66 |
| CONCLUSION..... | 83 |
| REFERENCES | 87 |

LIST OF FIGURES

- Figure 1. Environmental factors within the built environment and proposed modes of action by probiotic cleaners.** Potential pathogens can be deposited on surfaces by infected occupants, but their survival and transmission capability are dependent on many environmental factors, including temperature, light, humidity, occupant density, air flow, cleaning methods... 14
- Figure 2. Important molecules for germination and microbial inhibition by *Bacillus spp.*** The germination of *Bacillus* spores is triggered by either (A) *L*-alanine/*L*-valine or (B) a combination of *L*-asparagine, glucose, fructose, and potassium ions (103). Vegetative *Bacillus* cells can generate different compounds that can exclude pathogens, including: (C) the 16
- Figure 3. Experimental design of the surface and liquid germination experiments.** In the surface germination experiment (A), spores were diluted, mixed with a germination medium, inoculated onto a surface, and then sampled over time. A control experiment (B) was also performed in a larger liquid germination system. Surfaces were kept inside an incubation 29
- Figure 4. Germination ratio on a laminate surface at ambient humidity.** Each panel shows the mean Germination Ratio (GR) at each timepoint in the time series for the germinant media being tested: phosphate buffered saline (PBS), skim milk (SM), skim milk supplemented with 100 mM alanine (SMA), or tryptic soy broth (TSB). Error bars show 1 standard deviation 32
- Figure 5. Germination ratio on a vinyl surface at ambient humidity.** Each panel shows the mean Germination Ratio (GR) at each timepoint in the time series for the germinant media being tested: phosphate buffered saline (PBS), skim milk (SM), skim milk supplemented with 100 mM alanine (SMA), or tryptic soy broth (TSB). Error bars show 1 standard deviation from the 33
- Figure 6. Germination ratio on laminate at high humidity.** Each panel shows the mean Germination Ratio (GR) at each timepoint in the time series for the germinant media being tested: phosphate buffered saline (PBS), skim milk (SM), skim milk supplemented with 100 mM alanine (SMA), or tryptic soy broth (TSB). Error bars show 1 standard deviation from the 34
- Figure 7. Germination ratio on vinyl at high humidity.** Each panel shows the mean Germination Ratio (GR) at each timepoint in the time series for the germinant media being tested: phosphate buffered saline (PBS), skim milk (SM), skim milk supplemented with 100 mM alanine (SMA), or tryptic soy broth (TSB). Error bars show 1 standard deviation from the 35
- Figure 8. Germination ratio in liquid culture.** Each panel shows the mean Germination Ratio (GR) at each timepoint in the time series for the germinant media being tested: phosphate buffered saline (PBS), skim milk (SM), skim milk supplemented with 100 mM alanine (SMA), or tryptic soy broth (TSB). Error bars show 1 standard deviation from the mean. 36
- Figure 9. Representative HOBO output for high humidity timeseries.** Output from a HOBO sensor. Percent relative humidity (blue line) and temperature (black line) displayed. Sharp changes in temperature/humidity occur when the chamber is moved to a biosafety cabinet and opened for a sampling timepoint..... 37
- Figure 10. Representative HOBO output for low humidity timeseries.** Output from a HOBO sensor. Percent relative humidity (blue line) and temperature (black line) displayed. Sharp changes in temperature/humidity occur when the chamber is moved to a biosafety cabinet and opened for a sampling timepoint..... 37

| | |
|---|----|
| Figure 11. Setup of MRSA co-cultured with spores in droplets on surfaces. (A) Growth, dilution, and inoculation protocol for MRSA on surfaces. (B) Application of sterile media for the MRSA-only samples. (C) Dilution and inoculation protocol for the spore mix. (D) Sample swabbing, dilution, and plating..... | 51 |
| Figure 12. MRSA inhibition on tryptic soy agar plates. Images of each of individual strains used in the spore mixture. Each plate received three droplets, 5 μ L each, of 1) an overnight culture of the strain, 2) a 1:10 dilution of the strain, and 3) a 1:100 dilution of the strain. The strains used were (A) <i>B. inaquosorum</i> , (B) <i>B. velezensis</i> strain A, (C) <i>B. velezensis</i> strain | 52 |
| Figure 13. Representative HOBO output for high humidity timeseries. Output from a HOBO sensor. Percent relative humidity (blue line) and temperature (black line) displayed. Sharp changes in temperature/humidity occur when the chamber is moved to a biosafety cabinet and opened for a sampling timepoint..... | 53 |
| Figure 14. Representative HOBO output for ambient humidity timeseries. Output from a HOBO sensor. Percent relative humidity (blue line) and temperature (black line) displayed. Sharp changes in temperature/humidity occur when the chamber is moved to a biosafety cabinet and opened for a sampling timepoint..... | 53 |
| Figure 15. MRSA inhibition timeseries on laminate at ambient humidity. Mean number of MRSA CFUs in each type of media droplet, as determined via swabbing, dilution, plating, and CFU enumeration, and then adjustment for dilution factor. Phosphate buffered saline (PBS), skim milk (SM), skim milk supplemented with 100 mM alanine (SMA) and tryptic soy | 54 |
| Figure 16. MRSA inhibition timeseries on vinyl at ambient humidity. Mean number of MRSA CFU in each type of media droplet, as determined via swabbing, dilution, plating, and CFU enumeration, and then adjustment for dilution factor. Phosphate buffered saline (PBS), skim milk (SM), skim milk supplemented with 100 mM alanine (SMA) and tryptic soy. | 55 |
| Figure 17. MRSA inhibition timeseries on laminate at high humidity. Mean number of MRSA CFUs in each type of media droplet, as determined via swabbing, dilution, plating, and CFU enumeration, and then adjustment for dilution factor. Phosphate buffered saline (PBS), skim milk (SM), skim milk supplemented with 100 mM alanine (SMA) and tryptic soy | 56 |
| Figure 18. MRSA inhibition timeseries on vinyl at high humidity. Mean number of MRSA CFU in each type of media droplet, as determined via swabbing, dilution, plating, and CFU enumeration, and then adjustment for dilution factor. Phosphate buffered saline (PBS), skim milk (SM), skim milk supplemented with 100 mM alanine (SMA) and tryptic soy broth (TSB)..... | 57 |
| Figure 19. Test for germination efficiency of spores in 3D printed structures. A) Spores are serially diluted in phosphate buffered saline (PBS) and transferred in triplicate to a 24-well plate with tryptic soy broth (TSB). The last tube in the series is also used to inoculate five tryptic soy agar (TSA) plates. Wells C1-3 are not inoculated. B) Triplicate 3D printed structures with..... | 71 |
| Figure 20. Setup of MRSA inhibition by 3D printed spore structures. Serial dilution, plating, and inoculation of plates containing spores with structures, or no structures. A) An overnight culture of MRSA was serially diluted in phosphate buffered saline (PBS). Tube 6 was plated in triplicate on tryptic soy agar (TSA) plates for CFU enumeration and used to calculate the. | 73 |
| Figure 21. 3D printed structures on agar media. 3D printed structures containing <i>B. subtilis</i> TH002 spores (+) or structures without spores (-) were placed on tryptic soy agar (TSA) plates, | |

along with a 5 μ L droplet of an overnight culture of TH002 (S). A) Structures and TH002 droplet on TSA plate. B) Structures and TH002 droplet on TSA plates with 4 mg/L methicillin..... 75

Figure 22. Standard curves for each germination experiment. Each panel shows the standard curve generated for each of the four replicate germination experiments, G1 thru G4, along with the equation for the line of best fit, and the R^2 value..... 76

Figure 23. MRSA CFU per mL after 24 hours of incubation with or without 3D printed spore structures. Mean CFU in wells of a 24-well plate, with or without spore structures, which were inoculated with 900 μ L tryptic soy broth (TSB) and serial dilutions of MRSA in 100 μ L phosphate buffered saline (PBS)..... 78

LIST OF TABLES

| | |
|---|----|
| Table 1. Mann-Whitney test results between T0 and T72 for each germination timeseries. A Mann-Whitney test was performed for the first and last timepoint of each media under each combination of surface and humidity conditions. Media that were significantly different ($p < 0.05$) between T0 and T72 are highlighted in blue. | 38 |
| Table 2. Kruskal-Wallis test with Bonferroni Correction, significant results. Kruskal-Wallis test with Bonferroni correction to determine whether the surface material humidity significantly influenced the GR of each type of media at each timepoint. Only variables that were still significant ($p < 0.05$) after the correction are listed..... | 39 |
| Table 3. Mann-Whitney U test results at each timepoint, $p < 0.05$ only. Timepoints and incubation conditions (surface, humidity, and media type) where the mean CFU of MRSA incubated alone or in co-culture with the spore mix was significantly different ($p < 0.05$) using the Mann-Whitney test. Timepoints at which the MRSA co-cultured with the spore mix. | 58 |
| Table 4. Percentage change in CFUs between T0 and T24. The change in the mean number of CFUs, after accounting for dilution factor, was calculated for each set of conditions, media, and presence/absence of spores in the droplets. Phosphate buffered saline (PBS), skim milk (SM), skim milk supplemented with 100 mM alanine (SMA) and tryptic soy broth (TSB) were..... | 59 |
| Table 5. Percentage change in CFUs between T0 and T72. The change in the mean number of CFUs, after accounting for dilution factor, was calculated for each set of conditions, media, and presence/absence of spores in the droplets. Phosphate buffered saline (PBS), skim milk (SM), skim milk supplemented with 100 mM alanine (SMA) and tryptic soy broth (TSB) were..... | 60 |
| Table 6. Mean percentage change between MRSA abundance between start and end of timeseries. The percentage change in the MRSA CFUs was calculated based on each of the 4 variables in the experiment: humidity level, ambient or high; surface type, laminate or vinyl; type of media, phosphate buffered saline (PBS), skim milk (SM), skim milk with alanine (SMA).... | 61 |
| Table 7. Germinated spores per structure. Four germination experiments, G1 thru G4, were conducted using structures printed with <i>B. subtilis</i> strain TH002. Three replicates were used for each experiment, with the mean and standard deviation displayed for each individual experiment. | 77 |
| Table 8. MRSA abundance per well, incubated overnight with or without spore structures. Dilution factor adjusted CFU counts for MRSA growth after 24-hour incubation with or without 3D printed structures with spores. | 78 |

ACKNOWLEDGEMENTS

The introduction chapter, in full, is a reprint of the material as it appears in *The ISME Journal*, Volume 18, Issue 1, under the title “Biocontrol in built environments to reduce pathogen exposure and infection risk”. Neil R Gottel, Megan S Hill, Maxwell J Neal, Sarah M Allard, Karsten Zengler, Jack A Gilbert. Oxford University Press, 2024. The dissertation author was the primary investigator and author of this paper. The authors are funded by NSF ENG-EPSRC EFRI ELiS: Developing probiotic interventions to reduce the emergence and persistence of pathogens in built environments (UCSD 2223669) and NASA ROSBIO: Quantifying selection for pathogenicity and antibiotic resistance in bacteria and fungi on the ISS—a Microbial Tracking Study (80NSSC19K1604).

Chapter 1, in part is currently being prepared for submission for publication of the material. Gottel, Neil; Hill, Megan S; Allard, Sarah M; Salas Garcia, Mariana; Gilbert, Jack A. The dissertation/thesis author was the primary investigator and author of this material.

Chapter 2, in part is currently being prepared for submission for publication of the material. Gottel, Neil; Hill, Megan S; Allard, Sarah M; Salas Garcia, Mariana; Gilbert, Jack A. The dissertation/thesis author was the primary investigator and author of this material.

Chapter 3, in part is currently being prepared for submission for publication of the material. Gottel, Neil; Hill, Megan S; Allard, Sarah M; Huang, Lin; Gilbert, Jack A. The dissertation/thesis author was the primary investigator and author of this material.

VITA

2009 Bachelor of Science in Integrative Biology, University of Illinois Urbana-Champaign

2024 Doctor of Philosophy in Marine Biology, University of California San Diego

PUBLICATIONS

Gottel, Neil R., Megan S. Hill, Maxwell J. Neal, Sarah M. Allard, Karsten Zengler, and Jack A. Gilbert. “Biocontrol in built environments to reduce pathogen exposure and infection risk”; *The ISME Journal* (2024): wrad024.

ABSTRACT OF THE DISSERTATION

Germination and Inhibitory Activity of Spore-Forming Microbes on Surface Materials Used in Healthcare Settings

by

Neil Gottel

Doctor of Philosophy in Marine Biology

University of California San Diego, 2024

Professor Jack Gilbert, Chair

Surfaces in healthcare settings are colonized by pathogens, where they persist and are transmitted to other locations. Cleaning solutions that contain bacterial spores are an alternative to current methods for cleaning healthcare surfaces. My dissertation investigates how effectively these spores germinate on surfaces used in healthcare settings, whether they inhibit the survival

of methicillin-resistant *Staphylococcus aureus* (MRSA), and if incorporated into a 3D printed structure, how effectively they germinate and inhibit MRSA.

The first chapter investigates the germination efficiency of bacterial spores on surfaces from healthcare settings. Droplets of media containing a mixture of 5 *Bacillus* spp. and *Priestia* spp. were placed on laminate or vinyl, at either ambient or elevated relative humidity, then collected over a three-day timeseries via swabbing, followed by heat shocking and plating to determine the ratio of germinated spores to the total number of spores and cells. I found that there was a low, baseline level of germination, and that only very nutrient rich media would achieve high germination rates. The type of surface and the humidity also had a significant influence, but only at later timepoints in the experiments.

The second chapter focuses on the inhibition of MRSA using the spore mix from chapter 1. Droplets containing MRSA by itself or in co-culture with the spore mix were placed on laminate or vinyl and incubated at over a three-day timeseries. CFU enumeration was used to determine whether the survival of MRSA was influenced by the spore mix. Surface, humidity, and competition medium significantly influenced the survival of MRSA, but the presence of the spore mix did not inhibit MRSA survival.

The third chapter uses 3D printed structures that contain a strain of *B. subtilis* shown to have potent anti-MRSA inhibitory activity. Using optical density readings and CFU enumeration, the germination and growth of *B. subtilis* out of the structure and its inhibition of MRSA was investigated. Approximately 20% of the spores in the structures germinate and move out of the structure in liquid culture to inhibit MRSA, but the structures do not completely eliminate MRSA in either liquid culture or on solid agar surfaces.

INTRODUCTION

BIOCONTROL IN BUILT ENVIRONMENTS TO REDUCE PATHOGEN EXPOSURE AND INFECTION RISK

Abstract

The microbiome of the built environment comprises bacterial, archaeal, fungal, and viral communities associated with human-made structures. Even though most of these microbes are benign, antibiotic-resistant pathogens can colonize and emerge indoors, creating infection risk through surface transmission or inhalation. Several studies have catalogued the microbial composition and ecology in different built environment types. These have informed *in vitro* studies that seek to replicate the physicochemical features that promote pathogenic survival and transmission, ultimately facilitating the development and validation of intervention techniques used to reduce pathogen accumulation. Such interventions include using *Bacillus*-based cleaning products on surfaces or integrating bacilli into printable materials. Though this work is in its infancy, early research suggests the potential to use microbial biocontrol to reduce hospital- and home-acquired multidrug-resistant infections. Although these techniques hold promise, there is an urgent need to better understand the microbial ecology of built environments and to determine how these biocontrol solutions alter species interactions. This review covers our current understanding of microbial ecology of the built environment and proposes strategies to translate that knowledge into effective biocontrol of antibiotic-resistant pathogens.

Intro

Cleaning and disinfection practices in homes and hospitals to combat bacteria, fungi, and viruses have a long history. Ancient civilizations used various disinfection methods to remove

“pestilence”, from the rudimentary practices of boiling and sunlight exposure to the use of natural substances like vinegar and sulfur (1). However, it was not until the 19th century that the age of modern infection control began to take shape with targeted cleaning practices (1). For example, Ignaz Semmelweis introduced hand disinfection in hospitals (2), and Florence Nightingale introduced best practices to decrease infection rates and improve patient healing (3). In the following decades, the use of carbolic acid by Joseph Lister for surgical instrument sterilization, in conjunction with other antiseptic methods, further enhanced pathogen control in clinical settings (4). By the early-to-mid 20th century, the discovery of antibiotics and the development of chemical disinfectants, such as phenol and bleach, provided a newfound defense against infectious agents (5). Though antibiotics have been highly successful and saved many lives, the overuse of these drugs has led to the emergence of antibiotic-resistant bacteria, such as Methicillin-resistant *Staphylococcus aureus* (MRSA) and Vancomycin-resistant *Enterococcus* (VRE), making traditional antibiotics less effective (6). Additionally, pathogens are evolving resistance to biocidal compounds used in traditional cleaning solutions (7). However, chemical treatments such as phenol and bleach remain effective despite providing only temporary removal of pathogens on surfaces.

To reduce the risks associated with various disinfection cleaning agents, hospitals now more frequently use a variety of cleaning strategies for disinfection, including advanced technologies like exposure to ultraviolet (UV) light and hydrogen peroxide vapor (8). Despite these powerful treatments, outbreaks of *Clostridioides difficile* (9) and other antimicrobial-resistant (AMR) organisms (10–14) have continued to rise within healthcare settings, highlighting the enduring challenge of simultaneously disinfecting an area while avoiding selection for traits that increase pathogenic potential. Reducing the spread of AMR pathogens is

a crucial priority for global human health. In 2019, 1.27 million deaths were directly caused by AMR pathogens globally (15), and they are projected to cause an additional 10 million deaths annually by 2050 (16). We must therefore bolster our defenses against persistent and emerging pathogens, safeguarding global health and well-being amidst the evolving landscape of microbial threats (17).

The inability of current hospital disinfection methods to fully combat these challenges emphasizes the crucial need for continuous research, development, and adaptation of infection control methods. Although traditional cleaning methods have helped to reduce the emergence and spread of antibiotic-resistant bacteria and viruses in the built environment, using microbes sourced from different environments to inhibit pathogen survival and transmission is an intriguing new tool that is poised to further improve the health of people indoors. Reintroducing specific microbes into buildings can potentially revolutionize how we prevent the emergence and persistence of unwanted microbes. However, deploying what could be called a microbial biocontrol product is hampered by a lack of basic understanding of the mechanisms of action for this ecological strategy to control disease. Despite this knowledge gap, cleaning products containing bacteria that demonstrate antimicrobial activity have been developed (18) and are already publicly available for purchase. *Bacillus* spores are often used because many species are generally recognized as safe, non-pathogenic, produce a wide variety of antimicrobial compounds (19), and remain viable over long periods of time (20). Though it is unknown how effectively these spores germinate on dry, nutrient-depleted surfaces in built environments, it is important to determine why they are found to be associated with a reduction in the abundance of hospital-associated pathogens (21–24). It is unclear whether there is an actual competitive exclusion or inhibition effect or if the spores occupy niches on surfaces, thereby denying this

space to pathogens. Alternatively, the spores may mask any detectable signal of the pathogens, as determined via DNA sequencing methods. If the latter is true, this could mean that the pathogens remain viable and can cause infection. Answering this open question and moving the field toward improved public health objectives will require using a diverse suite of experimental and analytical approaches, including techniques that have been so far underutilized in built environment research.

In the last decade there have been critical innovations in the methods, study approaches, and experimental designs used to characterize diversity, survival, distribution, transmission, and health risk of microbes found in our buildings. A rapid explosion in observational studies over the last 15 years has provided a baseline analysis of the microbial diversity in built environments. High-throughput sequencing of bacterial 16S rRNA and fungal ITS genes has demonstrated that microbes colonize and spread throughout buildings in predictable ways (25–30). In addition, shotgun metagenomic sequencing has been used to characterize the spread of AMR genes (31) and to quantify the relative abundance of microbial taxa across surfaces and on the skin of indoor environment occupants (32). Also, quantitative PCR (qPCR) has been employed to determine the absolute abundance of specific AMR genes (33, 34) or species of interest (35) in a diverse set of environments such as soil, water, air, feces, and sediments. Further, targeted and untargeted metabolomics have been employed to characterize the distribution of chemicals around built spaces and infer the metabolic ecology of species interactions in experimental systems and real-world environments (36–38). These methods can be enhanced using specialized DNA extraction techniques and internal standards to compensate for the low biomass typically recovered in built environment samples (32, 39, 40).

Investigations in real-world built spaces have led to numerous new hypotheses regarding microbial survival and transmission, and the metabolic interactions that underpin these properties. Robustly testing these hypotheses has required innovations in experimental laboratory-based studies. Despite laboratories being built spaces themselves, recreating the inherent ecological dynamics that define the indoor microbiome has proven difficult and has required a reimagining of traditional microbiology techniques. Microbes in the built environment are generally assumed to be starving, dying, or dead (41). We are, therefore, attempting to study life on the edge of survival. Many microorganisms are unable to survive on surfaces, but some pathogens have demonstrated the ability to survive on surfaces common to the built environment. For example, methicillin-resistant *Staphylococcus aureus* shows robust viability on surfaces such as vinyl and plastic over days (42). Traditional microbiology cultivates microbes using media optimized over decades of experimentation to encourage their growth. Such conditions are unlikely to replicate microbial interactions in the built environment. So, it is necessary to use techniques that more closely reproduce the harsh conditions of most built environment surfaces to more accurately examine how microbes survive, grow, and interact in this environment.

Observational studies and laboratory investigations inform intervention studies in ways that help determine the potential benefit of removing species of concern or introducing potentially beneficial microbes, both for the integrity of the building structure and the health of the occupants. Intervention studies have been performed in mock built environment microcosms, as well as in full-scale field trials and are now elucidating the ecological dynamics of these environments. Unfortunately, due to the cost and added risk of conducting an intervention within buildings such as hospitals, only a few full-scale tests of these intervention techniques have been completed. This review will discuss recent advances in built environment microbiome research,

with a focus on strategies related to the understanding and translation of biocontrol practices used to reduce antibiotic-resistant pathogens on surfaces in real-world clinical settings.

Techniques for Investigating the Microbiome of the Built Environment

Observational studies have investigated microbial dynamics in the built environment, detecting broad trends in the microbial composition and indoor ecological dynamics. For example, these studies describe how the diversity, composition, and functional potential of communities change over time and how occupants and building operations influence these interactions. Many built environments have been explored in this way, including workplaces (43–45), homes (46–49), and public transportation (50, 51). Of critical importance to understanding the interaction between surface-associated microbial ecology and pathogenic activity, hospital environments have been well characterized (25, 26, 52), providing some of the most compelling results to justify further intervention studies. For example, one investigation demonstrated surfaces in a newly built hospital were inoculated with microbes that closely resembled the outside environment (25). However, when that hospital became operational and therefore densely populated with patients and healthcare workers, the surface-associated microbiome began to resemble that of the occupants' skin and respiratory tract. In addition, following the start of operational activity, hospital custodians cleaned surfaces with defined periodic frequency, which also influences microbial dynamics (25). Similar trends have been observed in studies that focused on closed hospital wards that were renovated and reopened for use (27). Using metagenomic reconstruction of bacterial genomes in hospitals over dense time series has demonstrated that bacteria in the hospital environment have increased selection pressure for the acquisition and accumulation of antimicrobial resistance genes (25). Although

the mechanism of action has not been elucidated, bacterial adaptation and resistance to disinfectants (such as those used to clean the hospital) is well known (53), and we hypothesize that genetic adaptation to survival against such disinfection may also be concomitant with other genetic survival strategies, such as antimicrobial resistance. However, further research is needed to uncover the explicit relationship between these phenomena.

Over the last 15 years, observational studies have generally applied relatively affordable microbiome analysis techniques, such as 16S rRNA or ITS gene sequencing, to characterize the diversity and taxonomic composition of bacterial and fungal communities, and qPCR of targeted genes to determine absolute abundances of microbial community members (54–58). Although approaches such as metagenomics, metatranscriptomics, metabolomics, and application of qPCR to quantify a variety of genes and microbial activity (e.g., the abundance of antibiotic resistance genes) can dramatically increase experimental costs, they can significantly improve our understanding of microbial interactions in these settings (59–61). These methods can be implemented to identify patterns of microbial metabolism in complex systems (62), or when observed over time, these data can reveal temporal dynamics. However, the implementation of these other ‘omics approaches is challenging due to the low microbial biomass found on surfaces in buildings, especially where resources such as water, carbon, nitrogen, and other essential nutrients to sustain life are limited and there is frequent cleaning (41, 45). Additionally, although observing spatial or temporal trends in microbiome composition or metabolism is useful, it is hard to identify the features that influence these dynamics due to our inability to control for every factor in a real-world environment. Targeted interventions or manipulations of the environment and the subsequent measurement of the magnitude of effect are needed to better understand how to optimize beneficial change. Even in an observational study such as the

Hospital Microbiome Project (25), where we can observe a pseudo-intervention, in this case a change in occupancy status in real-time, it is not possible to explicitly track the movement of individual microbes or infer microbial metabolic interactions and competitive dynamics. However, it is possible to predict how microbes interact with each other and model their behavior in these environments using metabolic models (63).

Modelling Microbial Metabolism

To improve our understanding of microbial activity and ecology in these extreme environments, it is necessary to fundamentally understand their metabolic potential. Genome-scale metabolic models (GSMMs) are mathematical models of metabolic networks reconstructed from the organism's annotated genome (63, 64). Genome-scale metabolic modelling can help facilitate a clear understanding of the mechanisms that microbes deploy to survive, germinate, and compete for resources. These models predict growth rates in a simulated medium and determine what reaction rates are needed to support growth. Pairs or larger groups of models can be connected to determine which metabolites are being readily exchanged (commensally or symbiotically) and which limited nutrients drive competition between the organisms (65, 66). These models can make predictions for hundreds of conditions within seconds, allowing for the rapid identification of important nutrients, uptakes, and secretions, thereby rationally informing the design of subsequent experiments. In an iterative process, experimental data can be incorporated into GSMMs, contextualizing the data and further refining their predictions. Transcriptomics can also be used to detect reactions associated with low-transcription genes, increasing the specificity of the model to the environment of interest (67). The refined model then yields insights into the biological relevance of transcriptional changes by identifying how

they affect the expression of larger metabolic pathways. These models can also facilitate the analysis of multi-omics data, by integrating them into an interpretable scaffold, which can then be used to predict how changes in the genome or to the environment influence survival or competitive outcomes. Using these modelling techniques on samples from the International Space Station, an extreme built environment, revealed beneficial interactions between the pathogen *Klebsiella pneumoniae* and bacterial species of the genus *Pantoea* and the family *Enterobacteriaceae* (68). The model also predicted *K. pneumoniae* is parasitic towards the fungal genus *Aspergillus*, which was confirmed experimentally via co-culture (68). Predicting microbial interactions in built environments via modelling is a powerful technique to inform efficacious biocontrol strategies by identifying novel species interactions and predicting their differential effect in a range of scenarios. This information can be generated based solely on ‘omics data and subsequently confirmed in laboratory studies.

Interpreting Metabolic Ecology

Studies in controlled laboratory settings typically, but not always (69), use microcosms that contain small pieces of construction materials relevant to the built environment of interest, and conditions (e.g., humidity and temperature) are varied to determine whether they have an effect on microbial activity and survival. To mimic realistic microbial community interactions and successional dynamics, studies have seeded surface materials with microbes by leaving them exposed within built environments prior to initiating challenge studies. In a study of microbial metabolic dynamics (60), coupons of oriented strand board (OSB), medium-density fiberboard (MDF), regular gypsum wallboard, and mold-resistant gypsum were naturally inoculated by passive colonization in homes and in a laboratory. Following this seeding, the coupons were

either soaked in water to simulate a water leak or kept dry, and then all coupons were incubated for an additional 30 days within a high humidity (~94%) chamber. Swabs of the coupons were collected every five days and analyzed with 16S/ITS rRNA gene amplicon sequencing and metabolomics to determine how these communities changed taxonomically and metabolically in response to wetting. Wetted coupons were dominated by the bacterial genera *Bacillus*, *Erwinia*, and *Pseudomonas* and the fungal genera *Eurotium* and *Penicillium*. When coupons had been wetted, *Bacillus* and *Pseudomonas* species were almost always negatively correlated in relative abundance, suggesting competitive exclusion. Even though *Bacillus* species are known to produce antifungal compounds (70–72), only the mold-resistant gypsum was dominated by *Bacillus*. The antibacterial compounds Nigragillin and Fumigaclavine C were found in high abundance. They were positively correlated with the presence of *Aspergillus* and negatively correlated with the abundance of *Bacillus* and *Pseudomonas* (60). These results suggest that the presence of *Bacillus* is not sufficient to prevent fungal growth on built environment surfaces. Although they did not purposefully inoculate surfaces with *Bacillus*, this study suggests that this genus did proliferate when coupons were wetted, but it only dominated on mold-resistant gypsum, which inherently inhibits fungal growth, and as such the naturally occurring *Bacillus* species may not have antifungal activity.

Semi-*in vitro* investigations are effective at discovering novel microbial interactions, but ecological dynamics can also be inferred from applying multi-omic techniques to controlled building environments. For example, one study characterized the chemical and microbial compositions of two frequently wet surfaces in a residential setting, specifically the kitchen sink and bathroom shower (73). This study used a combination of culture-dependent and independent techniques, including transcriptional analysis of the 16S rRNA gene to determine which bacteria

were active at the time of sampling, and assessment of both volatile and soluble chemicals to explore the links between the observed microbiota and chemical exudates. Adams and colleagues concluded that microbes play a critical role in structuring the chemical profiles of surfaces in built environments, particularly in kitchen sinks and shower stalls. The microbial VOCs (mVOCs) were predominantly associated with fatty acid processing, and the composition of these mVOCs appeared more stable than that of the microbial communities themselves, which showed variations in response to changing environmental conditions. A second example demonstrated microbial colonization, succession and viability in a tightly controlled restroom environment (61). This study focused on the ecological succession and viability of human-associated microbiota on restroom surfaces, including floors, toilet seats, and soap dispensers. The study demonstrated that a late-successional microbial community develops on restroom surfaces within 5 to 8 hours of decontamination. This community showed remarkable stability over weeks to months, indicating a quick establishment and persistence of specific microbial assemblages. The authors also showed that fecal taxa, particularly those able to enter a dormant phase, can persist for extended periods on restroom surfaces. This insight into microbial survival strategies in dry and nutrient-poor environments of built environments is crucial for understanding disease transmission, ecology, and environmental health. This study also found a significant positive correlation between bacterial and viral abundances, but with an unexpectedly low virus-to-bacterium ratio of nearly 1:1. This suggests that many bacteria on restroom surfaces are in a dormant state, influencing the dynamics of phages in these environments. Understanding microbial ecological dynamics in these systems is essential if we are to be able to control the survival, emergence and persistence of pathogens. Next, we explore how biocontrol may be

applied to manipulate these ecosystems to reduce the persistence of pathogens in the built environment.

Biocontrol in the built environment

In agriculture, biocontrol has been rigorously investigated as a replacement for pesticidal, antimicrobial, and antifungal compounds used to eliminate disease-causing organisms (74, 75). As many plant-associated microbes are naturally antagonistic towards human-associated pathogens (76), the adaptation of this method in built environments has become an emerging area of research.. The *Bacillus* species used in probiotic cleaning products are also often associated with plants and soil (77). Additionally, *Priestia megaterium* (previously *Bacillus megaterium*) is often included in these formulations due to its biocontrol activity in agriculture (78). Some *Bacillus* species are also part of the healthy human microbiome and can confer health benefits when administered as an oral probiotic. For example, consuming *B. subtilis* spores can decolonize *S. aureus* from the human gut (79). *S. aureus* is an opportunistic pathogen and present in approximately one-third of the human population (80–82), suggesting that decolonization can lower the overall risk of developing future *S. aureus* infections; although we also concede that removal of beneficial *Staphylococcus* species and strains may have negative health impacts.

Bacillus species form spores when starved for nutrients, making them resistant to damage by heat, UV, chemicals, and desiccation. Spores remain in this dormant state until conditions improve, then germinate upon exposure to certain amino acids, such as *L*-alanine, *L*-valine, and *L*-asparagine (83). This makes them ideal for inclusion in cleaning solutions because unlike probiotics that contain vegetative cells (which must be refrigerated), a spore-containing solution can be stored at room temperature indefinitely. Additionally, *Bacillus* spores will remain viable

on built environment surfaces for at least 72 hours (84), can be incorporated into materials (85) where they can repair microfractures (86), and facilitate changes to a material's shape in response to changes in humidity (87). In the future, building materials might contain spores for the purpose of maintaining structural integrity and improving the health of occupants via biocontrol mechanisms and immune stimulation (88, 89); although research in this area is still in the very early stages.

We posit that there are two potential mechanisms by which biocontrol bacteria, such as *Bacillus* spp., may regulate pathogen exposure in built environments: (i) competitive exclusion, either through competition for nutrients or through antibiotic production; and (ii) enhancing the ecological stability and pathogen exclusion potential of the native surface microbiome (Fig. 1). Additionally, as outlined below, studies have shown that *Bacillus* administration in hospitals leads to a significant reduction in the abundance of known pathogens on surfaces (22–24, 84, 90, 91). This could be due to competitive exclusion or by influencing the ecological stability of the native community; another possibility is that the application of billions of *Bacillus* spores leads to overwhelming numerical dominance (iii) that results in a decrease in the ability to detect pathogens, and maybe diminished likelihood of occupant exposure due to a reduction in the probability of encountering a pathogenic cell (Fig. 1). Below we explore specific examples that may help elucidate which mechanism or mechanisms is most likely.

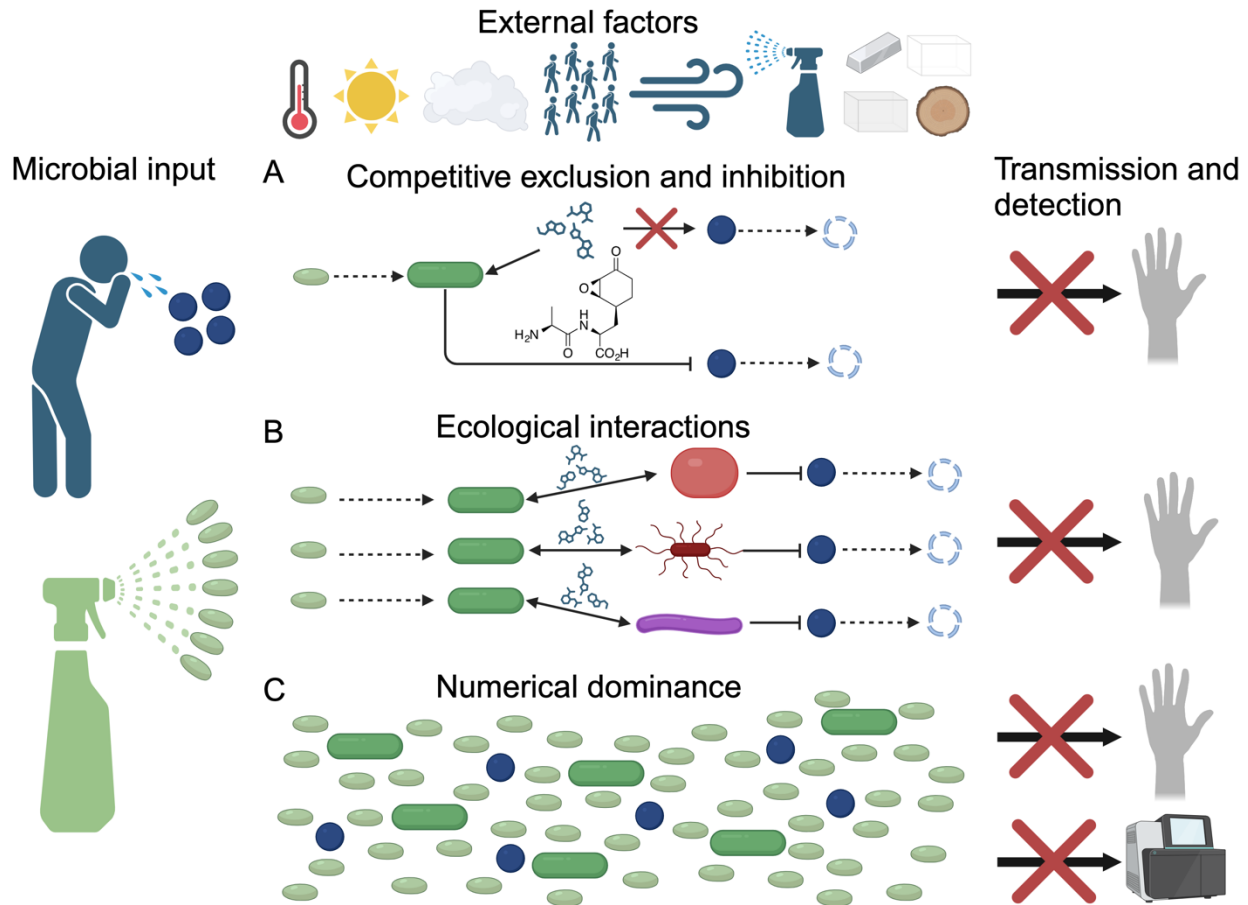


Figure 1. Environmental factors within the built environment and proposed modes of action by probiotic cleaners. Potential pathogens can be deposited on surfaces by infected occupants, but their survival and transmission capability are dependent on many environmental factors, including temperature, light, humidity, occupant density, air flow, cleaning methods, and surface material type (43, 92–96). However, this rate of accumulation and transmission can also be altered through manipulation of surface ecology by introducing bacteria into the environment. Here, we propose three potential modes of action for how probiotics can decrease pathogen exposure and infection risk. (A) Bacterial spores germinate and exclude pathogenic bacteria through direct consumption of resources or by inhibiting pathogen growth via the production of inhibitory molecules, such as bacilysin (97). (B) Germinated probiotic bacteria alter microbial community interactions through metabolic exchange, leading to the inhibition of pathogens (98). (C) Cleaner-associated bacterial cells outnumber cells of potential pathogens, resulting in numerical dominance. We hypothesize this could then reduce the rate of occupant interaction, or it may reduce the detection of pathogens by sequencing techniques.

Bacillus species can competitively exclude other organisms through the preferential uptake of nutrients from their surrounding environment. For example, iron, an important element for all life due to its frequent use as a cofactor in enzymes, can be sequestered by siderophores

secreted by *Bacillus* species (99). These molecules bind tightly to individual iron atoms and require specialized membrane transport proteins for uptake and utilization by a cell. Cells without the proper transportation proteins are unable to import and use the iron, thereby inhibiting their growth (100). Competitive inhibition of pathogens can also occur via the direct production of antagonistic compounds by *Bacillus* species, including surfactin, iturin, fengycin/plipastatin, bacillomycin, and bacilysin (Fig. 2; (101)); although, the effectiveness of these compounds has not specifically been demonstrated in the built environment. Several studies have demonstrated that *Bacillus* intervention enhances the pathogen exclusion properties of the extant surface microbiome (98, 102). However, the lack of a defined mechanism of action behind such biocontrol suggests an urgent need to perform new studies aimed at elucidating these modalities. This is especially important due to the proliferation of commercial probiotic cleaners, whose efficacy should be validated against traditional cleaning methods, and any impact on material integrity or human health assessed. However, studies that seek to demonstrate the effectiveness of an intervention against pathogen reduction cannot introduce pathogens into the environment to start the experiment and instead must rely on already existing exposure events, such as those occurring in hospitals. Additionally, there is a lack of control for complex factors such as occupancy rates, sunlight, and seasonality, which makes these studies susceptible to misleading conclusions (Fig. 1).

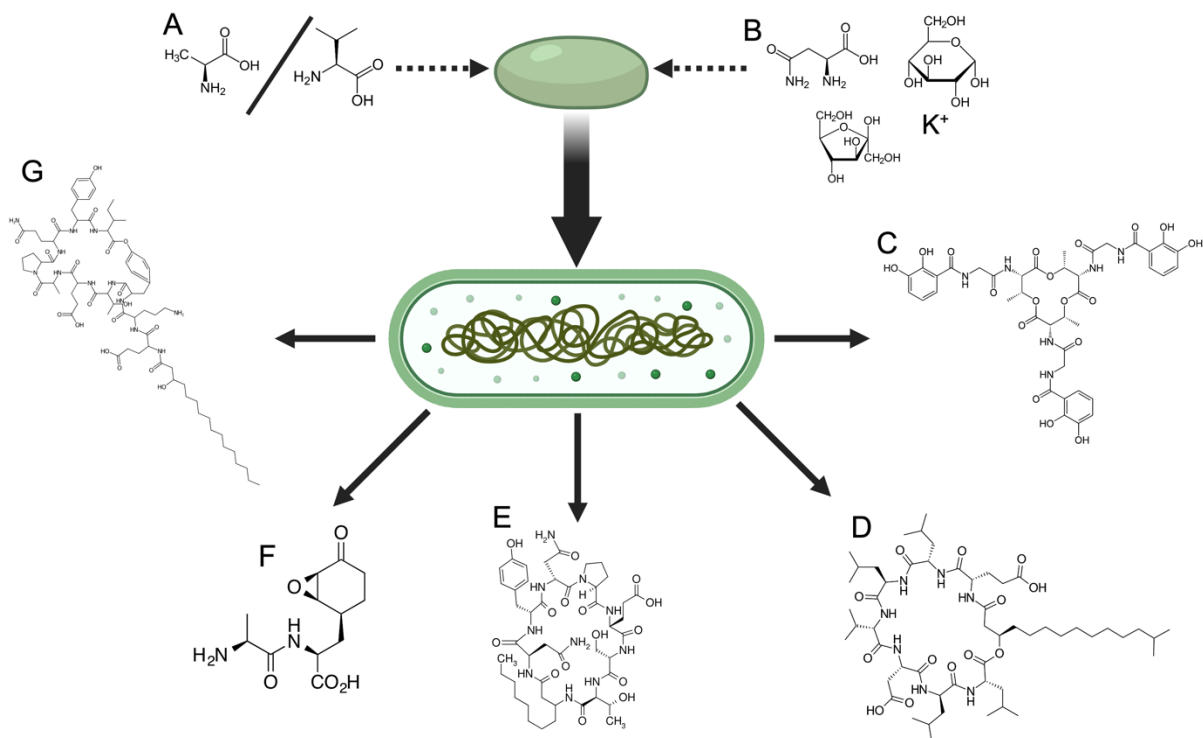


Figure 2. Important molecules for germination and microbial inhibition by *Bacillus* spp.

The germination of *Bacillus* spores is triggered by either (A) *L*-alanine/*L*-valine or (B) a combination of *L*-asparagine, glucose, fructose, and potassium ions (103). Vegetative *Bacillus* cells can generate different compounds that can exclude pathogens, including: (C) the siderophore bacillibactin, which binds iron and is involved in competitive exclusion of nearby microbes (104); (D) surfactin, which has antimicrobial properties and also aids in movement across surfaces (105); (E) bacillomycin, which has potent antibacterial activity (106); (F) bacilysin (97) and (G) fengycin (107), which are both antifungal compounds.

A recent study showed it was possible to impregnate materials with a bacterial spore-containing medium, either through direct inoculation (108) or through embedding spores in 3D printed materials (85). Spores of genetically modified *Bacillus* have been printed into soft hydrogel materials, where they remain viable and become metabolically reactive in response to a pathogen (e.g., *Staphylococcus aureus*), resulting in the biocidal activity of those agents (85). Using sprays, materials can also be seeded with microbial spores. To test the activity of these spore sprays, a commercially available cleaner containing either *Bacillus* spp. spores or a spore-free version of the cleaner was applied to steel coupons; then the coupons were inoculated with either *Acinetobacter baumannii* or *Klebsiella pneumoniae* (102). The coupons were sampled at 3, 24, and 72 hours for colony forming unit (CFU) enumeration to determine whether the presence of the cleaner, with or without *Bacillus* spores, decreased the survival rate of the pathogens compared to cleaner-free controls (102). However, there was no significant difference in *A. baumannii* survival rates in the presence or absence of the cleaner, with or without *Bacillus*. *K. pneumoniae* survival was significantly reduced when exposed to any cleaner, and the presence of *Bacillus* did not enhance this effect. In partial explanation for this finding, metatranscriptomic sequencing data suggested a low (~1% of reads) recovery of *Bacillus* when in spore form, whereas samples with vegetative cells had ~40% of reads identified as *Bacillus*. The absence of any impact of *Bacillus* on pathogen survival, coupled with the lack of vegetative transcriptional activity, suggests that most of the spores failed to germinate and hence had no inhibitory effect on the pathogens. Another study tested the natural seeding of blocks of ceramic, linoleum, and stainless steel in both indoor and outdoor environments that were periodically cleaned over eight months using either bleach, tap water, soap, or a *Bacillus*-containing probiotic cleaner (98). Following this seeding period, clinical *E. coli* and *S. aureus* strains were deposited on the blocks

and desiccated. Their survival was then assessed after 24 hours via CFU enumeration. Blocks cleaned with either soap or the probiotic cleaner had almost no viable pathogens after 24 hours; however, pathogen abundance on the tap water and bleach-cleaned blocks was significantly higher. Additional linoleum blocks were seeded and cleaned as before, then inoculated with a GFP-labelled *P. aeruginosa* strain. Following a 48-hour incubation within a flow cell with tryptic soy broth, the blocks were imaged to assess the extent of surface colonization by *P. aeruginosa*. Almost no growth was observed for the blocks cleaned with tap water or soap, but there was extensive colonization by *P. aeruginosa* on the bleach and probiotic cleaner blocks. These lab-based studies shed light on how *Bacillus*, the primary biocontrol bacteria used in commercial probiotic cleaning products, behaves in different environments and varied microbial communities. However, some lab studies show that *Bacillus* mostly fails to germinate and has a limited impact on the survival of pathogens like *A. baumannii* and *K. pneumoniae* (102). Conversely, using a probiotic cleaner appears to establish a microbial ecosystem that effectively kills or inhibits pathogens, but that cleaning with soap also leads to a microbial community that is just as effective at pathogen inhibition (98). However, the *Bacillus* cleaner did not appear to prevent the accumulation of *P. aeruginosa* when inoculated in a rich media, suggesting that environmental conditions are important for metabolic ecology. Although each study used different methods and conditions, they together reveal that *Bacillus* species do not automatically thrive and effectively compete with other microbes on surfaces. There appear to be only specific situations where *Bacillus* can effectively compete against other microbes in the built environment, which highlights the need for detailed investigation of biocontrol microbes on varied surface types before wide-scale deployment.

An important early study on the effectiveness of biocontrol cleaning methods used a solution containing *B. subtilis*, *B. pumilus* and *P. megaterium* spores (21) over 24 weeks. These spores reduced the CFUs recovered from coliforms, *S. aureus*, *C. difficile*, and *Candida albicans* on surfaces by 50 to 89% after 3-4 weeks of application as compared to surfaces cleaned using standard cleaning methods. The observed reduction remained steady throughout the remaining four months of the study, but pathogen abundance rebounded when traditional cleaning was reintroduced. A subsequent study focused on the resistance of the surface microbial community to antibiotics when a probiotic cleaning solution was used, as well as whether patients were colonized by the *Bacillus* species in the cleaner and if the *Bacillus* germinated on the surfaces (84). Spores were found to germinate on the dry, relatively nutrient deficient surfaces but were not found in samples of blood and urine from patients. Again, a decrease in pathogen abundance was observed on surfaces, as well as a reduction in the abundance of genes associated with antibiotic resistance. The study found no evidence that the *Bacillus* spp. were acquiring antibiotic resistance genes from the native microbial community.

These results prompted a large multicenter study focused on investigating whether *Bacillus*-based cleaning products could reduce the resistome of hospital-associated pathogens (109). A previous study demonstrated that healthcare-associated pathogens tended to acquire additional antibiotic resistance and virulence genes over time in the hospital (25). The Internal Medicine wards of five Italian hospitals were enrolled and samples were collected for an initial 6-month period, during which traditional cleaning methods were continued. Following this baseline period, a 6-month intervention was carried out using a Probiotic Cleaning Hygiene System (PCHS) that consisted of *B. subtilis*, *B. pumilus* and *P. megaterium* spores, after which there was a 6-month post-intervention period. The use of PCHS was associated with an up to

99% reduction in AMR genes contained in the hospital microbiome, with a 33%–100% decrease in the presence of resistant strains. The use of PCHS was also associated with a 60% decrease in the consumption of antimicrobial drugs by patients, leading to a 75% reduction in the costs associated with treating AMR infections. The cumulative incidence of healthcare-associated infections decreased significantly in the post-PCHS treatment period compared to the conventional treatment phase, from 4.8% to 2.3% ($P < 0.0001$). These results are promising, but replication by other research teams is necessary to increase confidence in this approach, as well as further investigations into mechanisms of action. Lacking this knowledge severely limits our ability to refine the process and to understand the ecological dynamics that underpin the observations.

Additional follow-up studies have confirmed the effectiveness of probiotic surface treatments in reducing the abundance of AMR genes and the potential pathogens that often harbor them. For example, bacteriophages are an attractive fast-acting alternative to spores. In a study using the PCHS combined with phage targeting *Staphylococcus* in hospital bathrooms, an 87% reduction in *Staphylococcus* species (including non-pathogenic strains) was observed after only one day of phage treatment (90). After six additional days, there was a 97% reduction in *Staphylococcus* observed, but there was a return to pre-intervention levels after four days of treatment cessation. Resuming the treatment for seven days resulted in a reduction like that observed in the first treatment period. A larger follow-up study at two hospitals using the combined PCHS+Phage treatment had mixed results. One hospital showed a significant reduction in *Staphylococcus*, but the other did not (24). This study was performed during the COVID-19 pandemic, which led to the use of emergency applications of 3% NaClO disinfectant. One hospital used a greater number of NaClO applications, and this increase was correlated with

an order of magnitude reduction in *Bacillus* and phage abundance, likely leading to a reduction in the effectiveness of the probiotic intervention (24). These results support an earlier study, also performed during the COVID-19 pandemic, that found a reduction in pathogen load through the use of PCHS was reversed when emergency 5% NaClO was implemented (91). These recent studies highlight the importance of understanding the dynamic nature of real-world applications, the limits of using phage as a treatment, and how probiotic cleaning methods might be rendered ineffective when harsh bleach cleaning agents are used in tandem.

Conclusions and Future Directions

Probiotic intervention studies in hospitals (22–24, 110, 111) have demonstrated the potential to revolutionize cleaning approaches in healthcare facilities. However, much is still unknown about their mechanism of action, as well as how additional factors could influence their efficaciousness *in situ*. Further investigation of how spores germinate and competitively exclude other microbes in these dry, nutrient-depleted environments is needed for the successful development and broad deployment of probiotic cleaners. To answer these questions, we must use a variety of experimental strategies, including varied application methods (i.e., how the cleaner is applied and at what concentration is the cleaner most effective), inclusion of taxonomically diverse pathogenic microbes at varied concentrations, and a characterization of whole community dynamics in response to cleaner application. These experiments will require highly controlled and easily manipulatable conditions, and therefore, laboratory testing will be essential for determining the relative importance of factors associated with method of use, humidity, nutrient availability, surface material type, and cleaning regimes. Further, simulating

transmission events of microbes from surfaces to humans will be needed to more fully understand how probiotic cleaners influence transmission rates of taxa of interest.

Differential use patterns of healthcare facilities might alter best practices for probiotic cleaner use. For example, it is unknown how the magnitude of response might vary between different wards or rooms. Patient rooms and bathrooms have been the primary focus of intervention studies; however, other shared spaces, such as hallways or visitor areas, also carry the potential for pathogen accumulation and transmission risk. Additionally, long-term monitoring is crucial to detect whether the pathogens in these environments begin to adapt to this new cleaning method and therefore become resistant to biocontrol. Such a situation could start an evolutionary “arms race” with unknown outcomes. It is crucial to consider the health and emotional impacts on the patients and staff. Sociological studies on healthcare workers and patients are necessary to understand the perception that patients, staff, and the public have about the use of these novel products and to involve their feedback in product design and application. The popularity of probiotics in popular foods and drinks could help alleviate concerns, but deploying them in hospitals, especially around high-risk patients, will likely be controversial. Understanding the perception of these products, and explaining how and why they work, will aid in successful widespread adoption across healthcare systems. As seen in studies conducted during the COVID-19 pandemic, harsh cleaning treatments using bleach may inhibit the probiotic and phage cleaners, so it will be imperative that staff are trained in how to properly treat surfaces cleaned with probiotics.

Beyond direct application to the engineering of probiotic materials (85), 3D printing is primed to be the future of microbial biocontrol in built environments. Recent advances in 3D printing have resulted in materials that can be printed at low enough temperatures that spores and

even live bacteria are not harmed during the assembly process. Unlike previous efforts, which used hydrogels (85), these new approaches can enable the printing of ceramics or hard plastics with improved utility as building materials. Using genome-enabled metabolic modelling to select bacteria that are optimized for these printing processes presents unique opportunities for built environment-specific designs that could be used to manipulate the ecology of these environments in prescribed ways. If this trend continues, we may soon be able to print tiles, furniture, or even entire structures out of sustainably produced microbially-active materials (108). Establishing the efficacy of these products through well-designed field intervention studies that are informed by lab-based experiments is an exciting subfield of built environment microbiome research and will ultimately lead to better products, building materials, and design techniques in buildings to improve occupant health and well-being.

Acknowledgements

The introduction chapter, in full, is a reprint of the material as it appears in *The ISME Journal*, Volume 18, Issue 1, under the title “Biocontrol in built environments to reduce pathogen exposure and infection risk”. Neil R Gottel, Megan S Hill, Maxwell J Neal, Sarah M Allard, Karsten Zengler, Jack A Gilbert. Oxford University Press, 2024. The dissertation author was the primary investigator and author of this paper. The authors are funded by NSF ENG-EPSC EFRI ELiS: Developing probiotic interventions to reduce the emergence and persistence of pathogens in built environments (UCSD 2223669) and NASA ROSBIO: Quantifying selection for pathogenicity and antibiotic resistance in bacteria and fungi on the ISS—a Microbial Tracking Study (80NSSC19K1604).

Chapter 1 GERMINATION OF BACILLUS AND PRIESTIA SPORES ON HEALTHCARE-ASSOCIATED SURFACE MATERIALS

Abstract

Members of the *Firmicutes* phylum, such as the *Bacillus* and *Priestia* genera, can form spores in response to nutritional stress and are resistant to other stressors such as heat and desiccation. These spores remain viable indefinitely and can later germinate and resume vegetative growth upon detection of nutrients such as amino acids. The long-term viability of spores at typical room temperatures, along with the inhibitory compounds produced when in the metabolically active, vegetative form, make them an attractive target for development into microbially-based cleaning products (MBCPs) that can be used in the built environment. Understanding how effectively spores in MBCPs germinate is critical to their development into viable cleaning solutions, but little is known about how these spores germinate in built environments. We investigated the germination efficiency of a mixture of spores applied to vinyl and laminate surfaces, which are commonly found in healthcare settings. The spores of five strains belonging to the genera *Bacillus* and *Priestia* were suspended in droplets containing varying levels of nutrients, then deposited on laminate and vinyl surfaces. These surfaces were incubated at room temperature at either an ambient or elevated humidity. Droplets were collected via swabbing over a three-day timeseries. After sample collection, the spores were resuspended and divided into two aliquots, one of which was plated immediately, and the other heat shocked and then plated. Following CFU enumeration, the ratio of germinated cells to the total number of spores and cells was calculated. We found that a low baseline of germination occurred, that this was not greatly enhanced using a germinant like skim milk, but strong germination occurred when skim milk was supplemented with alanine, or when tryptic soy broth was used. Humidity

and the type of surface had a significant effect, but only at later timepoints in the timeseries. This study shows that germinant availability is the most important factor influencing the germination of spores from MBCPs on healthcare relevant surfaces.

Introduction

Harsh chemical cleaners are an effective way to decrease microbial transmission in the built environment, especially in hospitals (112–114). However, antibacterial cleaning and hygiene products can contribute to the development of antibiotic resistance in bacteria (115). An alternative to these types of cleaning products are microbially-based cleaning products (MBCPs) that contain bacteria known to exhibit biocontrol properties, such as the inhibition and destruction of competing microbial species (116). Previous work suggests that *Bacillus* can reduce the abundance of the *Pseudomonas* genera on materials commonly used in constructing buildings (60). Therefore, using MBCPs that contain spores of species from the genus *Bacillus* and the closely related *Priestia*, could be used to inhibit microbial growth on other materials, such as those used in healthcare settings. The use of biocontrol microbes in the built environment has been shown to reduce multi-drug resistant *Staphylococcus aureus* on hard surfaces by 50–89% when compared to existing cleaning products (21). These biocontrol microbes were applied while in their spore form, and presumably had to germinate to inhibit other microbes on the surface. Spore germination has been studied extensively in the context of industrial food preparation and storage (117–119), and laboratory studies have shown that spore populations are highly heterogenous with respect to sensitivity to germinants (120, 121). However, the germination of spores in the built environment has not typically been the focus of germination studies, and how effectively they germinate in these environments is not well established.

Therefore, a better understanding of germination by spores on built environment surfaces is important for ensuring they perform as intended when used in MBCPs.

Bacillus spores germinate through the activation of germinant receptors (GRs) in the inner membrane (IM) by specific amino acids (l-alanine, l-valine, and l-asparagine) or D-sugars (103). Stimulated GRs cause channels in the IM to open and release monovalent cations like H⁺, K⁺, and Na⁺. Following the cation release, Ca²⁺ dipicolonic acid (CaDPA) is rapidly released from the cortex, and the spore core is partially rehydrated. The cortex peptidoglycan layer is hydrolyzed, and the spore core expands, increasing to 80% water content. This germinated spore can then begin metabolism and macromolecular biosynthesis and resume vegetative growth.

While there is evidence of the benefit of MBCPs as biocontrol agents in the BE (21, 22, 24), further development of these cleaners would benefit from investigating the germination of the spores used in MBCPs under different humidity levels and materials. Different surface materials can have dramatically different hydrological properties, which can influence the survival and growth of different bacterial species. For example, the surface adhesion properties of *Bacillus* species are highly dependent on the relative hydrophobicity of both the surface and the bacterium (122–125).

Here, we quantified the germination efficiency of four species of sporulating bacteria, including *Bacillus inaquosorum*, *Bacillus pumilus*, two strains of *Bacillus velezensis*, and *Priestia megaterium* on vinyl and laminate, two materials commonly used in the construction of surfaces in healthcare settings. We also tested the effect of ambient versus elevated humidity conditions on the germination efficiency. A three-day time series was used to assess how the length of time spent on the surface materials could influence germination efficiency. A variety of

germination media was also used, to determine the effect of nutrient availability on spore germination efficiency.

Materials and Methods

Strains used in study. We acquired strains of *B. inaquosorum*, *B. pumilus*, *P. megaterium*, and two strains of *B. velezensis* from a private collection as a mixture in equal ratios stored in the preservative phenoxyethanol(126, 127), at a total spore concentration of 2×10^9 per mL.

Experimental Setup of Surface materials. Laminate (model #050141211408000) and vinyl (model #7208GA) were purchased from Home Depot and cut into 15 cm x 10 cm coupons. Coupons were surface sterilized using 70% EtOH wipes followed by one hour of UV exposure, then taped down in chambers (27 cm x 20 cm x 6 cm) containing either a reservoir of 25 mL water for the high humidity condition then sealed in a bag or left cracked open to allow the humidity to equalize with the ambient room humidity ambient humidity condition (Fig. 1C). A HOBO humidity sensor (Onset) was placed in each chamber to monitor humidity. Chambers with water had > 90% relative humidity (RH), while the ambient humidity ranged from 60% to 75% RH.

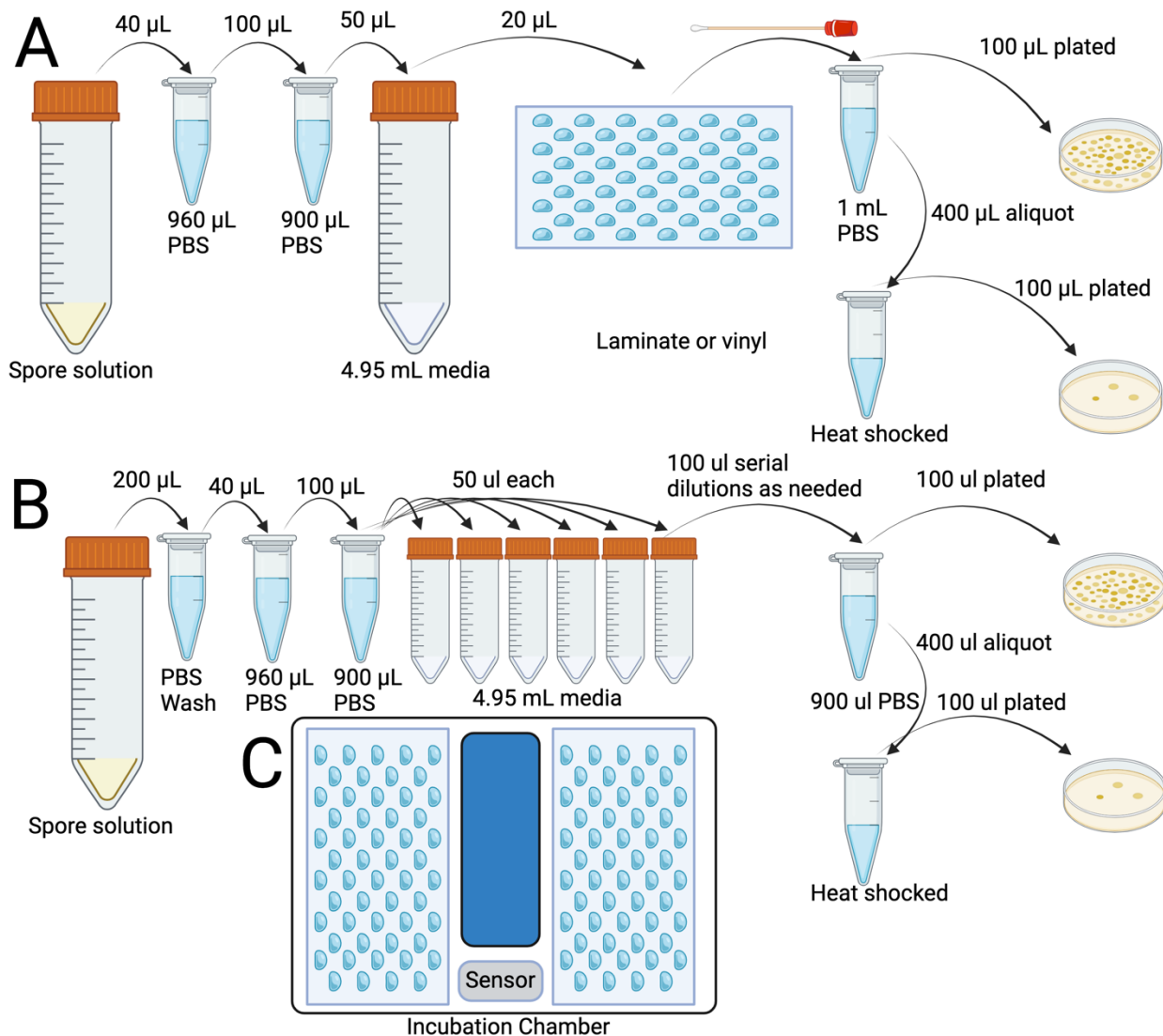


Figure 3. Experimental design of the surface and liquid germination experiments. In the surface germination experiment (A), spores were diluted, mixed with a germination medium, inoculated onto a surface, and then sampled over time. A control experiment (B) was also performed in a larger liquid germination system. Surfaces were kept inside an incubation chamber (C), 2 surfaces per chamber, with a reservoir that was either dry or filled with water, and a humidity sensor.

Spore germination protocol. Spores were suspended in either PBS, skim milk supplemented with either 10% molecular grade water (SM) or 100 mM alanine (SMA), or tryptic soy broth (TSB), then applied to a surface (Fig. 1A) The media were chosen to obtain a wide range of nutrients that could be available for the spores. PBS has no nutrients, skim milk has a

relatively low level of nutrients, skim milk supplemented with 100 mM alanine has a high concentration of a specific germinant, and TSB is a rich media with a relatively high amount of nutrients available to the spores. 200 μL of the spore solution was spun down at 10,000 x g, the preservative removed, and the remaining spore pellet resuspended in 200 μL PBS via vigorous pipetting (Fig. 1A). 40 μL of the washed spores was diluted 1:25 in 960 μL of PBS, vortexed, then 100 μL was transferred to 900 μL PBS, vortexed, then 50 μL transferred to 4.95 mL of each germination medium for a final concentration of 8×10^4 spores per mL. After the four media types were inoculated with spores, rows of six droplets, 20 μL each, were deposited on a coupon, one coupon per media. After inoculating all four coupons, the first row of six droplets from each coupon was sampled via swabbing with a cotton swab that was moistened with PBS. The swab was briefly dipped into PBS, then rubbed against the droplet location while slowly rotating the swab handle for five seconds. After sampling, the swab tip was broken off into a 1.5 mL microfuge tube containing 1 mL PBS. After sampling from all four coupons, the 24 swab tubes were vortexed at medium-high intensity for 30 seconds. Following vortexing, 400 μL of the resulting spore suspension was transferred to a new tube. This aliquot was heat shocked by insertion into a dry bead bath set to 80 °C for 10 minutes. During the heat shock, 100 μL of the spore suspension in the swab tube was plated onto tryptic soy agar (TSA) plates. After 10 minutes, 100 μL from each heat-shocked tube was plated on TSA plates. Additional timepoints were collected at 1.5, 3, 6, 12, 24, 48, and 72 hours after inoculation. TSA plates were incubated overnight at 37 °C, then colony forming units (CFU) were counted.

As a positive control, a liquid culture control experiment was used (Fig. 1B). The spores were diluted using the same method as the surface germination experiment, then 50 μL of diluted spores were transferred to 50 mL tubes containing 4.95 mL of media. Sets of six tubes per media

type were inoculated, then incubated at room temperature while shaking at 180 rpm, and then sampled, heat shocked, and plated at the same frequency as the surface germination experiment. Additional serial dilutions at the 24, 48, and 72 hour timepoints was used to account for cell growth and division.

Data Analysis. Following CFU enumeration, the number of germinated cells in each replicate was determined by subtracting the CFU count of each heat shocked replicate from the CFU count of its corresponding non-heat shocked replicate to determine how many vegetative cells and germinated spores were present in each sample. This value was divided by the CFU count of the non-heat shocked replicate, to yield a germination ratio (GR) of vegetative cells and germinated spores (“Germinated Cells”) to the total number of vegetative cells, germinated spores, and non-germinated spores (“Total Cells”). A GR close to 1 indicates that most of the spores in a sample germinated, while a GR close to 0 means that most of the spores did not germinate.

Using a Shapiro-Wilk test, we found that the data was non-normally distributed ($p < 2.2e-16$). Therefore, to determine whether there was a significant difference in the GR between the first and last timepoint of each media, we used a Mann-Whitney test with a significance level of $p < 0.05$. To determine whether surface type or humidity level significantly influenced the germination efficiency, a Kruskal-Wallis test with Bonferroni correction was used to analyze each timepoint for the four kinds of media.

Results

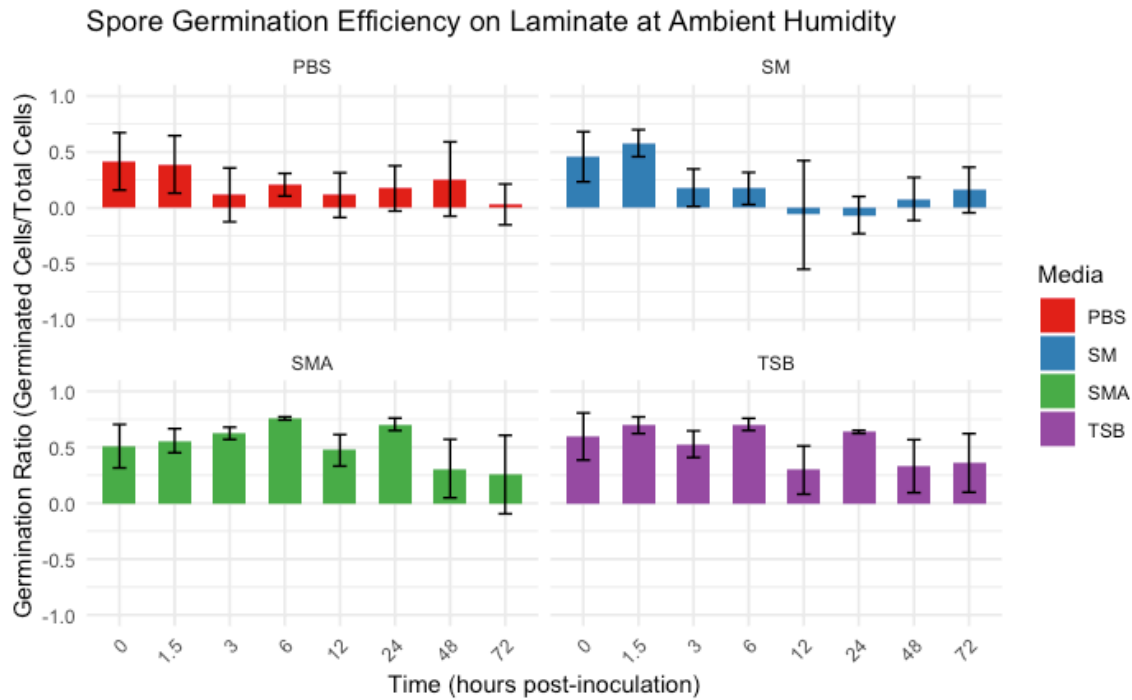


Figure 4. Germination ratio on a laminate surface at ambient humidity. Each panel shows the mean Germination Ratio (GR) at each timepoint in the time series for the germinant media being tested: phosphate buffered saline (PBS), skim milk (SM), skim milk supplemented with 100 mM alanine (SMA), or tryptic soy broth (TSB). Error bars show 1 standard deviation from the mean.

Spore germination on laminate at ambient humidity. The Germination Ratio (GR) was significantly greater at the earliest timepoint, T0, than at the last timepoint, T72, for the PBS and SM media (Mann-Whitney test, $p < 0.05$; Table 1) when the spores were incubated on laminate at ambient humidity (Fig. 4). TSB and SMA were not significantly different ($p > 0.05$) between the first and last timepoint, although the GR for SMA significantly increased ($p = 0.015$) during the first six hours. The GR for SMA and TSB both nearly reached one after six hours of incubation on the surface; however, both declined through the remainder of the timeseries.

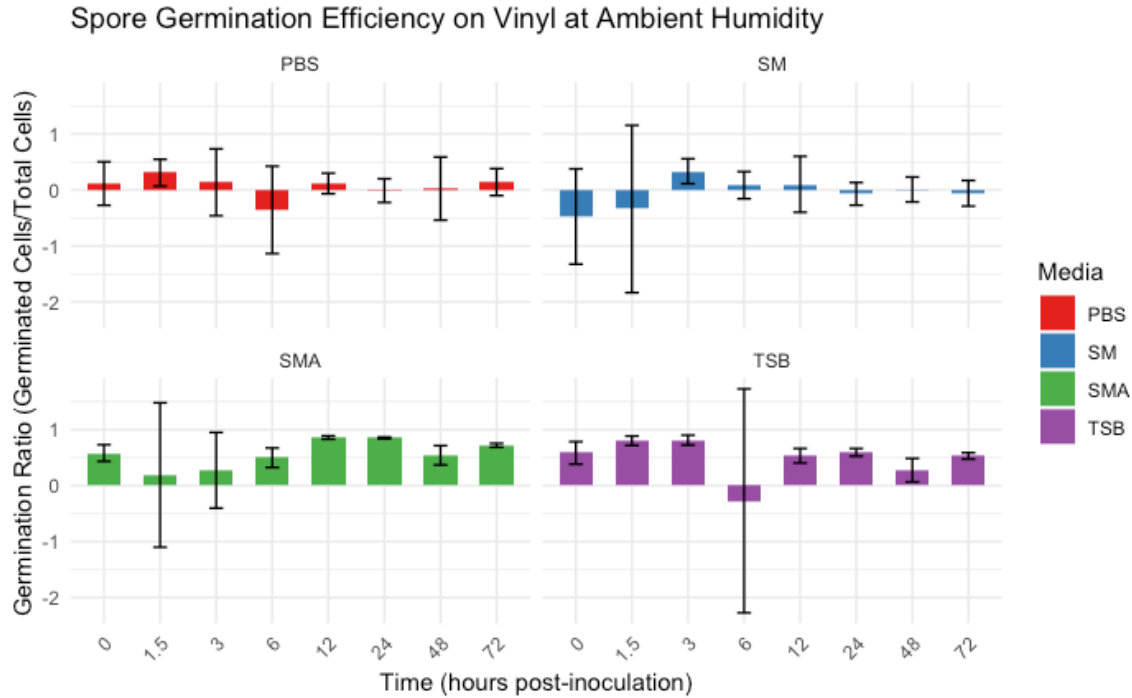


Figure 5. Germination ratio on a vinyl surface at ambient humidity. Each panel shows the mean Germination Ratio (GR) at each timepoint in the time series for the germinant media being tested: phosphate buffered saline (PBS), skim milk (SM), skim milk supplemented with 100 mM alanine (SMA), or tryptic soy broth (TSB). Error bars show 1 standard deviation from the mean.

Spore germination on vinyl at ambient humidity. The GR at T0 and T72 for all four media types was not significantly different ($p > 0.05$; Table 1). However, the GR for SMA was significantly elevated at T12 ($p = 0.016$) and T24 ($p = 0.0043$). The mean GR for both PBS and TSB remained close to zero throughout the timeseries, with higher GR occurring in the high nutrient media, SMA and TSB (Fig. 5).

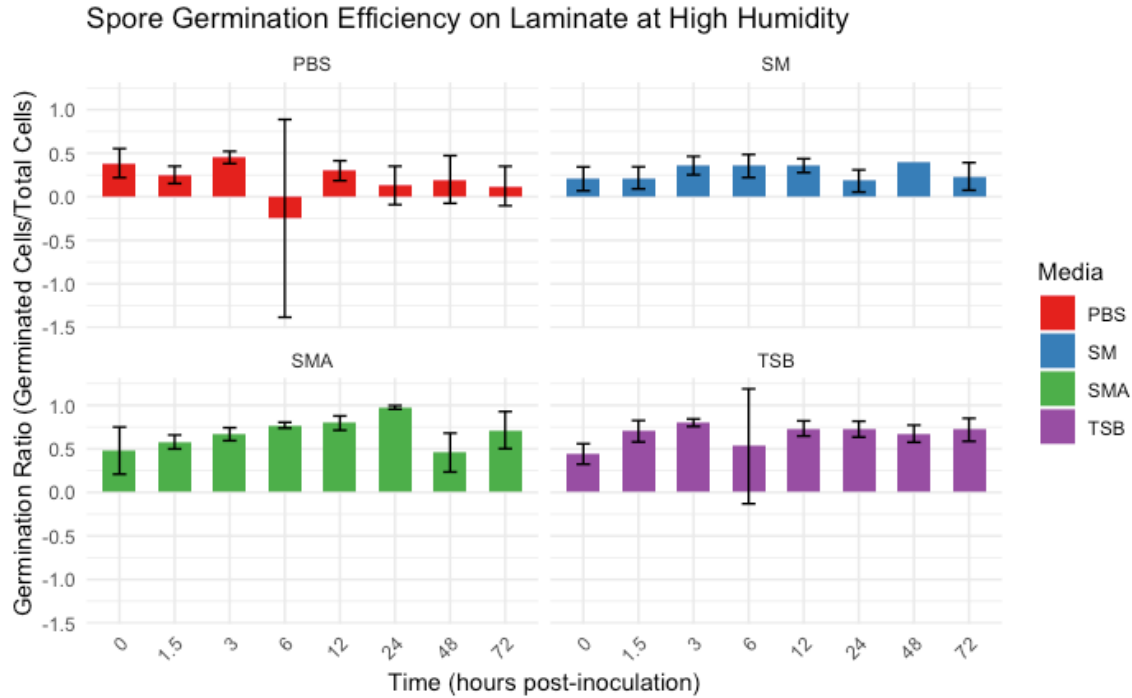


Figure 6. Germination ratio on laminate at high humidity. Each panel shows the mean Germination Ratio (GR) at each timepoint in the time series for the germinant media being tested: phosphate buffered saline (PBS), skim milk (SM), skim milk supplemented with 100 mM alanine (SMA), or tryptic soy broth (TSB). Error bars show 1 standard deviation from the mean.

Spore germination on laminate at high humidity. The GR of TSB between the first and last timepoints significantly increased ($p < 0.05$), while the other three media types were not significantly different ($p > 0.05$; Table 1). However, the GR in SMA media significantly increased through the first 24 hours of the experiment ($p = 0.0022$), then declined (Fig. 6).

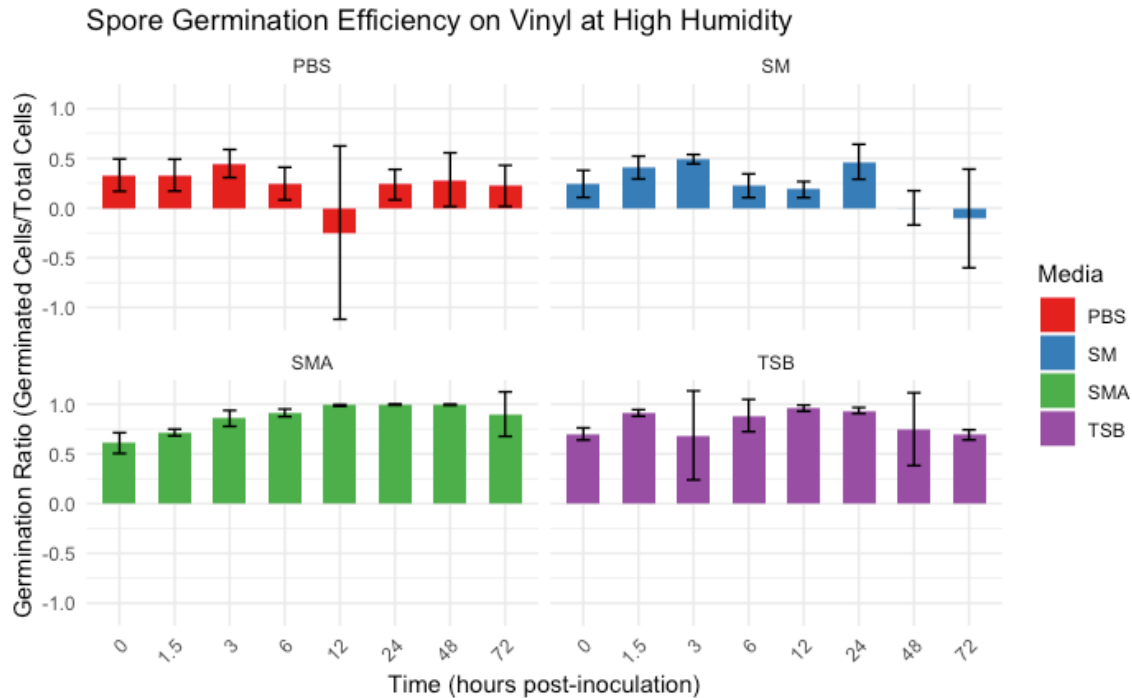


Figure 7. Germination ratio on vinyl at high humidity. Each panel shows the mean Germination Ratio (GR) at each timepoint in the time series for the germinant media being tested: phosphate buffered saline (PBS), skim milk (SM), skim milk supplemented with 100 mM alanine (SMA), or tryptic soy broth (TSB). Error bars show 1 standard deviation from the mean.

Spore germination on vinyl at high humidity. The GR for all four media at T0 and T72 was not significantly different ($p > 0.05$; Table 1). However, three of the media had, at later timepoints, significantly greater GRs than at the start of the timeseries (Fig. 7). For TSB, the GR had significantly increased by T1.5 ($p = 0.0022$). At T3, the GR was significantly greater for both SMA ($p = 0.0043$) and SM ($p = 0.0022$). The GR of SMA continued increasing throughout the timeseries until the last timepoint. The GR for PBS did not significantly change throughout the timeseries ($p > 0.05$; Fig. 7).

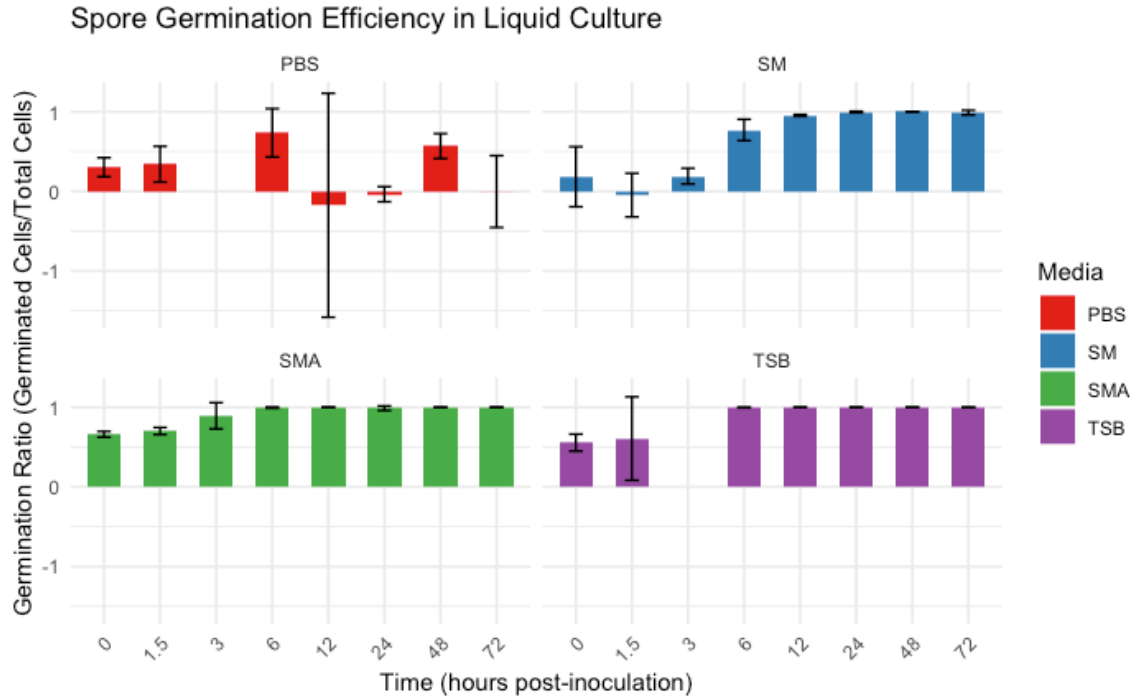


Figure 8. Germination ratio in liquid culture. Each panel shows the mean Germination Ratio (GR) at each timepoint in the time series for the germinant media being tested: phosphate buffered saline (PBS), skim milk (SM), skim milk supplemented with 100 mM alanine (SMA), or tryptic soy broth (TSB). Error bars show 1 standard deviation from the mean.

Spore germination in liquid culture. In liquid media, SM, SMA, and TSB had significantly different GRs between T0 and T72 ($p < 0.05$; Table 1). By T12, the GRs of SM, SMA, and TSB ($p = 0.036$, $p = 0.0091$, and $p = 0.0039$, respectively) were significantly greater than at T0, and would not decrease again (Fig. 8). The GR of PBS at T6 was significantly greater ($p = 0.035$) than at the start of the timeseries but declined through the rest of the experiment.

Stability of humidity and temperature. The HOBO humidity and temperature sensors were used to monitor the humidity and temperature within the chambers and verify that the water reservoir kept the humidity elevated above ambient conditions. The humidity in the chambers with the water reservoirs maintained humidity above 90% (Fig. 9), while the ambient humidity chambers maintained humidity between 50% and 80% (Fig. 10).

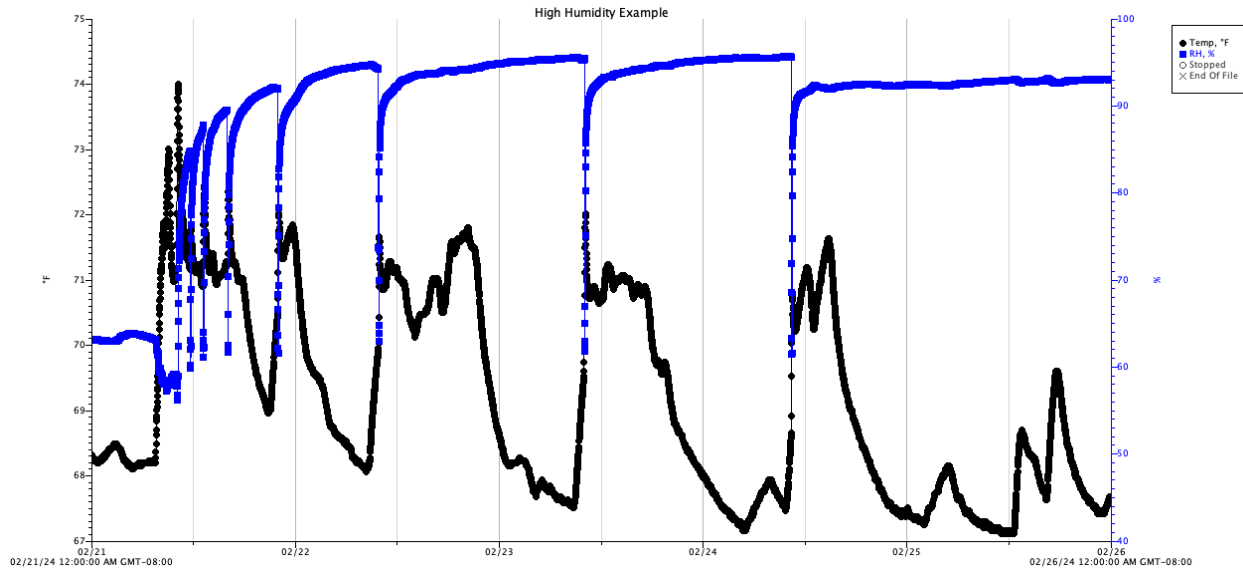


Figure 9. Representative HOBO output for high humidity timeseries. Output from a HOBO sensor. Percent relative humidity (blue line) and temperature (black line) displayed. Sharp changes in temperature/humidity occur when the chamber is moved to a biosafety cabinet and opened for a sampling timepoint.

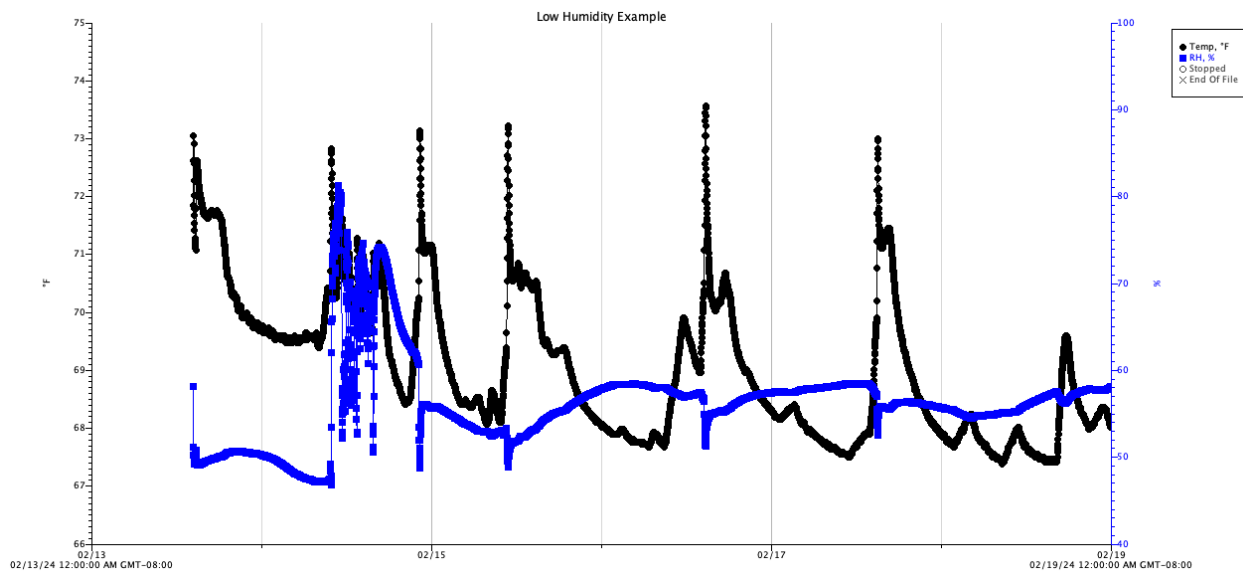


Figure 10. Representative HOBO output for low humidity timeseries. Output from a HOBO sensor. Percent relative humidity (blue line) and temperature (black line) displayed. Sharp changes in temperature/humidity occur when the chamber is moved to a biosafety cabinet and opened for a sampling timepoint.

Table 1. Mann-Whitney test results between T0 and T72 for each germination timeseries. A Mann-Whitney test was performed for the first and last timepoint of each media under each combination of surface and humidity conditions. Media that were significantly different ($p < 0.05$) between T0 and T72 are highlighted in blue.

Mann-Whitney Tests, T0 vs T72

| | Media | U Statistic | P Value |
|---|--------------|--------------------|----------------|
| Laminate, ambient humidity | TSB | 23 | 0.1775 |
| | PBS | 22 | 0.0381 |
| | SM | 27 | 0.0303 |
| | SMA | 16 | 0.1905 |
| Vinyl, ambient humidity | TSB | 15 | 0.6905 |
| | PBS | 15 | 0.6884 |
| | SM | 11 | 0.5368 |
| | SMA | 6 | 0.1255 |
| Laminate, high humidity | TSB | 0 | 0.0043 |
| | PBS | 24 | 0.1255 |
| | SM | 13 | 0.7922 |
| | SMA | 6 | 0.0649 |
| Vinyl, high humidity | TSB | 7 | 0.8571 |
| | PBS | 12 | 0.5476 |
| | SM | 24 | 0.1255 |
| | SMA | 6 | 0.1122 |
| Liquid culture | TSB | 0 | 0.0055 |
| | PBS | 28 | 0.1320 |
| | SM | 0 | 0.0055 |
| | SMA | 0 | 0.0168 |

Table 2. Kruskal-Wallis test with Bonferroni Correction, significant results. Kruskal-Wallis test with Bonferroni correction to determine whether the surface material humidity significantly influenced the GR of each type of media at each timepoint. Only variables that were still significant ($p < 0.05$) after the correction are listed.

| Kruskal-Wallis Test With Bonferroni Correction | | | | |
|---|----------------|--------------|-------------|--------------------------|
| Variable | P Value | Media | Time | P Value, Adjusted |
| Surface | 0.000342 | TSB | 12 | 0.0219 |
| Humidity | 0.000082 | TSB | 12 | 0.0052 |
| Humidity | 0.000524 | TSB | 72 | 0.0336 |
| Surface | 0.000567 | SM | 24 | 0.0363 |
| Humidity | 0.000532 | SM | 24 | 0.0340 |
| Surface | 0.000241 | SM | 72 | 0.0154 |
| Surface | 0.000030 | SMA | 12 | 0.0019 |
| Humidity | 0.000045 | SMA | 24 | 0.0029 |
| Surface | 0.000198 | SMA | 48 | 0.0127 |

A Kruskal-Wallis test, with Bonferroni correction, was used to determine whether the humidity or the surface type significantly influenced the GR at each timepoint. After the correction, humidity was found to have a significant effect at 4 timepoints, while surface had a significant effect at 5 timepoints (Table 2). For TSB, both surface type and humidity level significantly influenced the GR at T12 ($p=0.0219$, $p=0.0052$, respectively), and the humidity level was significant at T72. For SM, surface and humidity had a significant effect at T24 ($p=0.0363$ and $p=0.0340$, respectively), and surface type was significant at T72 ($p=0.0154$). Surface type significantly affected the GR for SMA samples at T12 and T48 ($p=0.0019$ and $p=0.0127$, respectively) and the humidity level was significant for T24 ($p=0.0029$). There were no timepoints at which surface type or humidity level significantly affected the GR in PBS ($p > 0.05$).

Discussion

The germination of the spores in MBCPs is a critical component of the overall effectiveness of these cleaners. Understanding the factors that influence spore germination is

therefore key to the development and deployment of MBCPs. This study used two levels of humidity (ambient and elevated), two types of surfaces (lamine and vinyl), and 4 different germination media.

Effect of humidity. Two levels of relative humidity were used in this study: the ambient humidity of the laboratory (~60% to 75% RH), and a high ambient humidity condition (>95% RH) that was achieved using a reservoir of water and completely sealing the chamber. The high humidity condition prevented the media droplets from drying out during the 3-day timeseries, while the droplets under ambient humidity shrank throughout the first day of the experiment and were dry by the next day. The difference in drying likely explains why the Kruskal-Wallis test found that humidity significantly affected the GR only at timepoints that were after T6 (Table 2). Rehydration of the spore cortex is a critical step in germination (103), which may explain the significant decrease in GR between T0 and T72 observed for spores in the PBS and SM media when incubated at ambient humidity on laminate (Table 1, Fig. 4), although no significant change in GR was observed between T0 and T72 for vinyl at ambient humidity (Table 1, Fig. 5). The shape, size, and mechanical properties of spores changes in response to increasing relative humidity (128, 129), which may prime spores for germination. Increases in salinity, which occurs as a droplet dries out and the salts are concentrated, also inhibits germination, but does not fully prevent it from occurring (130).

Effect of surface type. The two types of surfaces used, vinyl and laminate, are commonly used as flooring materials in hospitals. Their relatively smooth surface reduces bacterial colonization when compared to more porous materials (131). Using a Kruskal-Wallis Test with Bonferroni correction, the type of surface had a significant effect ($p < 0.05$) on the GR at 5 timepoints: TSB at T12, SM at T24 and T72, and SMA at T12 and T48.

Effect of germination media. Four different kinds of germination media were used for this study. PBS is commonly used when performing dilutions and washes of bacterial cells to reduce osmotic stress and does not contain nutrients like amino acids that could lead to the activation of germinant receptors. Therefore, we expected this media to not show significant levels of germination. However, we found that germination occurred when using PBS, specifically during the timepoints that were collected in the first six hours of each timeseries (Figs. 4, 6, and 7) , except for vinyl at ambient humidity (Fig. 5). It is possible that some of the spores were inactivated by the 10-minute, 80°C heat shock treatment. Temperature, composition of the sporulation medium, and the method of spore preparation used can all influence the heat resistance of spores (*132*), and it is likely there are some spores within a spore solution that are, by chance, more sensitive to heat than the rest of the population. Additionally, there is evidence that spores will spontaneously germinate in the absence of germinants (*133*), so there may have been a small fraction of germinated spores within the spore solution that were inactivated by the heat shock treatment.

Skim milk was selected as one of the germinant media because it has a wide variety of nutrients like amino acids (*134*), but is not as nutrient rich as TSB media. Additionally, the germination of spores in milk has been well-studied since standard pasteurization does not inactivate them in dairy products and leads to early spoilage (*135*). Spores in skim milk displayed low germination, especially under ambient humidity conditions (Fig. 4 and Fig. 5). The germinant alanine is present at ~14 mM in skim milk (*136*), so we also used an additional media type by supplementing skim milk with alanine. With 100 mM alanine, this supplemented skim milk was expected to have a strong impact on germination (*137*). This supplement enhanced the GR of the spores, and under high humidity conditions resulted in a GR very close

to 1 (Figs. 6 and 7). TSB was the fourth media used for this study and was an effective germinant, like SMA. TSB is a commonly used rich medium for bacterial cultivation and was expected to have a high GR across all the experimental conditions.

Limitations to the study. There are several technical limitations to this study, such as the use of heat shock followed by CFU enumeration. Each step of the sampling process (swabbing, dilution, plating) introduces additional random error, which may explain why some timepoints have very large error bars, such as T6 of TSB on vinyl at ambient humidity (Fig. 5). Additionally, due to the production of surfactin by members of the *Bacillus* (138) and *Priestia* (139) genera, any excess moisture on the plates could lead to the spread of a colony across the entire plate when incubated overnight and therefore ruin that replicate. Additionally, the differing colony sizes and shapes of each strain prevented the use of automated colony counting methods (140, 141). Besides technical limitations, this study did not include the chemicals that are standard components of a MBCP, such as detergents. These chemicals may influence the germination efficiency of the spores, as well as the long-term survival of the vegetative form of the cell. This study also did not determine whether spores germinated and then re-entered the sporulated form, or if they remained in the spore form for the entire duration of the timeseries. We also did not investigate the interaction between the different members of the species used in the study. However, these interactions may only matter under certain conditions, such as when an extremely high density of spores are utilized, or if the surface they are applied to is so hydrated that the cells can move freely across the surface.

Further research into the germination of spores in built environments is needed to enhance the reliability of MBCPs when they are deployed in real-world conditions. A wider range of materials could be studied, such as stainless steel, fabrics, and wood could be

investigated. Additionally, media that more closely resembles contamination from human occupants, such as blood, spit, and sweat could be used. Examining how easily spores are removed from surfaces by incidental interactions, such as brushing against a surface with a hand or clothing fabric, will be necessary to determine how often a MBCP should be reapplied to a surface. Also, the impact of cleaning with traditional products should be determined. Previous research on MBCPs conducted during the COVID-19 pandemic found that the increased cleaning of surfaces using bleach inactivated the biological component of the cleaner, likely leading to their decreased effectiveness against pathogens (91).

Conclusion

Spores used in MBCPs can effectively germinate on surfaces commonly used in healthcare settings, although how many germinate is impacted by the availability of nutrients, the humidity, and the type of surface they've been applied onto. Our study found that skim milk, a medium containing many nutrients that should induce germination, were only marginally more effective than PBS. High levels of germination required very nutrient rich media, such as TSB and skim milk supplemented with alanine. The type of surface and the humidity had a significant influence, but only at later timepoints in the experiments. This study shows that nutrient availability is by far the most important factor when considering the effectiveness of germination by spores in MBCPs.

Acknowledgements

Chapter 1, in part is currently being prepared for submission for publication of the material. Gottel, Neil; Hill, Megan S; Allard, Sarah M; Salas Garcia, Mariana; Gilbert, Jack A. The dissertation/thesis author was the primary investigator and author of this material.

Chapter 2 INHIBITION OF STAPHYLOCOCCUS AUREUS BY BACILLUS AND PRIESTIA SPORES ON HEALTHCARE RELEVANT SURFACES

Abstract

The rise of antibiotic-resistant pathogens within healthcare settings necessitates investigating new cleaning methods to combat their spread. The application of bacterial spores to surfaces in these settings is an under-explored alternative to using harsh chemical cleaners. In this study we investigated the use of a mixture of *Bacillus* and *Priestia* spores to inhibit the survival of methicillin-resistant *Staphylococcus aureus* on surfaces commonly used in healthcare settings. Timeseries experiments showed that MRSA survival decreases over time at ambient humidity conditions in droplets containing low to no nutrients, but tends to remain stable at elevated humidity, regardless of surface type (vinyl or laminate) tested. Differences in the CFU counts between MRSA incubated on a surface by itself versus in the presence of spores were almost always not significant. In the limited number of timepoints where a significant difference was found, it was usually an increase in survival of MRSA in the presence of spores, potentially because of nutrient availability due to microbial necromass. These results suggest that while species may demonstrate antimicrobial action against MRSA on agar plates or in liquid media under ideal conditions, they may not inhibit MRSA when co-cultured in droplets on common building materials. Therefore, bacterial spore associated cleaners may offer no benefit in hospital sanitation practices.

Introduction

Antimicrobial resistant (AMR) bacterial infections are a serious global health concern, with an estimated 5 million deaths associated with AMR globally in 2019 (15). These infections can spread between patients in healthcare settings, leading to longer hospital stays, costs, and increased risk of serious illness and death. One of the leading causes of hospital acquired

infections (HAI), methicillin-resistant *Staphylococcus aureus* (MRSA), resulted in 120,000 infections and 23,000 deaths in 2017 in the United States (142). One of the primary routes for MRSA transmission in hospitals is through fomites, which are objects or materials likely to harbor infective agents and facilitate transmission between patients (143).

The use of chemical cleaners is generally accepted as the standard method for removing pathogens from hospital surfaces (113). However, this cleaning may encourage the development of antimicrobial resistance in pathogens (115). Additionally, the persistence of MRSA infections and deaths, even with the widespread knowledge of the risk of fomite transmission in hospitals, presents an opportunity for the development and deployment of microbially-based cleaning products (MBCPs) in healthcare settings. MBCPs often contain spores from species in the *Bacillus* genus, which produce a wide variety of antimicrobial compounds (19, 144, 145). When co-cultured on agar plates, *B. subtilis* inhibits the growth and virulence factor expression of nearby *S. aureus* cells (146). *B. subtilis* is also active against *S. aureus* that has colonized the gut and nares, significantly reducing its prevalence when administered as a probiotic (79). In the built environment, surfaces cleaned using MBCPs in an Italian hospital reduced the prevalence of HAI-related pathogens by 50 to 89% compared to surfaces cleaned using traditional methods (21). However, in another study comparing probiotic, soap, and disinfectant-based cleaning in hospital settings, no significant difference in HAI rates was observed (147). This variability in the perceived effectiveness of MBCPs warrants more controlled analysis of their bactericidal potential in controlled laboratory settings.

In this study, we used two surface materials commonly found in hospital construction, two levels of relative humidity to reflect differences found in ambient conditions in hospitals due to changes in seasonal weather (e.g. (148)), and four types of spore carrier media to investigate

how surface type, humidity, and nutrient availability influence the survival of MRSA with and without the presence of *Bacillus* and *Priestia* spores. Droplets of MRSA were inoculated onto a surface, and then either sterile media or media inoculated with an equivalent number of *Bacillus* and *Priestia* spores were added to these droplets. Droplets were collected via swabbing, then diluted and plated for CFU enumeration over a three-day timeseries. Following colony counting, the significance of difference in the mean number of MRSA cells in the droplets with or without spores was calculated.

Materials and Methods

Bacterial strains. We acquired *B. inaquosorum*, *B. pumilus*, *P. megaterium*, and two strains of *B. velezensis* from a private collection as individual dry spore preparations, as well as a liquid mixture in equal ratios at a total spore concentration of 2×10^9 per mL stored in the preservative phenoxyethanol (126, 127). The MRSA strain was purchased from the American Type Culture Collection, *S. aureus* subsp. *aureus* Rosenbach BAA-1717.

Experimental Setup for agar plate competition studies. To determine whether the five *Bacillus* and *Priestia* strains would inhibit MRSA on agar plates, each strain and the MRSA strain were grown separately overnight in 5 mL of tryptic soy broth at 37 °C, shaking at 180 rpm. The overnight MRSA culture was diluted 1:100 in PBS, then 100 µL was spread on five tryptic soy agar (TSA) plates. Each plate received three 5 µL droplets of: 1) an overnight culture of one of the *Bacillus* and *Priestia* strains, 2) a 1:10 dilution of this culture in PBS, and 3) a 1:100 dilution of this culture in PBS. The plates were grown overnight at 37 °C, then imaged to determine whether a zone of inhibition had formed.

Experimental Setup of Surface materials. Laminate and vinyl were chosen as representative surface materials commonly used in hospital settings. Laminate and vinyl are

commonly used in hospitals because they are durable, easy to clean, resistant to stains and moisture, and cost-effective. Additionally, they offer comfort and safety with non-slip surfaces and come in various colors and patterns. Laminate (model #050141211408000) and vinyl (model #7208GA) were purchased from Home Depot and cut into 15 cm by 20 cm coupons, 2 surfaces of the same type were taped down in a 27 x 20 x 5.5 cm container. The coupons were surface sterilized using 70% EtOH wipes followed by 1 hour of UV exposure in a biological safety cabinet. After inoculation (see below), either an empty reservoir, or a reservoir containing 25 mL of dH₂O were placed in the chamber to increase humidity. A HOBO humidity sensor (Onset) was also placed in the chamber. For the high humidity condition, the chamber was sealed within a 7.5 L plastic bag. For the ambient humidity condition, the lid of the chamber was left slightly cracked open and was not sealed in a bag. The containers with water maintained relative humidity >90%, while the containers without water, maintained humidity between 50% and 80%.

Media preparation. A prepared 5 strain mixture of *Bacillus* and *Priestia* spores (with an equal number of spores per strain) were suspended in either phosphate buffered saline (PBS), skim milk (SM), SM supplemented with 100 mM alanine (SMA), or tryptic soy broth (TSB). PBS is commonly used for dilutions and washes of bacterial cells, and prevents osmotic damage to the cells, but does not provide additional nutrients for growth. SM has a wide range of nutrients, but is not as nutrient dense as a rich growth medium like TSB (136). Alanine is an effective germinant, and at 100 mM ensure strong germination of spores (137). Skim milk was prepared by dissolving skim milk powder (Sigma, cat # 1153630500) 10% w/v in dH₂O and autoclaved for 20 minutes. SMA was prepared by mixing 9 parts sterilized SM with 1 part filter-

sterilized 1M L-alanine. TSB was prepared per manufacturer's (Millipore, cat # 22092) instructions.

Standard curve for MRSA. The target concentration of MRSA cells in the competition was 2×10^6 cells per mL. This concentration ensured that there would be sufficient resources for the MRSA to grow, while also providing germinants for the spores and nutrients to enable their growth and antimicrobial activity against MRSA. A standard curve was made by growing MRSA at 37 °C in TSB, shaking at 180 rpm. Once the absorbance of the culture reached ~0.1 (blank adjusted), an aliquot from the culture was serially diluted every half hour for 2 hours, and 5 replicates were plated for CFU enumeration. Using the absorbance and CFU enumeration, a standard curve was calculated, and used for determining how much to dilute MRSA cultures to achieve a $\sim 2 \times 10^6$ cells per mL abundance to start each competition.

Surface competition setup. MRSA was streaked on a tryptic soy agar (TSA) plate and grown overnight at 37 °C (Fig. 11A). The next day, a colony was picked and resuspended in tryptic soy broth (TSB). A plate reader was used to measure the absorbance at an optical density (OD) of 600 nm. When the absorbance was between 0.2 and 0.4, the culture was first diluted 1:10 in the media being used for the experimental timeseries (PBS, SM, SMA, or TSB), then diluted again according to the standard curve, resulting in a total volume of 5 mL and a MRSA concentration of $\sim 2 \times 10^6$ per mL. The diluted MRSA solution was poured in a reservoir, and using a multichannel pipette, 10 μ L droplets were deposited on the surface (laminar or vinyl), six droplets per timepoint (T0, T24, T48, T72, and an extra row in case of sample loss). One combination of humidity and surface type (laminar ambient humidity, vinyl ambient, laminar high humidity, or vinyl high) was tested for each timeseries, using five chambers. Four of the five chambers contained each type of media being tested, with or without the spore mix (details

below). An additional chamber with two droplets of each type of media, without MRSA or spores, served as negative controls to confirm sterility of the media.

Once the MRSA was distributed to the surfaces, 10 μL of sterile media was added to one half of the droplets in each chamber (Fig. 11B). Then, 100 μL of the spore solution was diluted in 900 μL PBS, vortexed, then diluted again by transferring 50 μL to 4.95 mL of media to obtain a 2×10^6 spores per mL solution (Fig. 11C). 10 μL droplets of the diluted spore solution were transferred to the other half of the MRSA droplets that did not receive the sterile media.

Surface competition sample collection. After droplets were deposited on the surfaces, the first row of six droplets was collected via swabbing with a cotton tipped swab, then the tip was broken off into 1 mL of PBS. Once all the samples for the first timepoint, T0, were collected, the tubes containing the tips were vortexed at medium intensity for 30 seconds, then 100 μL was transferred to a tube with 900 μL PBS. These tubes were vortexed for 5 seconds, and then 100 μL from each tube was plated on TSA plates made with 4 mg methicillin per L of agar media, to prevent the growth of the spores that germinated. The controls for sterility were plated on TSA plates that did not contain methicillin. Plates were incubated for 2 days at 37 $^{\circ}\text{C}$, and then the colonies counted. Additional samples were collected 24, 48, and 72 hours after the initial surface inoculation.

Data analysis. CFU counts were adjusted based on the dilution factor prior to plating. Using the Shapiro-Wilk test for normality, the data was found to not be normally distributed. Therefore, the significance of the difference between the mean of MRSA in droplets with and without spores was calculated using a Mann-Whitney test. A Kruskal-Wallis test was used to

determine the mean percentage change in MRSA abundance during the course of the timeseries and the significance of each variable tested (humidity, media, surface, spore presence/absence).

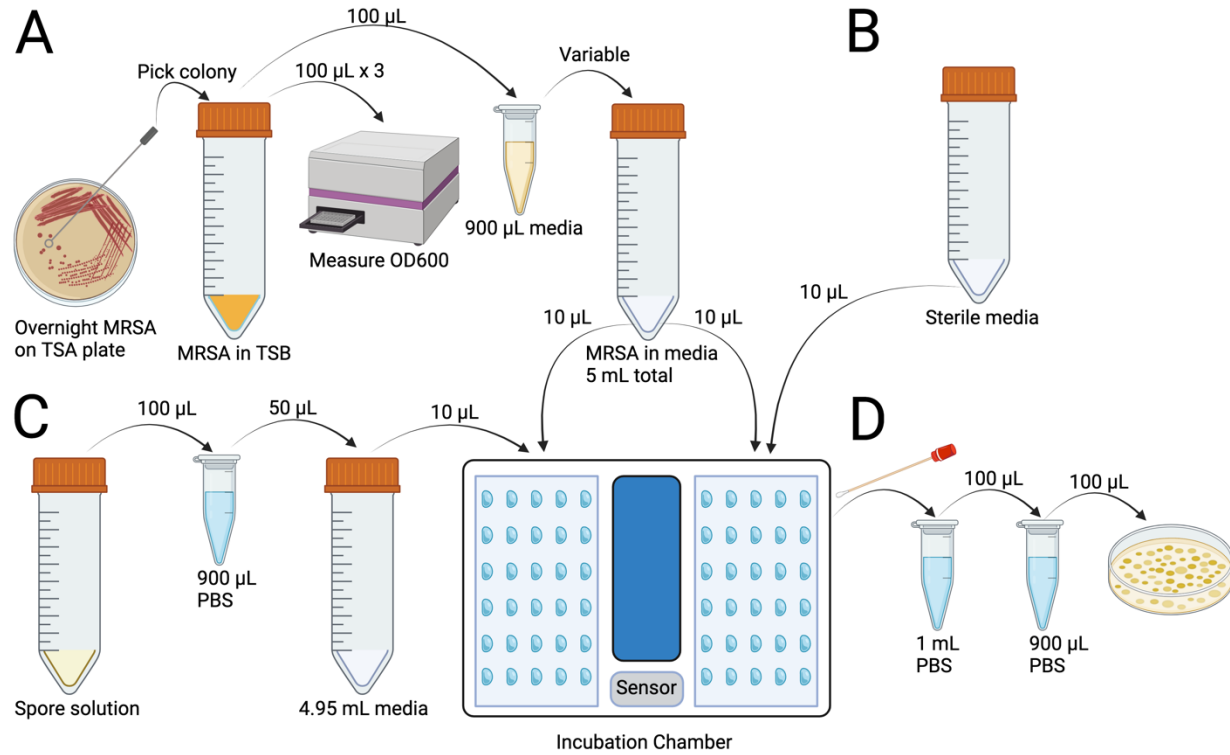


Figure 11. Setup of MRSA co-cultured with spores in droplets on surfaces. (A) Growth, dilution, and inoculation protocol for MRSA on surfaces. (B) Application of sterile media for the MRSA-only samples. (C) Dilution and inoculation protocol for the spore mix. (D) Sample swabbing, dilution, and plating.

Results

Inhibition of MRSA by individual strains used in study. Plating of the five *Bacillus* and *Priestia* strains at 3 different levels of dilution of an overnight culture with 1) no dilution, 2) a 1:10 dilution, and 3) a 1:100 dilution showed that four of the five strains had inhibition zones (white halos around the dark circular colonies labeled 1, 2 and 3), but *P. megaterium* did not make a zone of inhibition in the MRSA lawn (Fig. 12). The *B. velezensis* strains grew poorly in

the liquid culture and were outcompeted by MRSA on the TSA plates when diluted (Fig. 12B, C).

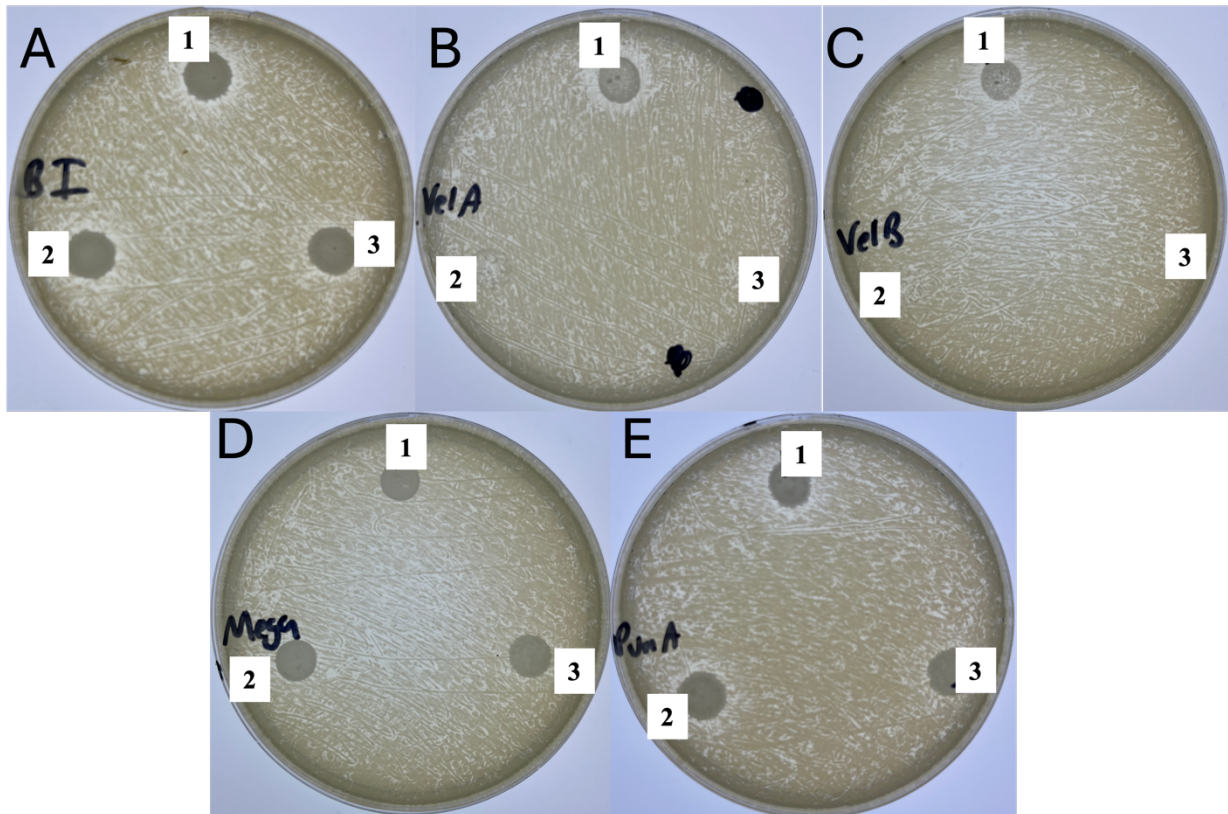


Figure 12. MRSA inhibition on tryptic soy agar plates. Images of each of individual strains used in the spore mixture. Each plate received three droplets, 5 μ L each, of 1) an overnight culture of the strain, 2) a 1:10 dilution of the strain, and 3) a 1:100 dilution of the strain. The strains used were (A) *B. inaquosorum*, (B) *B. velezensis* strain A, (C) *B. velezensis* strain B, (D) *P. megaterium*, and (E) *B. pumilus*.

Humidity within chambers. HOBO sensors inside the chambers were used to monitor the humidity throughout the experiment. The high humidity condition maintained relative humidity above 90% (Fig. 13), while the relative humidity in the ambient humidity chambers was between 50% and 80% (Fig. 14).

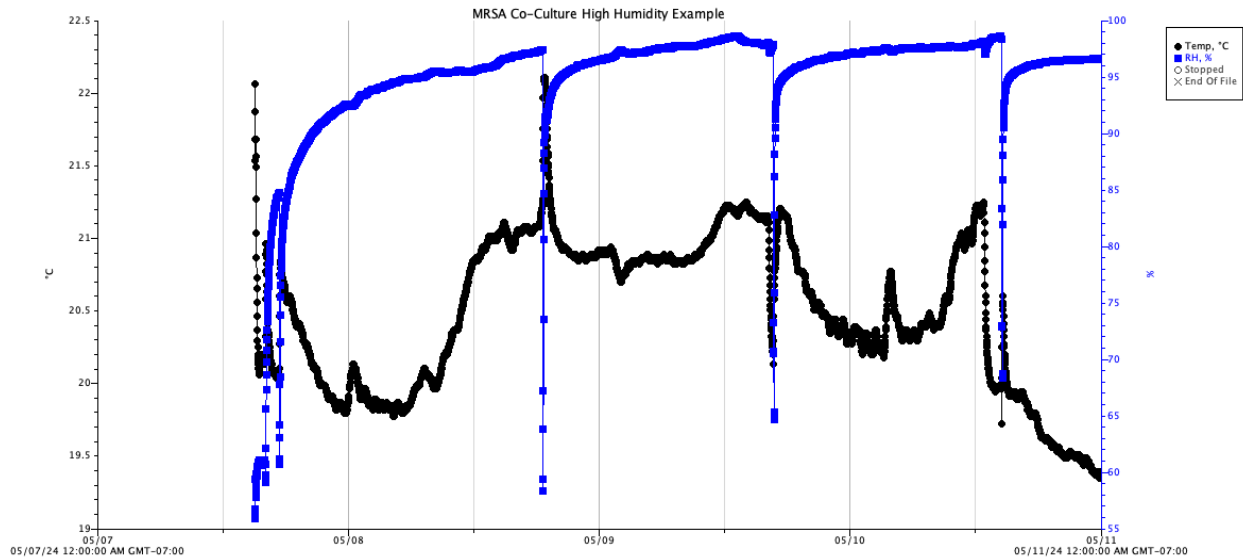


Figure 13. Representative HOBO output for high humidity timeseries. Output from a HOBO sensor. Percent relative humidity (blue line) and temperature (black line) displayed. Sharp changes in temperature/humidity occur when the chamber is moved to a biosafety cabinet and opened for a sampling timepoint.

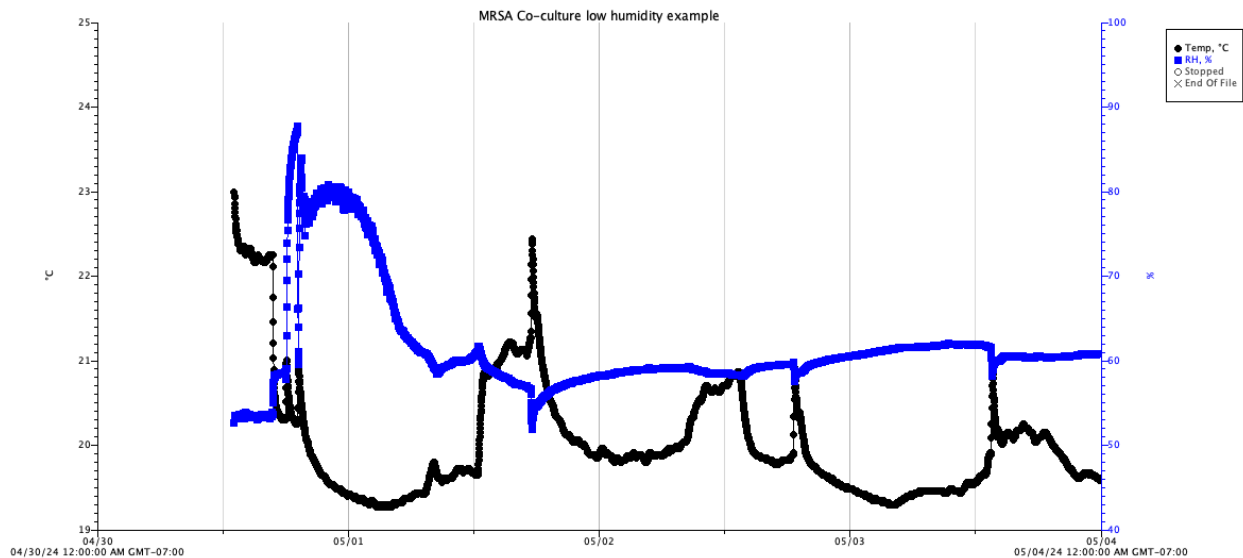


Figure 14. Representative HOBO output for ambient humidity timeseries. Output from a HOBO sensor. Percent relative humidity (blue line) and temperature (black line) displayed. Sharp changes in temperature/humidity occur when the chamber is moved to a biosafety cabinet and opened for a sampling timepoint.

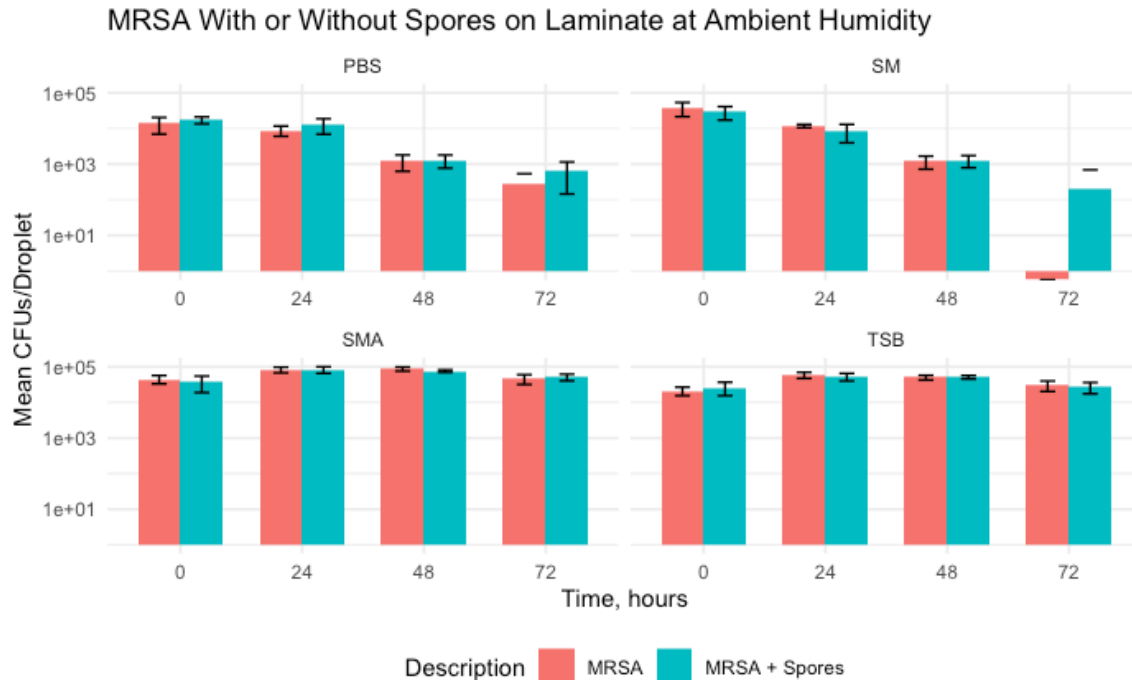


Figure 15. MRSA inhibition timeseries on laminate at ambient humidity. Mean number of MRSA CFUs in each type of media droplet, as determined via swabbing, dilution, plating, and CFU enumeration, and then adjustment for dilution factor. Phosphate buffered saline (PBS), skim milk (SM), skim milk supplemented with 100 mM alanine (SMA) and tryptic soy broth (TSB) were used as the competition medium.

The mean number of MRSA CFU in the PBS and SM droplets decreased throughout the laminate, ambient humidity timeseries (Fig. 15). Between T0 and T72, the mean CFU of MRSA by itself in PBS decreased by 98.1%, and when cultured with spores, by 96.2% (Table 5). In SM, CFUs decreased by 100% for MRSA alone, and by 99.3% with spores. Growth of MRSA was observed for SMA and TSB in the first 24 hours of the timeseries. CFUs of MRSA incubated by itself increased by 83.5% in SMA, and by 177.5% in TSB, while CFUs of MRSA with the spore mix increased by 124% in SMA and by 102% in TSB (Table 4). Between T0 and T72, MRSA CFUs had an overall increase in SMA (2.39% MRSA alone, 38.5% with spores) and in TSB (42.8% alone, 2.56% with spores). There was no statistically significant difference ($p > 0.05$)

between MRSA incubated by itself, or when co-cultured with the spore mix at any of the timepoints in the timeseries (Table 3).

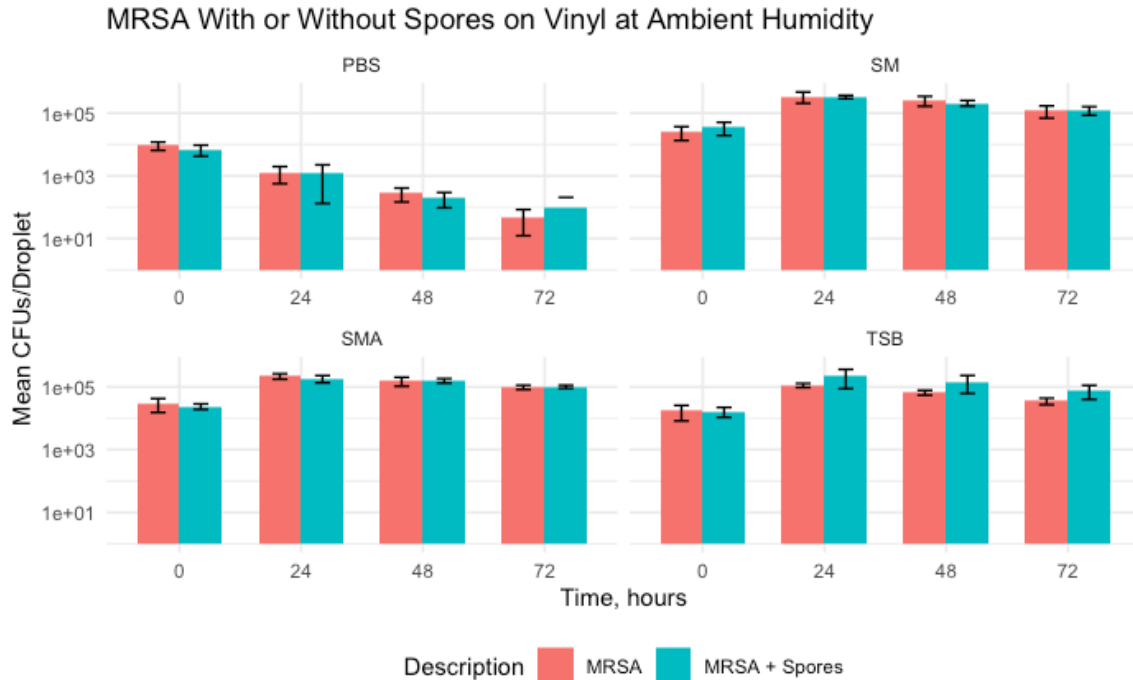


Figure 16. MRSA inhibition timeseries on vinyl at ambient humidity. Mean number of MRSA CFU in each type of media droplet, as determined via swabbing, dilution, plating, and CFU enumeration, and then adjustment for dilution factor. Phosphate buffered saline (PBS), skim milk (SM), skim milk supplemented with 100 mM alanine (SMA) and tryptic soy broth (TSB) were used as the competition medium.

The mean MRSA CFU decreased during the timeseries for MRSA incubated alone (-99.5%) and with the spore mix (-98.6%) in PBS on vinyl at ambient humidity (Fig. 16). For the other types of media (SM, SMA, and TSB), the CFU increased between T0 and T24 (Table 4), then decreased, but remained elevated when comparing between T0 and T72 (Table 5). Only one timepoint, TSB at T72, had significantly different ($p=0.0152$) MRSA CFUs between MRSA incubated alone and MRSA with spores, with the CFU abundance of MRSA incubated alone being greater (Table 3).

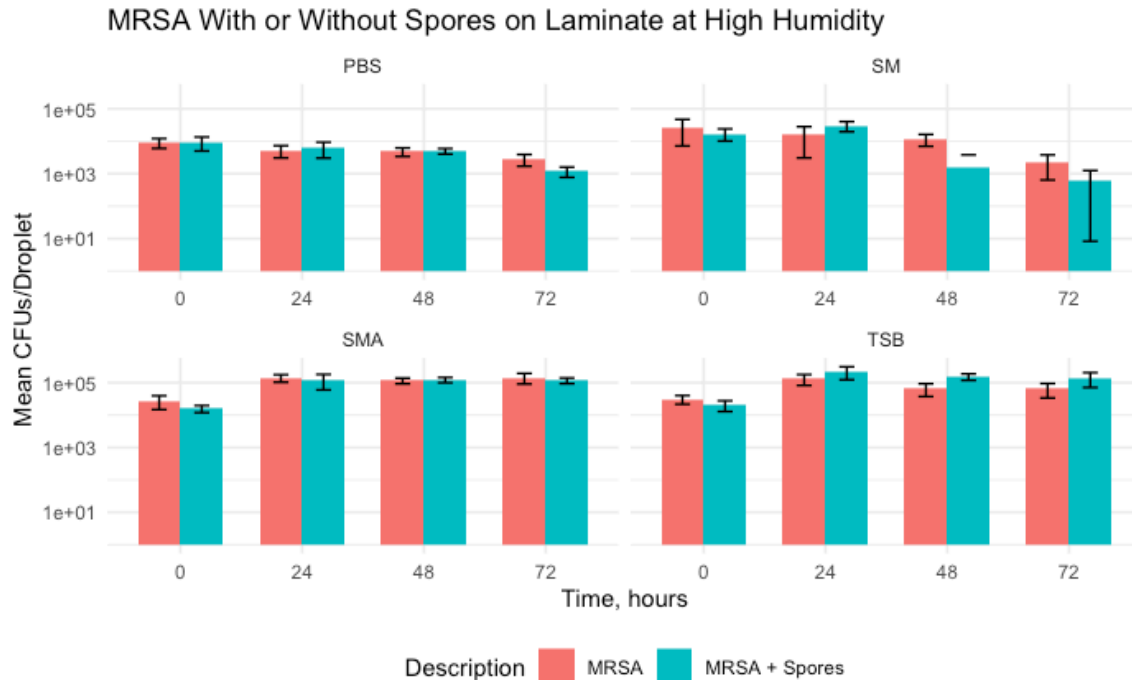


Figure 17. MRSA inhibition timeseries on laminate at high humidity. Mean number of MRSA CFUs in each type of media droplet, as determined via swabbing, dilution, plating, and CFU enumeration, and then adjustment for dilution factor. Phosphate buffered saline (PBS), skim milk (SM), skim milk supplemented with 100 mM alanine (SMA) and tryptic soy broth (TSB) were used as the competition medium.

MRSA CFUs on laminate at high humidity decreased over the course of the timeseries (Table 5) when incubated with or without spores in droplets of PBS and SM (Fig. 17). In SMA and TSB, there was an increase in MRSA CFUs between T0 and T24 (Table 4) for both MRSA by itself and with the spore mix. CFUs remained elevated through the rest of the timeseries (Table 5). Three timepoints for this set of conditions had significantly less ($p < 0.05$) MRSA CFUs in droplets with the spore mix, SMA T0, SM T48, PBS T72, and two timepoints where MRSA incubated by itself was lower than when incubated with the spore mix, TSB T48 and TSB T72 (Table 3).

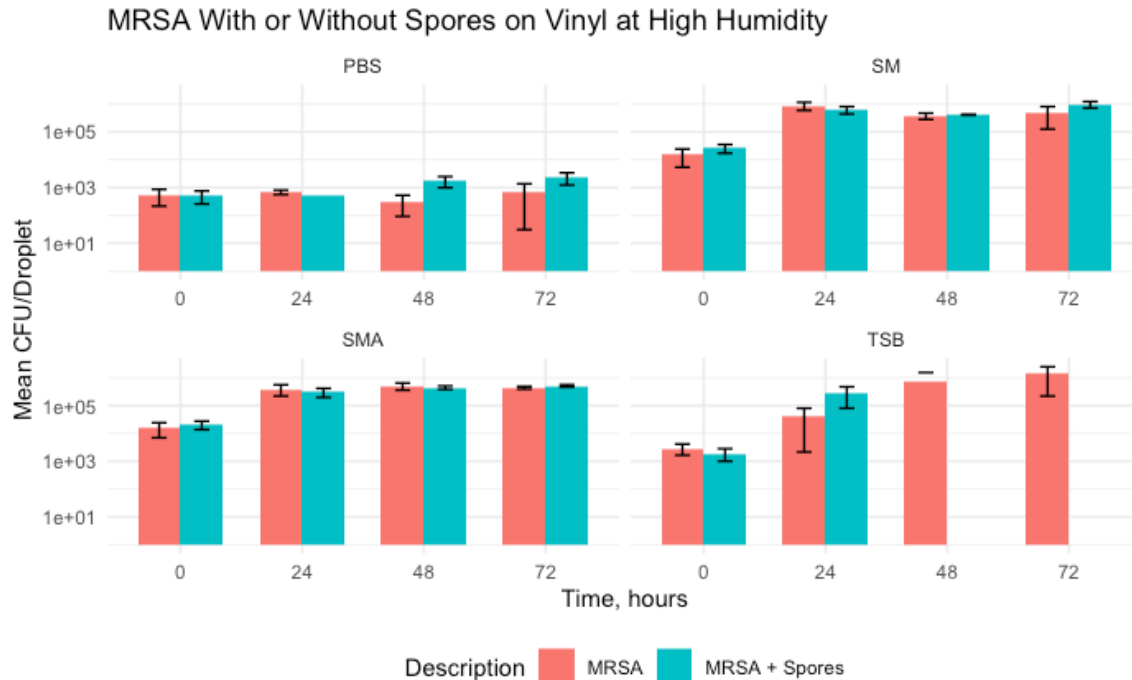


Figure 18. MRSA inhibition timeseries on vinyl at high humidity. Mean number of MRSA CFU in each type of media droplet, as determined via swabbing, dilution, plating, and CFU enumeration, and then adjustment for dilution factor. Phosphate buffered saline (PBS), skim milk (SM), skim milk supplemented with 100 mM alanine (SMA) and tryptic soy broth (TSB) were used as the competition medium.

There was a positive percentage change in the mean MRSA CFU for all 4 media types and spore absence/presence between T0/T24 (Table 4) and T0/T72 (Table 5) for droplets on vinyl at high humidity (Fig. 18). The mean MRSA CFU was significantly lower when MRSA was incubated in the absence of spores at five timepoints (SM T0, TSB T24, PBS T48, SM T72, SMA T72; $p < 0.05$; Table 3). Two timepoints, TSB T48 and TSB T72, are not displayed; the high density of colonies prevented accurately counting the CFUs.

Table 3. Mann-Whitney U test results at each timepoint, p < 0.05 only. Timepoints and incubation conditions (surface, humidity, and media type) where the mean CFU of MRSA incubated alone or in co-culture with the spore mix was significantly different (p < 0.05) using the Mann-Whitney test. Timepoints at which the MRSA co-cultured with the spore mix was significantly lower than MRSA incubated by itself are highlighted in green. Phosphate buffered saline (PBS), skim milk (SM), skim milk supplemented with 100 mM alanine (SMA) and tryptic soy broth (TSB) were used as the competition medium.

| Surface | Humidity | Timepoint, hours | Media | p value | U statistic |
|----------|----------|------------------|-------|---------|-------------|
| Vinyl | Ambient | 72 | TSY | 0.0152 | 3 |
| Laminate | High | 0 | SMA | 0.0411 | 31 |
| Laminate | High | 48 | SM | 0.0077 | 35 |
| Laminate | High | 48 | TSY | 0.0022 | 0 |
| Laminate | High | 72 | PBS | 0.0043 | 35 |
| Laminate | High | 72 | TSY | 0.0152 | 3 |
| Vinyl | High | 0 | SM | 0.0411 | 5 |
| Vinyl | High | 24 | TSY | 0.0200 | 3 |
| Vinyl | High | 48 | PBS | 0.0081 | 1 |
| Vinyl | High | 72 | SM | 0.0260 | 4 |
| Vinyl | High | 72 | SMA | 0.0411 | 5 |

Table 4. Percentage change in CFUs between T0 and T24. The change in the mean number of CFUs, after accounting for dilution factor, was calculated for each set of conditions, media, and presence/absence of spores in the droplets. Phosphate buffered saline (PBS), skim milk (SM), skim milk supplemented with 100 mM alanine (SMA) and tryptic soy broth (TSB) were used as the competition medium.

| Conditions | Media | Description | CFUs, T0 | CFUs, T24 | Change, % |
|-----------------------------------|-------|---------------|----------|-----------|-----------|
| Laminate, ambient humidity | PBS | MRSA | 13720.0 | 8916.7 | -35.0 |
| | PBS | MRSA + Spores | 17300.0 | 12883.3 | -25.5 |
| | SM | MRSA | 37660.0 | 11850.0 | -68.5 |
| | SM | MRSA + Spores | 29200.0 | 8533.3 | -70.8 |
| | SMA | MRSA | 44683.3 | 82000.0 | 83.5 |
| | SMA | MRSA + Spores | 36600.0 | 82300.0 | 124.9 |
| | TSY | MRSA | 20916.7 | 58033.3 | 177.5 |
| | TSY | MRSA + Spores | 25920.0 | 52250.0 | 101.6 |
| Vinyl, ambient humidity | PBS | MRSA | 9216.7 | 1271.7 | -86.2 |
| | PBS | MRSA + Spores | 6933.3 | 1193.3 | -82.8 |
| | SM | MRSA | 25350.0 | 340733.3 | 1244.1 |
| | SM | MRSA + Spores | 35233.3 | 331600.0 | 841.2 |
| | SMA | MRSA | 29050.0 | 220800.0 | 660.1 |
| | SMA | MRSA + Spores | 23966.7 | 183533.3 | 665.8 |
| | TSY | MRSA | 17033.3 | 113133.3 | 564.2 |
| | TSY | MRSA + Spores | 16500.0 | 226266.7 | 1271.3 |
| Laminate, high humidity | PBS | MRSA | 9083.3 | 5200.0 | -42.8 |
| | PBS | MRSA + Spores | 9266.7 | 6196.7 | -33.1 |
| | SM | MRSA | 27333.3 | 15633.3 | -42.8 |
| | SM | MRSA + Spores | 17183.3 | 30033.3 | 74.8 |
| | SMA | MRSA | 27083.3 | 139433.3 | 414.8 |
| | SMA | MRSA + Spores | 15783.3 | 119683.3 | 658.3 |
| | TSY | MRSA | 30750.0 | 129900.0 | 322.4 |
| | TSY | MRSA + Spores | 20216.7 | 216133.3 | 969.1 |
| Vinyl, high humidity | PBS | MRSA | 533.3 | 682.0 | 27.9 |
| | PBS | MRSA + Spores | 500.0 | 550.0 | 10.0 |
| | SM | MRSA | 14733.3 | 864666.7 | 5768.8 |
| | SM | MRSA + Spores | 25916.7 | 618466.7 | 2286.4 |
| | SMA | MRSA | 15600.0 | 390933.3 | 2406.0 |
| | SMA | MRSA + Spores | 20650.0 | 305266.7 | 1378.3 |
| | TSY | MRSA | 2900.0 | 41166.7 | 1319.5 |
| | TSY | MRSA + Spores | 1916.7 | 276500.0 | 14326.1 |

Table 5. Percentage change in CFUs between T0 and T72. The change in the mean number of CFUs, after accounting for dilution factor, was calculated for each set of conditions, media, and presence/absence of spores in the droplets. Phosphate buffered saline (PBS), skim milk (SM), skim milk supplemented with 100 mM alanine (SMA) and tryptic soy broth (TSB) were used as the competition medium.

| Conditions | Media | Description | CFUs, T0 | CFUs, T72 | Change, % |
|-----------------------------------|-------|---------------|-----------|-----------|-----------|
| Laminate, ambient humidity | PBS | MRSA | 13720.0 | 266.7 | -98.1 |
| | PBS | MRSA + Spores | 17300.0 | 650.0 | -96.2 |
| | SM | MRSA | 37660.0 | 0.0 | -100.0 |
| | SM | MRSA + Spores | 29200.0 | 200.0 | -99.3 |
| | SMA | MRSA | 44683.3 | 45750.0 | 2.4 |
| | SMA | MRSA + Spores | 36600.0 | 50700.0 | 38.5 |
| | TSY | MRSA | 20916.7 | 29883.3 | 42.9 |
| | TSY | MRSA + Spores | 25920.0 | 26583.3 | 2.6 |
| Vinyl, ambient humidity | PBS | MRSA | 9216.7 | 48.3 | -99.5 |
| | PBS | MRSA + Spores | 6933.3 | 96.7 | -98.6 |
| | SM | MRSA | 25350.0 | 119983.3 | 373.3 |
| | SM | MRSA + Spores | 35233.3 | 124100.0 | 252.2 |
| | SMA | MRSA | 29050.0 | 98133.3 | 237.8 |
| | SMA | MRSA + Spores | 23966.7 | 102066.7 | 325.9 |
| | TSY | MRSA | 17033.3 | 35566.7 | 108.8 |
| | TSY | MRSA + Spores | 16500.0 | 76450.0 | 363.3 |
| Laminate, high humidity | PBS | MRSA | 9083.3 | 2805.0 | -69.1 |
| | PBS | MRSA + Spores | 9266.7 | 1186.7 | -87.2 |
| | SM | MRSA | 27333.3 | 2216.7 | -91.9 |
| | SM | MRSA + Spores | 17183.3 | 633.3 | -96.3 |
| | SMA | MRSA | 27083.3 | 141533.3 | 422.6 |
| | SMA | MRSA + Spores | 15783.3 | 116400.0 | 637.5 |
| | TSY | MRSA | 30750.0 | 63833.3 | 107.6 |
| | TSY | MRSA + Spores | 20216.7 | 137066.7 | 578.0 |
| Vinyl, high humidity | PBS | MRSA | 533.3 | 695.0 | 30.3 |
| | PBS | MRSA + Spores | 500.0 | 2287.5 | 357.5 |
| | SM | MRSA | 14733.3 | 464533.3 | 3052.9 |
| | SM | MRSA + Spores | 25916.7 | 964266.7 | 3620.6 |
| | SMA | MRSA | 15600.0 | 438600.0 | 2711.5 |
| | SMA | MRSA + Spores | 20650.0 | 513200.0 | 2385.2 |
| | TSY | MRSA | 2900.0 | 1351166.7 | 46492.0 |
| | TSY | MRSA + Spores | 1916.6667 | NA | NA |

Table 6. Mean percentage change between MRSA abundance between start and end of timeseries. The percentage change in the MRSA CFUs was calculated based on each of the 4 variables in the experiment: humidity level, ambient or high; surface type, laminate or vinyl; type of media, phosphate buffered saline (PBS), skim milk (SM), skim milk with alanine (SMA), or tryptic soy broth (TSB); and the presence or absence of spores. Chi-squared and p-values are derived from Kruskal-Wallis test for significance.

| Variable | Condition | Mean % Change | StDev % Change | Chi-Squared | p-value |
|----------|---------------|---------------|----------------|-------------|----------|
| Humidity | Ambient | 196 | 889 | 29.118 | 6.81E-08 |
| | High | 5457 | 21041 | | |
| Surface | Laminate | 93 | 294 | 40.668 | 1.81E-10 |
| | Vinyl | 5632 | 21147 | | |
| Media | PBS | -28 | 171 | 55.303 | 5.92E-12 |
| | SM | 1076 | 2118 | | |
| | SMA | 1064 | 1576 | | |
| | TSB | 9672 | 30422 | | |
| Spores | MRSA | 4726 | 20450 | 0.023808 | 0.8774 |
| | MRSA + Spores | 610 | 1210 | | |

Discussion

Microbial based cleaning products are a new alternative to traditional cleaning methods of surfaces in the built environment (149–151). These products, typically composed of bacterial spores and chemical detergents, could either replace or supplement methods currently used for cleaning, especially in healthcare settings, where there is a risk of pathogen transmission to at-risk patients (152). In this study, we tested the impact of a five-strain spore mixture on the survival of MRSA on surfaces commonly used in hospital flooring, vinyl and laminate. While the 4 of the 5 different strains were shown to be able to kill MRSA in agar plates (Fig. 12), over the course of a three-day timeseries we found that the survival of MRSA was significantly decreased by a mix of the five spores in only a three timepoints, all of which were under 95% humidity (Table 3). Contrary to expectation, the *Bacillus* and *Priestia* spore treatment resulted in a significant increase in the abundance of MRSA at eight different time points.

On tryptic soy agar plates MRSA was inhibited by four of the 5 *Bacillus* and *Priestia* strains. This supports data from other studies, that have demonstrated that *B. subtilis* colonies

inhibit nearby *S. aureus* colonies, through the production of surfactin and plipastatin by *B. subtilis* (146). Inhibition by *B. subtilis* of *S. aureus* also appears to happen *in vivo* when *B. subtilis* spores are administered as probiotics to individuals colonized by *S. aureus* (79). However, in a 3rd study, a probiotic cleaner containing a mix of *Bacillus* species was tested on the pathogens *Acinetobacter baumannii* and *Klebsiella pneumoniae*, and it was determined that only the chemical components of the cleaner impacted the survival of the pathogens (102).

Using a Kruskal-Wallis test, the mean percentage change in abundance of MRSA between the start and end of the timeseries was calculated (Table 6). The impact of the humidity level, surface type, and media used were all highly significant ($p=6.81E-8$, $p=1.81E-10$, and $p=5.92E-12$, respectively). However, the presence or absence of the spore mix in the MRSA droplets did not have a significant impact ($p=0.8774$). This lack of impact does not align with the results of studies done in hospitals using MBCPs (21, 23, 24), but does mirror the findings of studies using humidity-controlled microcosms (102).

A wide range of survival times for *S. aureus* on surfaces has been reported (153). At one extreme, when inoculated onto a surface that contains silver and zinc ions, *S. aureus* abundance is reduced from 8.7×10^4 CFU to 1.5×10^2 CFU in just one hour, while the same number of CFU inoculated on stainless steel resulted in 4.2×10^4 CFU after one hour (154), and below the detection limit of 10 CFU after 24 hours. At the other extreme, MRSA in dried suspensions of PBS with hospital dust, incubated at ambient humidity and temperature resulted in survival times of ~318 days (155). In our study, the abundance of MRSA suspended in droplets of PBS or SM and then incubated at ambient humidity on laminate and vinyl surfaces was reduced by >95% after 3 days (Table 5). The presence/absence of the spore mix did not significantly increase or decrease MRSA survival under these conditions (Table 3). The size of the droplets used in this

study, 20 μ L, ensured that they had completely dried by the day after inoculation, and so the MRSA and spores experienced desiccation throughout the experiment, as might be expected in the real-world. Tolerance to desiccation is key to surviving the dry conditions typically found on surfaces in the built environment (41), although an improved tolerance is not required for MRSA epidemic outbreaks to occur (156). The availability of water will also impact how microbes interact with each other in the built environment (96). In a controlled laboratory study, built environment materials that were either wetted or left dry, then incubated at a high humidity, demonstrated how the availability of water leads to very different microbial successional dynamics and interactions (60). Although all materials used were incubated at the high humidity condition, materials that experienced the wetting event had far greater microbial abundance, but lower diversity, likely due to competition between microbes and the elimination of weaker competitors. Interestingly, the proportion of *Bacillus* spp. were almost always negatively correlated with *Pseudomonas* spp. on surfaces that experienced the wetting event, suggesting competitive exclusion.

Although our study did not demonstrate significant inhibition and competition between MRSA and the *Bacillus/Priestia* spores on laminate or vinyl, further investigation, using more varieties of surfaces, humidities, and pathogens would be required to conclusively demonstrate that the microbial component of MBCPs is active, and the inhibitory activity demonstrated on agar plates can be replicated under controlled, realistic conditions in the lab. Longer timescales, on the order of weeks or months may have led to a significant difference between the survival of MRSA with and without the spores. The ratio of spores to MRSA cells may also impact the survival of MRSA: it may be necessary to use much higher numbers of spores to effectively eliminate MRSA from the surface. Additionally, there may be negative interactions between the

strains in the spore mix, resulting in competition between the spore strains, instead of with MRSA.

Conclusion

MBCPs are cleaners that typically contain bacterial spores that exhibit antimicrobial activity against pathogens in controlled nutrient rich laboratory settings, e.g. on agar plates or in liquid media cultures. Laboratory based demonstration of the bactericidal activity of strains of *Bacillus* against pathogens have shown variable success on agar and in liquid media cultures. Similarly, studies using MBCPs conducted in healthcare settings, have also had variable success in reducing in pathogen abundance on surfaces. In our study, a four out of five strains of *Bacillus* and *Priestia* spp. could inhibit MRSA growth on agar culture plates but failed to reliably reduce the abundance or viability of MRSA on two surface materials commonly used in hospitals, laminate and vinyl.

Acknowledgements

Chapter 2, in part is currently being prepared for submission for publication of the material. Gottel, Neil; Hill, Megan S; Allard, Sarah M; Salas Garcia, Mariana; Gilbert, Jack A. The dissertation/thesis author was the primary investigator and author of this material.

Chapter 3 GERMINATION AND PATHOGEN INHIBITION BY 3D PRINTED STRUCTURES CONTAINING *BACILLUS SUBTILIS* SPORES

Abstract

Spores of bacteria, including *Bacillus subtilis*, are often included in commercial cleaning products, to potentially improve cleaning performance and suppress the emergence and persistence of pathogenic bacteria on building surfaces. But these cleaning products require continual application. Creating building materials in which the bacterial spores are embedded and able to potentially reproduce through periodic germination provides another mechanism by which to deliver microbial biocontrol into the built environment. Here we screened *B. subtilis* strains for their inhibitory activity against Methicillin-resistant *Staphylococcus aureus* in vitro and identified *B. subtilis* TH002 as having potent inhibitory activity against MRSA. Spores of this strain were mixed with Poly(ethylene glycol) diacrylate (PEGDA) 700 and then 3-D printed using blue light to crosslink the material at low temperatures to ensure continued bacterial viability. We tested the germination and antimicrobial activity of the printed spores in these materials. *Bacillus* spores were able to germinate and form colonies on solid agar plates and in liquid TSB media, however, while an overnight liquid culture of *Bacillus* can inhibit MRSA, the *Bacillus* spores printed into the material lacked the ability to form a zone of inhibition of a lawn of MRSA.

Introduction

3D printed materials have the potential to revolutionize how we construct the built environment that humans occupy for over 95% of their lives (157). Recently, researchers have begun to incorporate living organisms into these materials, including microorganisms (158–160). Microorganisms have been 3D printed into materials for a variety of functions, such as bioremediation (161), enhancing the future recycling of the material (162), or providing self-

repair of the material (163). Incorporating spore-forming species, such as *Bacillus subtilis*, in soft hydrogel materials has resulted in sustainable microbial viability and also biocontrol of known pathogens (85); however, the *Bacillus* used were genetically modified and the hydrogels are not suitable for use as high-touch surface materials. Spore-forming species have several advantages, such as their tolerance to temperatures experienced during printing (162), and resistance to desiccation, UV light, and physical disruption (164), which enables them to potentially persist for years within a given material (20). While it has been demonstrated that these spore forming *Bacillus* can persist and remain antibacterial against known pathogens in soft hydrogels, no research has been done to demonstrate that they can survive and remain active in hard materials such as plastics.

Microbial-based cleaning products (MBCPs) have recently been developed as products for use by the general public (165), and have been deployed in studies in healthcare settings (22, 23, 90, 109). However, these microbes may not make their way deeper into the surface to reach pathogens that are established in pores and surface microfractures, and may be inactivated by cleaning measures like those deployed during the COVID-19 pandemic (91). Materials that have already incorporated microbes with antimicrobial activity into their structure ensures that there are microbes both near the surface, and deeper in the structure, where they may lie dormant until activated by germinants or changes in the environment (166).

In this study, we printed spores of *Bacillus subtilis* into Poly(ethylene glycol) diacrylate (PEGDA) 700. PEGDA is a biocompatible polymer used in various biomedical and industrial applications. It consists of PEG chains with acrylate end groups, enabling it to form hard hydrogels through polymerization. PEGDA 700 is commonly used for tissue engineering, drug delivery, 3D printing, and creating non-adhesive surface coatings. Its properties can be tailored

by adjusting the PEG chain length and cross-linking density, making it a versatile material for developing advanced materials and devices. The germination of *Bacillus subtilis* spores from the surface of these spore-containing materials was investigated, along with the potential of these materials to inhibit methicillin-resistant *Staphylococcus aureus* (MRSA), a common hospital-acquired infection (HAI). We found that *Bacillus* can germinate from these materials on agar and in liquid media, but that its ability to inhibit MRSA growth was lost on solid media, and dependent on the starting inoculation concentration of MRSA in liquid media. This suggests that while these spore-containing materials may be valuable for controlling MRSA growth, they would only be viable in environments where they were exposed to liquids.

Methods

Microbial strains and inhibition testing. The MRSA strain, *S. aureus* subsp. *aureus* Rosenbach BAA-171728, was purchased from the American Type Culture Collection. 28 *B. subtilis* strains were obtained from the Bacillus Genetic Stock Center (Columbus, OH), isolated from a diverse global distribution of locations. Each of the *Bacillus subtilis* strains was tested for its ability to inhibit MRSA by placing 5 μ L droplets of each strain onto a tryptic soy agar (TSA) plate that had received 100 μ L of a 1:100 dilution of a MRSA culture grown in tryptic soy broth (TSB) at 37 °C. The plate was incubated overnight at 37 °C, then observed for the appearance of a zone of inhibition in the MRSA lawn around the *B. subtilis* colony. Strain TH002 was chosen for its strong inhibition of MRSA (Fig. 16E).

Spore production and purification. TH002 was streaked out from a frozen stock on tryptic soy agar (TSA) plates (Millipore Sigma # 105458), then a single colony picked and inoculated into 200 mL of Difco Sporulation Medium (DSM) (167). This culture was grown at 37 °C for three days with shaking at 180 RPM. The culture was aliquoted into four 50 mL

centrifuge tubes, centrifuged for 30 min at 4,000 x g and the supernatant discarded. Each pellet was resuspended in 40 mL of cold (4 °C) sterile distilled water, then centrifuged for 30 min at 4,000 x g and the supernatant removed and discarded. The washed pellets were resuspended in 40 mL of cold distilled water and stored at 4°C overnight. The next day, the spores were centrifuged 30 min at 4,000 x g and the supernatant removed and discarded. Pellets from each 50 mL tube were resuspended in cold sterile distilled water and combined to obtain a ~8 mL spore solution. To this suspension, 9 mL of a filter sterilized potassium phosphate buffer consisting of 1.76 M K₂HPO₄ and 1.24 M KH₂PO₄, and a second 13.6 mL solution of autoclaved 50% w/v polyethylene glycol (PEG) 4000 was added. Then, enough cold sterile distilled water was added to bring the total volume up to 40 mL (168).

The two-phase extraction solution was vortexed for 15 minutes using a 50 mL vortex adapter, then centrifuged at 100 x g for three minutes. The top organic phase, containing spores, was removed, diluted in ~500mL of deionized water, and pelleted by centrifugation at 4000 x g for 30 minutes. This was done by adding 1 mL each of extracted top phase to 50 mL tubes with 49 mL deionized water. After pelleting, the supernatant was removed. Pellets from each 50 mL were combined in 10 mL cold sterile water and transferred to a single 15 mL Falcon tube, then centrifuged at 4000 x g for 20 min. The pellet was washed three more times in 10 mL of cold sterile distilled water.

To obtain a high-purity spore solution, a final histodenz separation was used (169). The spore pellet was resuspended in 200 µL of a histodenz 20% w/v solution, then transferred to a 2 mL microcentrifuge tube containing 1.5 mL of histodenz 50% w/v. The two-layer histodenz solution was centrifuged at 8000 x g for 10 min. Spores move through the histodenz and form a pellet. After removing the histodenz, the purified spore pellet was resuspended in cold distilled

water and centrifuged at 8000 x g for 10 min three more times. The purity of the spore solution was confirmed via phase microscopy on an agarose pad (170) to visualize the bright oval spores and confirm the absence of dark rod-shaped vegetative cells.

After confirming purity, the spore solution was serially diluted and plated on TSA plates for CFU enumeration. Following enumeration (8.16×10^7 CFU/mL \pm 1.06×10^7 CFU/mL (mean \pm standard deviation), the spores were further diluted in a solution consisting of 25 % Poly(ethylene glycol) diacrylate (PEGDA) 700, 0.25 w/v% LAP (photoinitiator), 0.01 w/v% tartrazine (photoinhibitor/yellow food dye) for a final concentration of $\sim 2 \times 10^6$ spores/mL (171, 172). The spore/PEGDA/LAP mixture was printed as structures measuring 9 mm x 9 mm x 0.3 mm onto circular glass coverslips in a 24-well plate at a wavelength of 405 nm in a Bionova X 3D bioprinter (BICO Group, Gothenburg, Sweden), washed with PBS, then stored in 1 mL PBS at 4 °C until used in an assay. The printed surfaces have a volume of 0.0243 cm³, and a surface area of 0.918 cm². At $\sim 2,000,000$ spores per mL, it's expected that each printed structure contains $\sim 48,600$ spores. Structures of the same size but without spores were printed with the same method.

3D printed structure germination efficiency. All wells of a 24-well plate were filled with 900 μ L TSB (Fig. 19). Wells A1-A3, B1-B3, and C1-C3 received 100 μ L of PBS. 3D printed structures were placed in wells A1-A3 using sterile tweezers (Fig. 19B). 3D printed structures without spores were added to wells B1-B3 using sterile tweezers (Fig. 19C). Spores of *B. subtilis* strain TH002 stored in PBS at 4 °C were vigorously vortexed, then 100 μ L was transferred to a tube containing 900 μ L PBS (Fig. 19A). After vortexing for five seconds, this transfer was repeated until 5 tubes had solutions of increasingly diluted spores. These tubes were used to inoculate wells D1-D3 (tube 1), A4-A6 (tube 2), B4-B6 (tube 3), C4-C6 (tube 4), and

D4-D6 (tube 5). Tube 5 was also used to plate five 100 μ L aliquots on TSA plates for CFU enumeration. The plate was transferred to a SpectraMax iD5 plate reader (Molecular Devices, San Jose, CA) set to 37 $^{\circ}$ C. The OD600 of each well was measured every 5 minutes for 24 hours, with five seconds of shaking before each reading. After 24 hours, the output from the plate reader was analyzed along with the CFU counts of the TSA plates to determine the number of spores that germinated from the structures.

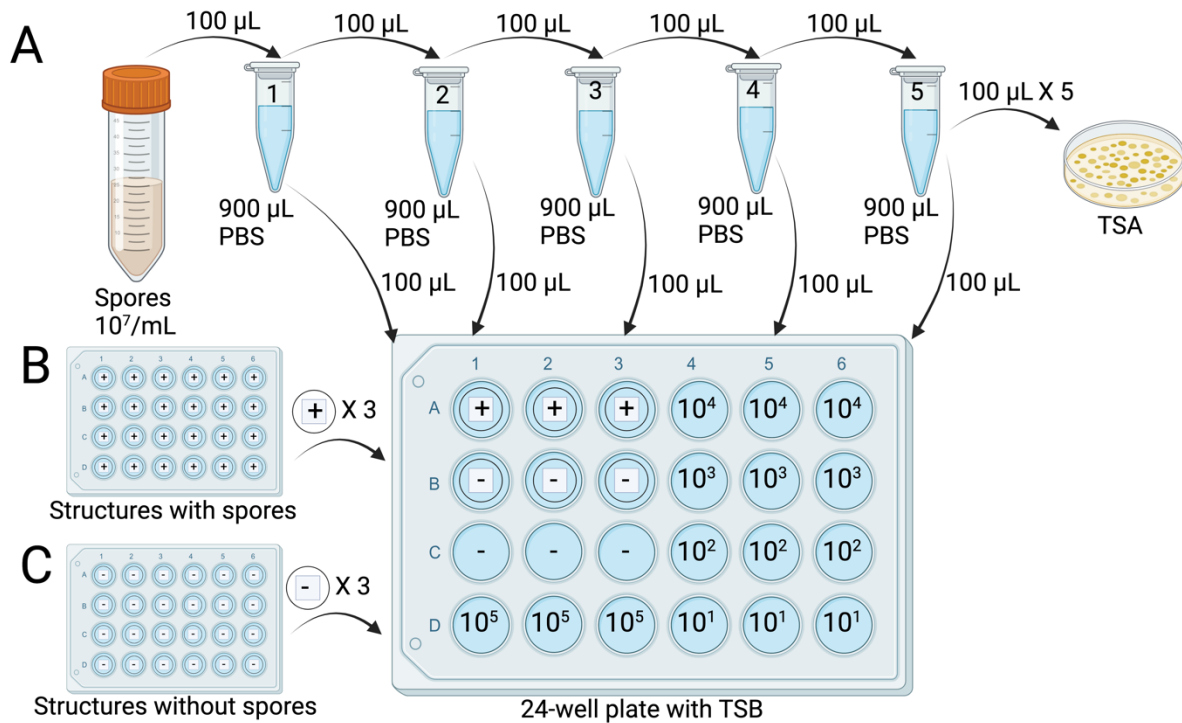


Figure 19. Test for germination efficiency of spores in 3D printed structures. A) Spores are serially diluted in phosphate buffered saline (PBS) and transferred in triplicate to a 24-well plate with tryptic soy broth (TSB). The last tube in the series is also used to inoculate five tryptic soy agar (TSA) plates. Wells C1-3 are not inoculated. B) Triplicate 3D printed structures with spores are transferred to wells A1-3. C) Triplicate 3D printed structures without spores are transferred to wells B1-3.

Data analysis of germination efficiency. The output from the plate reader and from the CFU counts was used to construct a standard curve, which was used to determine how many spores germinated from the 3D printed structures. The time at which each well of the plate reached an OD600 of 0.2 or greater was recorded. Combined with the CFU counts, the time at

OD600=0.2 and spore concentration of each well was plotted, and a line of best fit was applied to obtain a standard curve (Fig. 22) for each germination experiment. This standard curve was then used to calculate the number of spores that germinated from each structure by using the time at OD600=0.2 for wells A1-A3.

Germination of spores from structures and inhibition of MRSA on solid media. TSA plates with or without 4mg/L of methicillin, and with or without a lawn of MRSA, were made to test the germination of *B. subtilis* strain TH002 spores that were within a 3D printed structure. To each combination of testing conditions (TSA + no antibiotic, no MRSA; TSA + no antibiotic, MRSA; TSA+methicillin, no MRSA; and TSA+methicillin, MRSA), 3D printed structures with and without spores, and 5 μ L of an overnight TH002 culture, were placed on the plates. Plates were incubated overnight at 37 °C, then observed to determine whether growth occurred. Additionally, the plates that had a lawn of MRSA were checked for the presence of inhibition zones around the structures.

In addition to the structure testing, 5 μ L droplets of overnight growth of TH002 in TSB, along with 1:10 and 1:100 dilutions of the overnight growth, were placed on a TSA plate with a lawn of MRSA to detect whether a zone of inhibition was formed in the MRSA lawn.

Measuring inhibition of MRSA in liquid media

A pair of 24-well plates, one with 3D printed structures containing spores, the other without structures, was used to determine whether the 3D printed structures with spores would inhibit MRSA in liquid media. All wells of both plates received 900 μ L of TSB. An overnight culture of MRSA was serially diluted in PBS (Fig. 20A), then each tube was added in triplicate to both plates (Fig. 20B). 100 μ L of the sixth tube in the dilution series was plated in triplicate on TSA plates and incubated overnight at 37 °C for CFU enumeration the next day. The two plates

were incubated at 37 °C in a shaking incubator set to 120 rpm. The next day, the cultures of each 24-well plate were mixed via pipetting 5X with a P1000 multichannel pipet, then duplicate 100 μ L aliquots from wells A4-A6, B4-B6, C4-C6, and D1-D6 of both plates were serially diluted, plated, and incubated overnight at 37 °C. Plates with 10s to 100s of colonies were counted.

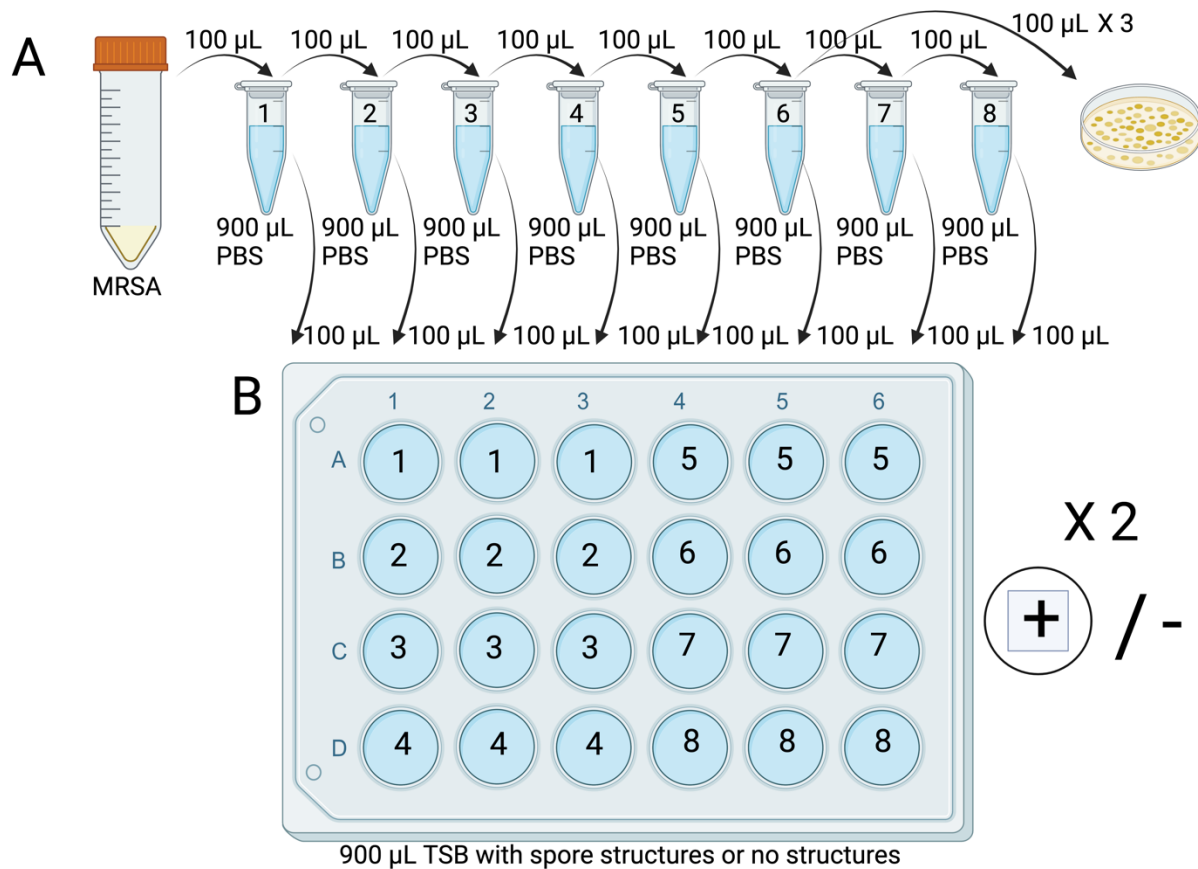


Figure 20. Setup of MRSA inhibition by 3D printed spore structures. Serial dilution, plating, and inoculation of plates containing spores with structures, or no structures. A) An overnight culture of MRSA was serially diluted in phosphate buffered saline (PBS). Tube 6 was plated in triplicate on tryptic soy agar (TSA) plates for CFU enumeration and used to calculate the starting inoculum per well. B) 100 μ L of each diluted culture was transferred in triplicate to two 24-well plates containing 900 μ L tryptic soy broth (TSB) in each well. The wells of one plate each contained 3D printed structures with spores; the wells of the other plate did not contain structures. Following incubation at 37 °C, 100 μ L aliquots of each well were diluted and plated on tryptic soy agar (TSA) plates supplemented with 4 mg/L methicillin for CFU enumeration.

Data analysis of MRSA inhibition by spore structures. Following CFU enumeration and accounting for the dilution factor of each plate, the technical replicates (2 per well) were averaged, then the mean and standard deviation of each well at each inoculation level was calculated and plotted. Welch's t-test was used to determine the significance of the differences between the MRSA CFU counts when testing the impact of the exposure to the 3D printed structures with spores.

Results

3D printed structures on solid media. 3D printed structures containing spores of *B. subtilis* strain TH002, or structures that were printed without spores, were placed on TSA plates and incubated overnight at 37 °C (Fig. 21A, B, C, D). Without methicillin, the spores germinated and grew outwards from the structure (Fig. 21A), while in the presence of methicillin the spores did not form a colony (Fig. 21B, D). When grown in the presence of MRSA without methicillin, the spores germinated and colonies grew, but no clear zone of inhibition in the lawn of MRSA was detected (Fig. 21C). The zone of inhibition suggests that TH002, does not actively kill MRSA, but instead locally inhibits its growth potentially through competition for resources. As a positive control, 5 uL TH002 grown overnight in TSB (S) did form a clear zone of inhibition in the MRSA in the absence of methicillin. Similarly, 5 µL droplets of TH002 grown undiluted overnight in TSB, and then diluted 1:10 or 1:100 in PBS all formed clear zones of inhibition on a lawn of MRSA (Fig. 21E). This suggests that the *Bacillus* spores do germinate from the 3D printed material but lost the ability to inhibit MRSA.

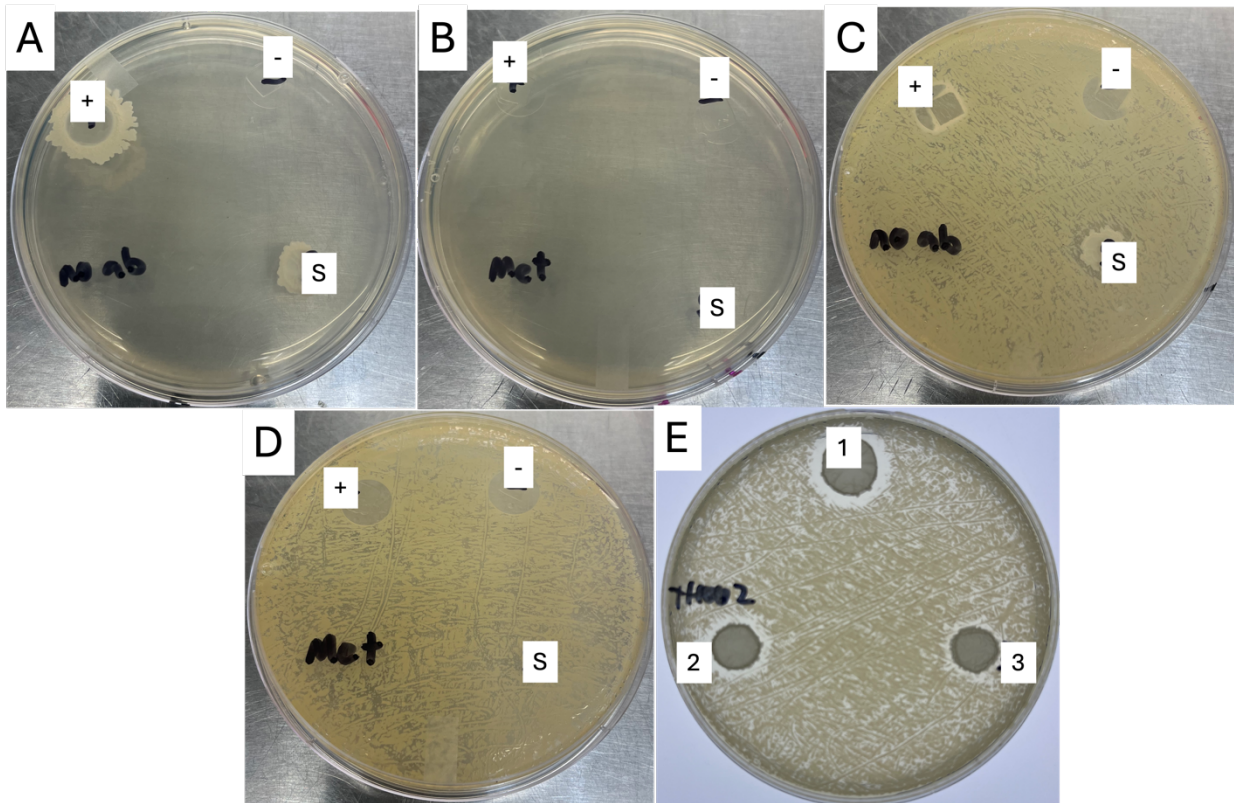


Figure 21. 3D printed structures on agar media. 3D printed structures containing *B. subtilis* TH002 spores (+) or structures without spores (-) were placed on tryptic soy agar (TSA) plates, along with a 5 μ L droplet of an overnight culture of TH002 (S). A) Structures and TH002 droplet on TSA plate. B) Structures and TH002 droplet on TSA plates with 4 mg/L methicillin. C) Structures and TH002 droplet on TSA plate with a lawn of MRSA. There is MRSA growth around the spore structure, but no zone of inhibition. D) Structures and TH002 droplet on TSA plate containing 4 mg/L methicillin on a lawn of MRSA. E) Droplets of an overnight culture of TH002, at either 1) undiluted, 2) 1:10 diluted in phosphate buffered saline (PBS), or 3) 1:100 diluted in PBS.

Germination of 3D printed structures in liquid media. Using the standard curves generated for each experiment (Fig. 22), and the time at which the media in the wells containing the 3D printed spore structures reached 0.2 at OD600, the number of spores that germinated from the structure was calculated (Table 7). Taken together, the four germination experiments showed that 9745 ± 3768 (mean \pm standard deviation) germinated from each structure when incubated in TSB at 37 $^{\circ}$ C with 5 seconds of shaking every 5 minutes over a minimum 9-hour time period.

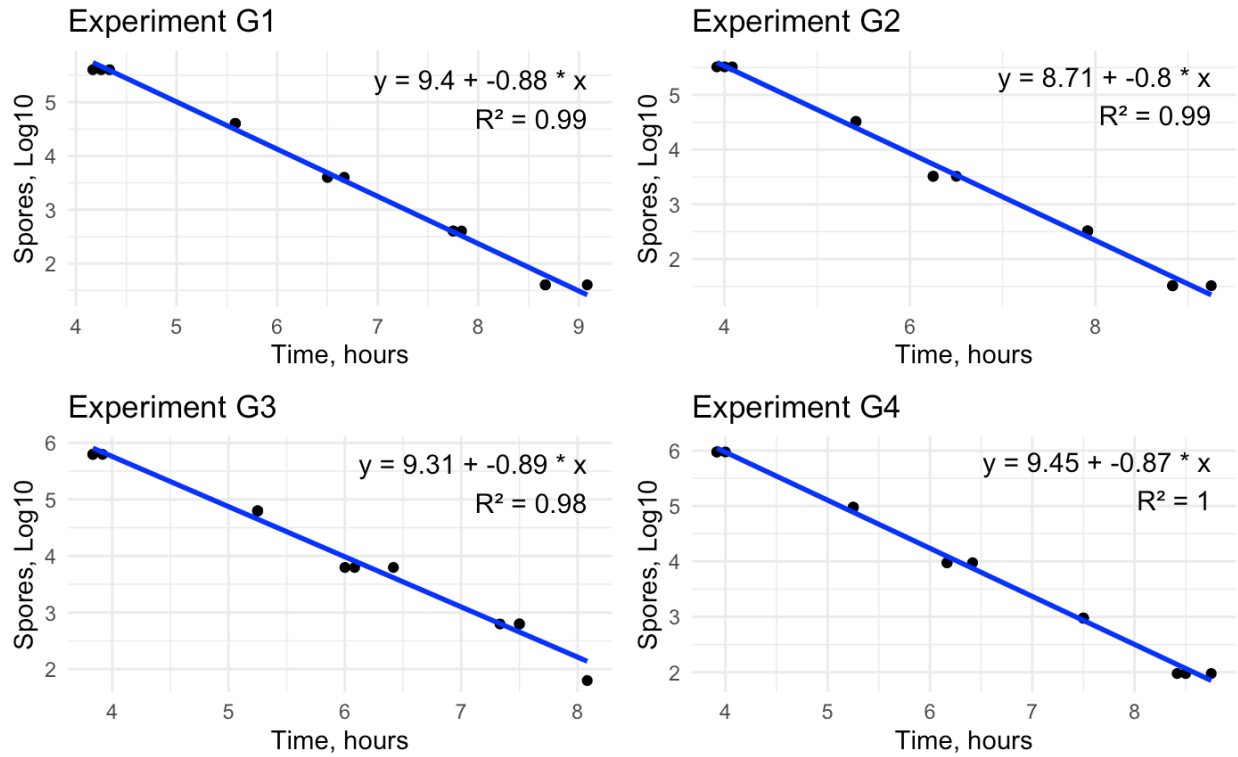


Figure 22. Standard curves for each germination experiment. Each panel shows the standard curve generated for each of the four replicate germination experiments, G1 thru G4, along with the equation for the line of best fit, and the R² value.

Table 7. Germinated spores per structure. Four germination experiments, G1 thru G4, were conducted using structures printed with *B. subtilis* strain TH002. Three replicates were used for each experiment, with the mean and standard deviation displayed for each individual experiment.

| | Germinated Spores per Structure | Mean | Standard Deviation |
|----------------|---------------------------------|-------|--------------------|
| G1 | 13389 | 9843 | 3070 |
| | 8071 | | |
| | 8071 | | |
| G2 | 6294 | 7391 | 1127 |
| | 7334 | | |
| | 8546 | | |
| G3 | 13588 | 8913 | 5095 |
| | 3482 | | |
| | 9668 | | |
| G4 | 12367 | 12832 | 4215 |
| | 17260 | | |
| | 8869 | | |
| All Structures | | 9745 | 3768 |

Inhibition of MRSA in liquid culture by spore structures

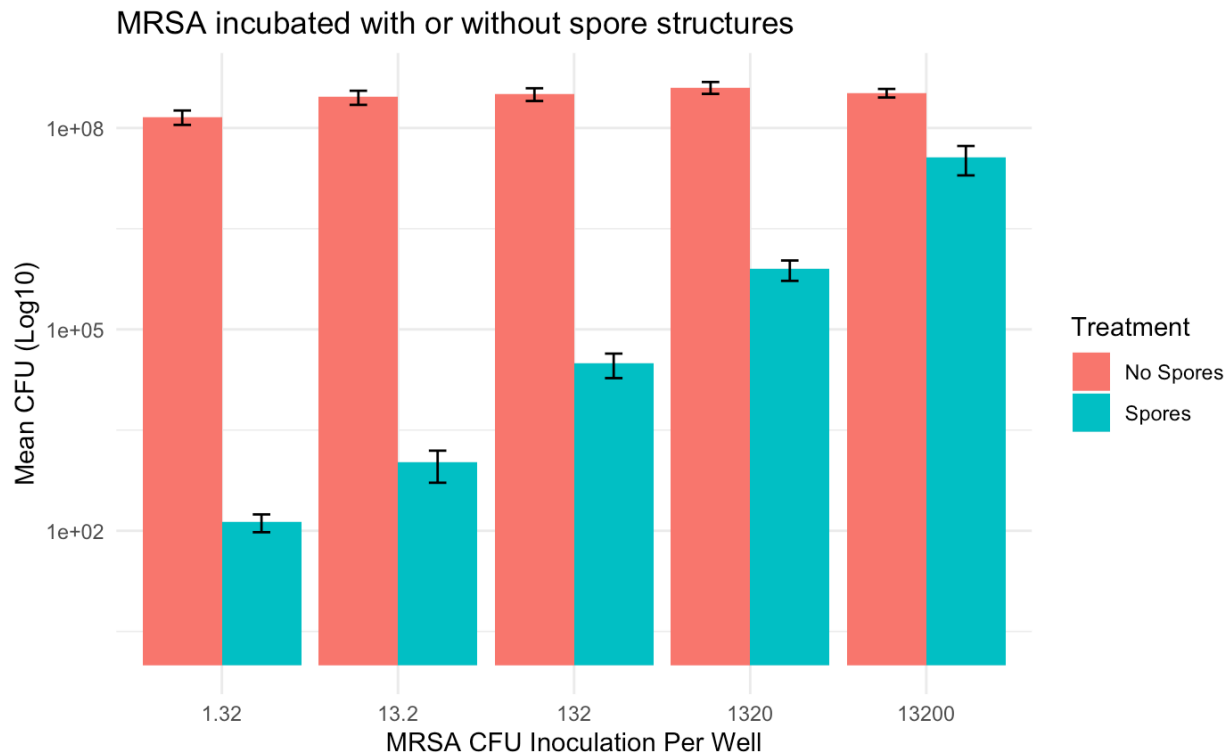


Figure 23. MRSA CFU per mL after 24 hours of incubation with or without 3D printed spore structures. Mean CFU in wells of a 24-well plate, with or without spore structures, which were inoculated with 900 μ L tryptic soy broth (TSB) and serial dilutions of MRSA in 100 μ L phosphate buffered saline (PBS).

Table 8. MRSA abundance per well, incubated overnight with or without spore structures. Dilution factor adjusted CFU counts for MRSA growth after 24-hour incubation with or without 3D printed structures with spores.

| Inoculation Per Well | Mean No Spores | Mean Spores | percent_reduction | t-statistic | p-value |
|----------------------|----------------|-------------|-------------------|-------------|----------|
| 1.32 | 146666667 | 135 | 99.99991 | -7.161332 | 0.002012 |
| 13.2 | 290000000 | 1040 | 99.99964 | -7.307287 | 0.001865 |
| 132 | 321666667 | 31167 | 99.99031 | -8.076016 | 0.001277 |
| 1320 | 403333333 | 795000 | 99.80289 | -8.625774 | 0.000993 |
| 13200 | 333333333 | 36816667 | 88.955 | -9.973030 | 0.000568 |

As the spore-structures were not able to inhibit MRSA on solid agar, we tested the potential of the structures to inhibit MRSA in liquid media. A dilution series of MRSA, comprising 10-fold dilutions from ~13,000 CFUs to ~1 CFU, was inoculated into wells of a 24-

well plate, with or without structures containing spores of TH002 (Fig. 23). The CFU abundance of MRSA after 24 hours of incubation at 37 °C was calculated. While the spore-structures did cause some inhibition of the MRSA growth, the level inhibition was correlated with the starting inoculation concentration of MRSA (Table 8). MRSA inoculated into wells without the spore structures resulted in approximately the same ending CFU abundance irrespective of starting inoculation concentration (Fig. 23).

Discussion

In this study, we printed spores of *B. subtilis* strain TH002, which was observed to inhibit MRSA growth, into small 3D structures of a common hard hydrogel material, Poly(ethylene glycol) diacrylate (PEGDA) 700. We then tested whether the spores remained viable and able to germinate from the material, and whether the spores retained their ability to inhibit the growth of MRSA following inclusion into these 3D printed PEGDA structures. We found that when placed on TSA plates, the spores would germinate and form extensive colonies. However, when these structures were placed on a lawn of MRSA, germination and growth would still occur, but it was limited to the area immediately around the structure and failed to inhibit MRSA growth. By contrast in liquid media, spore germination occurred and led to an MRSA-inoculant concentration dependent inhibition of the pathogen. One explanation for the contrast between the agar and liquid media observations is that each 3D printed PEGDA structure contains only a small number of spores (~48,600), which may not be sufficient to overcome an existing MRSA lawn on solid media but is sufficient to facilitate active growth and inhibition in a more favorable liquid media environment.

The germination of *Bacillus* spores from the 3D printed PEGDA materials in liquid media was considerable. Grown overnight in the right TSB media, an average of 9745 spores \pm 3768 (mean \pm standard deviation) would germinate and colonize the surrounding media. Given the size of the structure and number of spores contained within (~48,600), the growth suggests that ~20% of the spores germinated and became vegetative, which would further reduce the potential inhibitory effect of a particular PEGDA structure. The matrix created by the printing process is not an impermeable membrane (172), but is still thick enough to limit movement of vegetative cells buried deep in the structure, which may reduce the number of spores that can escape and germinate in either the solid or liquid medium. Additionally, since the structures are printed

directly onto a glass coverslip and are relatively thin (0.3 mm) compared to their width and length (9 mm x 9 mm), this means that many spores would be restricted in their movement, so the estimation of ~20% is likely an underestimate of germination and outgrowth. In rich media containing variable amounts of MRSA, the structures limit the growth of MRSA, but do not eliminate it completely, even when the starting concentration of MRSA is ~ 1 cell. On solid media growth occurs around the structure, but a zone of inhibition does not form (Fig. 21C), although inhibition does occur around the droplet. In contrast, patches of a 3D-printed hydrogel containing *B. subtilis* spores at an average concentration of 3.2×10^6 was found to eliminate MRSA when placed on an agar plate seeded with MRSA (85). However, this strain had been engineered to produce the antibiotics lysostaphin and thiocillin, suggesting that using wild-type strains in 3D-printed materials may not be sufficient to achieve the desired antimicrobial effect.

Conclusion

Light-based 3D printed PEGDA structures containing *B. subtilis* spores can be used to inhibit the growth of antibiotic-resistant pathogens such as MRSA in liquid media. When these structures are exposed to germinants, either in liquid or solid form, spores will germinate and grow out from the structure. However, only ~20% of the spores in a structure of PEGDA germinated, potentially because of being unable to reach the surface of the material to access the germinant. Additionally, while the germinating spores can inhibit MRSA growth in liquid media, they failed to inhibit or kill MRSA on solid media, potentially because of the small number of spores able to germinate. Future experiments must determine ways to enhance the ability of the spores in these structures to germinate when needed and to further inactivate or kill pathogens on surfaces more effectively.

Acknowledgements

Chapter 3, in part is currently being prepared for submission for publication of the material. Gottel, Neil; Hill, Megan S; Allard, Sarah M; Huang, Lin; Gilbert, Jack A. The dissertation/thesis author was the primary investigator and author of this material.

CONCLUSION

This dissertation has discussed the germination and antimicrobial potential of *Bacillus* spp. and *Priestia* sp. spores on surfaces used in hospitals and in 3D printed structures.

Preventing the spread of antibiotic-resistant pathogens like methicillin-resistant *Staphylococcus aureus* (MRSA) in hospitals is crucial to protecting the lives of patients and the safety of healthcare workers. Current cleaning techniques and technologies are important to combating the incidences of healthcare associated infections (HAIs), but infections still occur and are projected to cause increasingly more deaths in the future primarily driven by an increase in antibiotic resistance in bacteria. Therefore, there is a critical need for new approaches to combating the spread of these pathogens. Microbial based cleaning products (MBCPs) and 3D printed “living” structures which contain bacterial spores are promising new tools provide active microbial biocontrol of pathogen emergence and persistence in the built environment. However, we lack critical information needed to facilitate effective translation of these technologies. Understanding how spores in MBCPs and living materials germinate on built surfaces, how that germination is affected by temperature and humidity, and how effective the germinated spores are in inactivating known pathogens remain unanswered questions. In chapter 1, the effect of media, humidity, and physical surface type on the germination efficiency of *Bacillus* and *Priestia* spores was investigated. In chapter 2, the impact of media, humidity and surface type on the ability of germinated spores to inhibit MRSA was calculated. In chapter 3, the germination and inhibition of MRSA by spores actively printed into 3D structures was examined.

In hospitals, HAIs caused by pathogens like MRSA are typically spread by fomite transmission. Fomites that are highly porous, like fabrics and carpets, enhance the survival of microbes, and therefore relatively smooth surfaces that are easy to clean, such as laminate and vinyl, a more often used for hospital structures, like floors and high touch surfaces. However,

pathogens are still capable of remaining viable on these surfaces in between cleaning events, where they can later be transferred via touch to a susceptible patient. Studies have explored the potential MBCPs to reduce the persistence and viability of HAIs in hospitals, which have shown that pathogen load on surfaces cleaned using MBCPs is lower than those cleaned using standard cleaning products (chemical detergents and chlorine-based detergents). While these results are compelling, they have yet to be fully reproduced, and fundamental questions remain, such as the germination efficiency of the spores used in MBCPs, what factors influence the germination, and how these factors might influence the ability to control the persistence of pathogens in fomites.

Spores from the genera *Bacillus* and *Priestia* germinate in response to the presence and availability of specific nutrients, such as the amino acid L-alanine as well as the availability of free-water in an environment. In chapter 1, a mixture of *Bacillus* spp. and *Priestia* sp. spores suspended in small droplets of germination media were placed on vinyl and laminate, and then sampled over three days, to calculate the ratio of germinated spores to non-germinated spores. A low level of germination on vinyl and laminate surfaces was observed when using no nutrient and low nutrient mediums like phosphate buffered saline and skim milk. Supplementing skim milk with alanine, or using the rich media, tryptic soy broth, resulted in a strong germination response. Humidity and the type of surface, vinyl or laminate, had significant impacts on the germination rate, but only at specific time points, suggesting that these features may not be key drivers of germination efficiency. The availability of germinants for the spores contained in MBCPs should be considered when using these products, since germination may not be efficient on a surface that is an otherwise low nutrient environment, even if it is contaminated by a pathogen.

While studies have shown that deploying MBCPs in healthcare settings can reduce the abundance of known pathogens, few studies have examined how environmental features shape this response. In the laboratory environment, co-culturing microbial species on agar plates to observe zones of inhibition around nearby colonies is commonly used to determine whether one microbial species is antagonistic towards another. However, there is no guarantee that this inhibition will be replicated in other types of media, surfaces, and environmental conditions. As a result, just because a potential microbial biocontrol agent shows inhibitory activity against a pathogen in vitro, does not mean that this phenotype will be transferred to a hospital setting. Therefore, potential species for inclusion into MBCPs should be tested against pathogens under in vivo like conditions, such as on the surfaces they are expected to be used on and with humidities and nutrients that may be available in the hospital setting. In chapter 2, MRSA in droplets of germination media with or without *Bacillus* spp. and *Priestia* sp. spores were inoculated onto laminate and vinyl, at either ambient or elevated humidity, then samples over time. The colony forming units (CFUs) of MRSA were then quantified between the two treatments. While four out of five of the *Bacillus* spp. and *Priestia* sp. strains used in the spore mix formed zones of inhibition when co-cultured with MRSA on agar plates, they failed to significantly inhibit the survival of MRSA over the course of a three-day timeseries on vinyl or laminate surface materials. This observation was regardless of the surface type, humidity level, or type of germinant media used. This negative result for inhibition in droplets on laminate and vinyl demonstrates the importance of testing and validation of future MBCPs and their microbial constituents on the surfaces that they are intended to be used on. While the results of chapter 1 demonstrate that the spores in the spore mix will reliably germinate, especially in the presence of high levels of nutrients, they appear unable to significantly inhibit MRSA when deployed under

more realistic conditions. However, in this study only one ratio (one spore to one MRSA cell) was used, and it may be that a higher ratio of spores to MRSA cells would result in significant inhibition. Additionally, perhaps a combination of species could be more effective, or a longer experimental timeline may be required to result in pathogen inactivation. It is also possible that there may be a synergistic effect of using both spores and the chemical cleaners typically included in MBCPs that was not captured by the design of this study.

While deploying microbial biocontrol through cleaning products provides a readily accessible and versatile solution to applying these solutions into the built environment, creating ‘living’ surface materials that actively incorporate bacteria into their matrix has recently been explored. Spores of species like *Bacillus subtilis* are especially suitable for this application, since they are robust against stressors like heat, desiccation, and chemicals, that may be experienced during printing, and which would be lethal to vegetative cells. While spores should remain dormant into these materials, as they need a germinant and the right environmental conditions, they may activate during a water leak, food spill, or bodily fluid contamination event, that could provide sufficient nutrients and free water. In chapter 3, a strain of *B. subtilis* that inhibits MRSA on agar plates was printed into 3D PEGDA material, which forms a rigid hydrogel. The germination efficiency and ability to inhibit MRSA of the printed spore-materials was tested in both liquid media and on agar plates. Germination efficiency analysis suggested that only 20% of the spores in each structure were able to germinate in liquid media, which should be the most hospitable condition, suggesting that many of the spores likely remain trapped in the material matrix. Additionally, while there was partial inhibition of MRSA in a liquid culture exposed to the spore structure, the MRSA population was not eliminated, and the degree of inactivation was significantly correlated with the quantity of MRSA cells used to inoculate the liquid medium.

When only one MRSA cell was used as an inoculant, the spore-structure was able to inhibit MRSA growth by 6 orders of magnitude, but with an inoculum of ~10,000 MRSA cells, the spore structure inhibit MRSA growth by only a single order of magnitude. Importantly, when the spore structures were placed on an MRSA lawn on agar plates, the *Bacillus* did germinate and spread, but failed to develop a zone of inhibition. These results are in harmony with the conclusions of chapters 1 and 2, as while germination of spores may occur, it does not guarantee elimination of nearby pathogens.

The main takeaways of this dissertation are 1) the germination of spores on surfaces relevant to healthcare settings is dependent upon the availability of germinants, the type of surface, and the humidity; 2) no inhibition of MRSA on laminate and vinyl surfaces by the spores was observed regardless of the availability of germinant, humidity level, or surface type; and 3) spores contained within 3D printed structures can germinate and move out of the structure and display some inhibition of pathogens in liquid media, but they do not eliminate them completely.

REFERENCES

1. J. Blancou, History of disinfection from early times until the end of the 18th century. *Rev. Sci. Tech.* **14**, 21–39 (1995).
2. N. Kadar, Rediscovering Ignaz Philipp Semmelweis (1818-1865). *Am. J. Obstet. Gynecol.* **220**, 26–39 (2019).
3. H. A. Gilbert, Florence Nightingale’s Environmental Theory and its influence on contemporary infection control. *Collegian* **27**, 626–633 (2020).
4. M. Worboys, Joseph Lister and the performance of antiseptic surgery. *Notes Rec. R. Soc. Lond.* **67**, 199–209 (2013).
5. G. L. Armstrong, L. A. Conn, R. W. Pinner, Trends in infectious disease mortality in the United States during the 20th century. *JAMA* **281**, 61–66 (1999).

6. C. L. Ventola, The antibiotic resistance crisis: part 1: causes and threats. *P T* **40**, 277–283 (2015).
7. S. Mc Carlie, C. E. Boucher, R. R. Bragg, Molecular basis of bacterial disinfectant resistance. *Drug Resist. Updat.* **48**, 100672 (2020).
8. D. J. Weber, W. A. Rutala, D. J. Anderson, L. F. Chen, E. E. Sickbert-Bennett, J. M. Boyce, Effectiveness of ultraviolet devices and hydrogen peroxide systems for terminal room decontamination: Focus on clinical trials. *Am. J. Infect. Control* **44**, e77-84 (2016).
9. J. Czepiel, M. Drózdź, H. Pituch, E. J. Kuijper, W. Perucki, A. Mielimonka, S. Goldman, D. Wultańska, A. Garlicki, G. Biesiada, Clostridium difficile infection: review. *Eur. J. Clin. Microbiol. Infect. Dis.* **38**, 1211–1221 (2019).
10. R. Laxminarayan, The overlooked pandemic of antimicrobial resistance. *Lancet* **399**, 606–607 (2022).
11. L. Poirel, J.-Y. Madec, A. Lupo, A.-K. Schink, N. Kieffer, P. Nordmann, S. Schwarz, Antimicrobial Resistance in Escherichia coli. *Microbiol Spectr* **6** (2018).
12. C. Y. Effah, T. Sun, S. Liu, Y. Wu, Klebsiella pneumoniae: an increasing threat to public health. *Ann. Clin. Microbiol. Antimicrob.* **19**, 1 (2020).
13. C. Cillóniz, C. Garcia-Vidal, A. Ceccato, A. Torres, Antimicrobial Resistance Among Streptococcus pneumoniae. *Antimicrobial Resistance in the 21st Century*, 13 (2018).
14. R. Vázquez-López, S. G. Solano-Gálvez, J. J. Juárez Vignon-Whaley, J. A. Abello Vaamonde, L. A. Padró Alonzo, A. Rivera Reséndiz, M. Muleiro Álvarez, E. N. Vega López, G. Franyuti-Kelly, D. A. Álvarez-Hernández, V. Moncaleano Guzmán, J. E. Juárez Bañuelos, J. Marcos Felix, J. A. González Barrios, T. Barrientos Fortes, Acinetobacter baumannii Resistance: A Real Challenge for Clinicians. *Antibiotics (Basel)* **9** (2020).
15. C. J. L. Murray, K. S. Ikuta, F. Sharara, L. Swetschinski, G. Robles Aguilar, A. Gray, C. Han, C. Bisignano, P. Rao, E. Wool, S. C. Johnson, A. J. Browne, M. G. Chipeta, F. Fell, S. Hackett, G. Haines-Woodhouse, B. H. Kashef Hamadani, E. A. P. Kumaran, B. McManigal, R. Agarwal, S. Akech, S. Albertson, J. Amuasi, J. Andrews, A. Aravkin, E. Ashley, F. Bailey, S. Baker, B. Basnyat, A. Bekker, R. Bender, A. Bethou, J. Bielicki, S. Boonkasidecha, J. Bukosia, C. Carvalheiro, C. Castañeda-Orjuela, V. Chansamouth, S. Chaurasia, S. Chiurchiù, F. Chowdhury, A. J. Cook, B. Cooper, T. R. Cressey, E. Criollo-Mora, M. Cunningham, S. Darboe, N. P. J. Day, M. De Luca, K. Dokova, A. Dramowski, S. J. Dunachie, T. Eckmanns, D. Eibach, A. Emami, N. Feasey, N. Fisher-Pearson, K. Forrest, D. Garrett, P. Gastmeier, A. Z. Giref, R. C. Greer, V. Gupta, S. Haller, A. Haselbeck, S. I. Hay, M. Holm, S. Hopkins, K. C. Iregbu, J. Jacobs, D. Jarovsky, F. Javanmardi, M. Khorana, N. Kisoona, E. Kobeissi, T. Kostyanov, F. Krapp, R. Krumkamp, A. Kumar, H. H. Kyu, C. Lim, D. Limmathurotsakul, M. J. Loftus, M. Lunn, J. Ma, N. Mturi, T. Munera-Huertas, P. Musicha, M. M. Mussi-Pinhata, T. Nakamura, R. Nanavati, S. Nangia, P. Newton, C. Ngoun, A. Novotney, D. Nwakanma, C. W. Obiero, A. Olivas-Martinez, P. Olliaro, E. Ooko, E. Ortiz-Brizuela, A. Y. Peleg, C. Perrone, N. Plakkal, A. Ponce-de-Leon,

- M. Raad, T. Ramdin, A. Riddell, T. Roberts, J. V. Robotham, A. Roca, K. E. Rudd, N. Russell, J. Schnall, J. A. G. Scott, M. Shivamallappa, J. Sifuentes-Osornio, N. Steenkeste, A. J. Stewardson, T. Stoeva, N. Tasak, A. Thaiprakong, G. Thwaites, C. Turner, P. Turner, H. R. van Doorn, S. Velaphi, A. Vongpradith, H. Vu, T. Walsh, S. Waner, T. Wangrangsimaikul, T. Wozniak, P. Zheng, B. Sartorius, A. D. Lopez, A. Stergachis, C. Moore, C. Dolecek, M. Naghavi, Global burden of bacterial antimicrobial resistance in 2019: a systematic analysis. *Lancet* **399**, 629–655 (2022).
16. U. N. Environment, Bracing for Superbugs: Strengthening environmental action in the One Health response to antimicrobial resistance, *UNEP - UN Environment Programme* (2023). <https://www.unep.org/resources/superbugs/environmental-action>.
 17. F. Prestinaci, P. Pezzotti, A. Pantosti, Antimicrobial resistance: a global multifaceted phenomenon. *Pathog. Glob. Health* **109**, 309–318 (2015).
 18. J. Jeżewska-Frańkowiak, J. Żebrowska, E. Czajkowska, J. Jasińska, M. Pęksa, G. Jędrzejczak, P. M. Skowron, Identification of bacterial species in probiotic consortiums in selected commercial cleaning preparations. *Acta Biochim. Pol.* **66**, 215–222 (2019).
 19. C. Tran, I. E. Cock, X. Chen, Y. Feng, Antimicrobial Bacillus: Metabolites and Their Mode of Action. *Antibiotics (Basel)* **11** (2022).
 20. N. Ulrich, K. Nagler, M. Laue, C. S. Cockell, P. Setlow, R. Moeller, Experimental studies addressing the longevity of Bacillus subtilis spores - The first data from a 500-year experiment. *PLoS One* **13**, e0208425 (2018).
 21. A. Vandini, R. Temmerman, A. Frabetti, E. Caselli, P. Antonioli, P. G. Balboni, D. Platano, A. Branchini, S. Mazzacane, Hard surface biocontrol in hospitals using microbial-based cleaning products. *PLoS One* **9**, e108598 (2014).
 22. E. Caselli, S. Brusaferrero, M. Coccagna, L. Arnoldo, F. Berloco, P. Antonioli, R. Tarricone, G. Pelissero, S. Nola, V. La Fauci, A. Conte, L. Tognon, G. Villone, N. Trua, S. Mazzacane, SAN-ICA Study Group, Reducing healthcare-associated infections incidence by a probiotic-based sanitation system: A multicentre, prospective, intervention study. *PLoS One* **13**, e0199616 (2018).
 23. M. D’Accolti, I. Soffritti, F. Bini, E. Mazziga, S. Mazzacane, E. Caselli, Pathogen Control in the Built Environment: A Probiotic-Based System as a Remedy for the Spread of Antibiotic Resistance. *Microorganisms* **10** (2022).
 24. M. D’Accolti, I. Soffritti, F. Bini, E. Mazziga, L. Arnoldo, A. Volta, M. Bisi, P. Antonioli, P. Laurenti, W. Ricciardi, S. Vincenti, S. Mazzacane, E. Caselli, Potential Use of a Combined Bacteriophage-Probiotic Sanitation System to Control Microbial Contamination and AMR in Healthcare Settings: A Pre-Post Intervention Study. *Int. J. Mol. Sci.* **24** (2023).
 25. S. Lax, N. Sangwan, D. Smith, P. Larsen, K. M. Handley, M. Richardson, K. Guyton, M. Krezalek, B. D. Shogan, J. Defazio, I. Flemming, B. Shakhsher, S. Weber, E. Landon, S.

- Garcia-Houchins, J. Siegel, J. Alverdy, R. Knight, B. Stephens, J. A. Gilbert, Bacterial colonization and succession in a newly opened hospital. *Sci. Transl. Med.* **9** (2017).
26. T. E. Klassert, R. Leistner, C. Zubiria-Barrera, M. Stock, M. López, R. Neubert, D. Driesch, P. Gastmeier, H. Slevogt, Bacterial colonization dynamics and antibiotic resistance gene dissemination in the hospital environment after first patient occupancy: a longitudinal metagenetic study. *Microbiome* **9**, 169 (2021).
 27. J. Chopyk, K. Akrami, T. Bavly, J. H. Shin, L. K. Schwanemann, M. Ly, R. Kalia, Y. Xu, S. T. Kelley, A. Malhotra, F. J. Torriani, D. A. Sweeney, D. T. Pride, Temporal variations in bacterial community diversity and composition throughout intensive care unit renovations. *Microbiome* **8**, 86 (2020).
 28. B. Hickman, P. V. Kirjavainen, M. Täubel, W. M. de Vos, A. Salonen, K. Korpela, Determinants of bacterial and fungal microbiota in Finnish home dust: Impact of environmental biodiversity, pets, and occupants. *Front. Microbiol.* **13**, 1011521 (2022).
 29. H. Niculita-Hirzel, P. Wild, A. H. Hirzel, Season, Vegetation Proximity and Building Age Shape the Indoor Fungal Communities' Composition at City-Scale. *J Fungi (Basel)* **8** (2022).
 30. E. L. F. Estensmo, L. Morgado, S. Maurice, P. M. Martin-Sanchez, I. B. Engh, J. Mattsson, H. Kausrud, I. Skrede, Spatiotemporal variation of the indoor mycobiome in daycare centers. *Microbiome* **9**, 220 (2021).
 31. V. A. C. de Abreu, J. Perdigão, S. Almeida, Metagenomic Approaches to Analyze Antimicrobial Resistance: An Overview. *Front. Genet.* **11**, 575592 (2020).
 32. L. S. Zaramela, M. Tjuanta, O. Moyne, M. Neal, K. Zengler, synDNA-a Synthetic DNA Spike-in Method for Absolute Quantification of Shotgun Metagenomic Sequencing. *mSystems* **7**, e0044722 (2022).
 33. C. Ferreira, S. Otani, F. M. Aarestrup, C. M. Manaia, Quantitative PCR versus metagenomics for monitoring antibiotic resistance genes: balancing high sensitivity and broad coverage. *FEMS Microbes* **4**, xtad008 (2023).
 34. A. Abramova, T. U. Berendonk, J. Bengtsson-Palme, A global baseline for qPCR-determined antimicrobial resistance gene prevalence across environments. *Environ. Int.* **178**, 108084 (2023).
 35. Y. Liu, Y. Cao, T. Wang, Q. Dong, J. Li, C. Niu, Detection of 12 Common Food-Borne Bacterial Pathogens by TaqMan Real-Time PCR Using a Single Set of Reaction Conditions. *Front. Microbiol.* **10**, 222 (2019).
 36. C. A. Kapon, J. T. Morton, A. Bouslimani, A. V. Melnik, K. Orlinsky, T. L. Knaan, N. Garg, Y. Vázquez-Baeza, I. Protsyuk, S. Janssen, Q. Zhu, T. Alexandrov, L. Smarr, R. Knight, P. C. Dorrestein, Creating a 3D microbial and chemical snapshot of a human habitat. *Sci. Rep.* **8**, 3669 (2018).

37. M. Wang, J. J. Carver, V. V. Phelan, L. M. Sanchez, N. Garg, Y. Peng, D. D. Nguyen, J. Watrous, C. A. Kapon, T. Luzzatto-Knaan, C. Porto, A. Bouslimani, A. V. Melnik, M. J. Meehan, W.-T. Liu, M. Crüsemann, P. D. Boudreau, E. Esquenazi, M. Sandoval-Calderón, R. D. Kersten, L. A. Pace, R. A. Quinn, K. R. Duncan, C.-C. Hsu, D. J. Floros, R. G. Gavilan, K. Kleigrew, T. Northen, R. J. Dutton, D. Parrot, E. E. Carlson, B. Aigle, C. F. Michelsen, L. Jelsbak, C. Sohlenkamp, P. Pevzner, A. Edlund, J. McLean, J. Piel, B. T. Murphy, L. Gerwick, C.-C. Liaw, Y.-L. Yang, H.-U. Humpf, M. Maansson, R. A. Keyzers, A. C. Sims, A. R. Johnson, A. M. Sidebottom, B. E. Sedio, A. Klitgaard, C. B. Larson, C. A. B. P, D. Torres-Mendoza, D. J. Gonzalez, D. B. Silva, L. M. Marques, D. P. Demarque, E. Pociute, E. C. O’Neill, E. Briand, E. J. N. Helfrich, E. A. Granatosky, E. Glukhov, F. Ryffel, H. Houson, H. Mohimani, J. J. Kharbush, Y. Zeng, J. A. Vorholt, K. L. Kurita, P. Charusanti, K. L. McPhail, K. F. Nielsen, L. Vuong, M. Elfeki, M. F. Traxler, N. Engene, N. Koyama, O. B. Vining, R. Baric, R. R. Silva, S. J. Mascuch, S. Tomasi, S. Jenkins, V. Macherla, T. Hoffman, V. Agarwal, P. G. Williams, J. Dai, R. Neupane, J. Gurr, A. M. C. Rodríguez, A. Lamsa, C. Zhang, K. Dorrestein, B. M. Duggan, J. Almaliti, P.-M. Allard, P. Phapale, L.-F. Nothias, T. Alexandrov, M. Litaudon, J.-L. Wolfender, J. E. Kyle, T. O. Metz, T. Peryea, D.-T. Nguyen, D. VanLeer, P. Shinn, A. Jadhav, R. Müller, K. M. Waters, W. Shi, X. Liu, L. Zhang, R. Knight, P. R. Jensen, B. O. Palsson, K. Pogliano, R. G. Lington, M. Gutiérrez, N. P. Lopes, W. H. Gerwick, B. S. Moore, P. C. Dorrestein, N. Bandeira, Sharing and community curation of mass spectrometry data with Global Natural Products Social Molecular Networking. *Nat. Biotechnol.* **34**, 828–837 (2016).
38. L.-F. Nothias, D. Petras, R. Schmid, K. Dührkop, J. Rainer, A. Sarvepalli, I. Protsyuk, M. Ernst, H. Tsugawa, M. Fleischauer, F. Aicheler, A. A. Aksenov, O. Alka, P.-M. Allard, A. Barsch, X. Cachet, A. M. Caraballo-Rodríguez, R. R. Da Silva, T. Dang, N. Garg, J. M. Gauglitz, A. Gurevich, G. Isaac, A. K. Jarmusch, Z. Kamenik, K. B. Kang, N. Kessler, I. Koester, A. Korf, A. Le Gouellec, M. Ludwig, C. Martin H, L.-I. McCall, J. McSayles, S. W. Meyer, H. Mohimani, M. Morsy, O. Moyne, S. Neumann, H. Neuweger, N. H. Nguyen, M. Nothias-Esposito, J. Paolini, V. V. Phelan, T. Pluskal, R. A. Quinn, S. Rogers, B. Shrestha, A. Tripathi, J. J. J. van der Hooft, F. Vargas, K. C. Weldon, M. Witting, H. Yang, Z. Zhang, F. Zubeil, O. Kohlbacher, S. Böcker, T. Alexandrov, N. Bandeira, M. Wang, P. C. Dorrestein, Feature-based molecular networking in the GNPS analysis environment. *Nat. Methods* **17**, 905–908 (2020).
39. J. Shen, A. G. McFarland, R. A. Blaustein, L. J. Rose, K. A. Perry-Dow, A. A. Moghadam, M. K. Hayden, V. B. Young, E. M. Hartmann, An improved workflow for accurate and robust healthcare environmental surveillance using metagenomics. *Microbiome* **10**, 206 (2022).
40. J. J. Minich, Q. Zhu, S. Janssen, R. Hendrickson, A. Amir, R. Vetter, J. Hyde, M. M. Doty, K. Stillwell, J. Benardini, J. H. Kim, E. E. Allen, K. Venkateswaran, R. Knight, KatharoSeq Enables High-Throughput Microbiome Analysis from Low-Biomass Samples. *mSystems* **3** (2018).
41. S. M. Gibbons, The Built Environment Is a Microbial Wasteland, *mSystems*. **1** (2016). <https://doi.org/10.1128/mSystems.00033-16>.

42. C. Coughenour, V. Stevens, L. D. Stetzenbach, An evaluation of methicillin-resistant *Staphylococcus aureus* survival on five environmental surfaces. *Microb. Drug Resist.* **17**, 457–461 (2011).
43. A. J. Hoisington, C. E. Stamper, K. L. Bates, M. A. Stanislawski, M. C. Flux, T. T. Postolache, C. A. Lowry, L. A. Brenner, Human microbiome transfer in the built environment differs based on occupants, objects, and buildings. *Sci. Rep.* **13**, 6446 (2023).
44. H. Li, S.-Y.-D. Zhou, R. Neilson, X.-L. An, J.-Q. Su, Skin microbiota interact with microbes on office surfaces. *Environ. Int.* **168**, 107493 (2022).
45. J. Chase, J. Fouquier, M. Zare, D. L. Sonderegger, R. Knight, S. T. Kelley, J. Siegel, J. G. Caporaso, Geography and Location Are the Primary Drivers of Office Microbiome Composition. *mSystems* **1** (2016).
46. H. Amin, T. Šantl-Temkiv, C. Cramer, K. Finster, F. G. Real, T. Gislason, M. Holm, C. Janson, N. O. Jögi, R. Jogi, A. Malinovschi, I. P. G. Marshall, L. Modig, D. Norbäck, R. Shigdel, T. Sigsgaard, C. Svanes, H. Thorarinsdottir, I. M. Wouters, V. Schlünssen, R. J. Bertelsen, Indoor Airborne Microbiome and Endotoxin: Meteorological Events and Occupant Characteristics Are Important Determinants. *Environ. Sci. Technol.* **57**, 11750–11766 (2023).
47. Z. Wang, K. R. Dalton, M. Lee, C. G. Parks, L. E. Beane Freeman, Q. Zhu, A. González, R. Knight, S. Zhao, A. A. Motsinger-Reif, S. J. London, Metagenomics reveals novel microbial signatures of farm exposures in house dust. *Front. Microbiol.* **14**, 1202194 (2023).
48. M. Richardson, N. Gottel, J. A. Gilbert, J. Gordon, P. Gandhi, R. Reboulet, J. T. Hampton-Marcell, Concurrent measurement of microbiome and allergens in the air of bedrooms of allergy disease patients in the Chicago area. *Microbiome* **7**, 82 (2019).
49. C. K. Carstens, J. K. Salazar, S. V. Sharma, W. Chan, C. Darkoh, Evaluation of the kitchen microbiome and food safety behaviors of predominantly low-income families. *Front. Microbiol.* **13**, 987925 (2022).
50. M. H. Y. Leung, X. Tong, K. O. Boïfot, D. Bezdan, D. J. Butler, D. C. Danko, J. Gohli, D. C. Green, M. T. Hernandez, F. J. Kelly, S. Levy, G. Mason-Buck, M. Nieto-Caballero, D. Syndercombe-Court, K. Udekwu, B. G. Young, C. E. Mason, M. Dybwad, P. K. H. Lee, Characterization of the public transit air microbiome and resistome reveals geographical specificity. *Microbiome* **9**, 112 (2021).
51. R. B. Guevarra, J. Hwang, H. Lee, H. J. Kim, Y. Lee, D. Danko, K. A. Ryon, B. G. Young, C. E. Mason, S. Jang, Metagenomic characterization of bacterial community and antibiotic resistance genes found in the mass transit system in Seoul, South Korea. *Ecotoxicol. Environ. Saf.* **246**, 114176 (2022).
52. K. R. Chng, C. Li, D. Bertrand, A. H. Q. Ng, J. S. Kwah, H. M. Low, C. Tong, M. Natrajan, M. H. Zhang, L. Xu, K. K. Ko, E. X. P. Ho, T. V. Av-Shalom, J. W. P. Teo, C. C. Khor,

- MetaSUB Consortium, S. L. Chen, C. E. Mason, O. T. Ng, K. Marimuthu, B. Ang, N. Nagarajan, Cartography of opportunistic pathogens and antibiotic resistance genes in a tertiary hospital environment. *Nat. Med.* **26**, 941–951 (2020).
53. A. T. Köhler, A. C. Rodloff, M. Labahn, M. Reinhardt, U. Truyen, S. Speck, Evaluation of disinfectant efficacy against multidrug-resistant bacteria: A comprehensive analysis of different methods. *Am. J. Infect. Control* **47**, 1181–1187 (2019).
 54. A. Mahnert, C. Moissl-Eichinger, G. Berg, Microbiome interplay: plants alter microbial abundance and diversity within the built environment. *Front. Microbiol.* **6**, 887 (2015).
 55. S. W. Kembel, E. Jones, J. Kline, D. Northcutt, J. Stenson, A. M. Womack, B. J. Bohannon, G. Z. Brown, J. L. Green, Architectural design influences the diversity and structure of the built environment microbiome. *ISME J.* **6**, 1469–1479 (2012).
 56. R. R. Dunn, N. Fierer, J. B. Henley, J. W. Leff, H. L. Menninger, Home life: factors structuring the bacterial diversity found within and between homes. *PLoS One* **8**, e64133 (2013).
 57. R. I. Adams, A. C. Bateman, H. M. Bik, J. F. Meadow, Microbiota of the indoor environment: a meta-analysis. *Microbiome* **3**, 49 (2015).
 58. A. Checinska, A. J. Probst, P. Vaishampayan, J. R. White, D. Kumar, V. G. Stepanov, G. E. Fox, H. R. Nilsson, D. L. Pierson, J. Perry, K. Venkateswaran, Microbiomes of the dust particles collected from the International Space Station and Spacecraft Assembly Facilities. *Microbiome* **3**, 50 (2015).
 59. S. Lax, D. P. Smith, J. Hampton-Marcell, S. M. Owens, K. M. Handley, N. M. Scott, S. M. Gibbons, P. Larsen, B. D. Shogan, S. Weiss, J. L. Metcalf, L. K. Ursell, Y. Vázquez-Baeza, W. Van Treuren, N. A. Hasan, M. K. Gibson, R. Colwell, G. Dantas, R. Knight, J. A. Gilbert, Longitudinal analysis of microbial interaction between humans and the indoor environment. *Science* **345**, 1048–1052 (2014).
 60. S. Lax, C. Cardona, D. Zhao, V. J. Winton, G. Goodney, P. Gao, N. Gottel, E. M. Hartmann, C. Henry, P. M. Thomas, S. T. Kelley, B. Stephens, J. A. Gilbert, Microbial and metabolic succession on common building materials under high humidity conditions. *Nat. Commun.* **10**, 1767 (2019).
 61. S. M. Gibbons, T. Schwartz, J. Fouquier, M. Mitchell, N. Sangwan, J. A. Gilbert, S. T. Kelley, Ecological succession and viability of human-associated microbiota on restroom surfaces. *Appl. Environ. Microbiol.* **81**, 765–773 (2015).
 62. L. S. Zaramela, O. Moyne, M. Kumar, C. Zuniga, J. D. Tibocho-Bonilla, K. Zengler, The sum is greater than the parts: exploiting microbial communities to achieve complex functions. *Curr. Opin. Biotechnol.* **67**, 149–157 (2021).

63. A. Passi, J. D. Tibocho-Bonilla, M. Kumar, D. Tec-Campos, K. Zengler, C. Zuniga, Genome-Scale Metabolic Modeling Enables In-Depth Understanding of Big Data. *Metabolites* **12** (2021).
64. I. Thiele, B. Ø. Palsson, A protocol for generating a high-quality genome-scale metabolic reconstruction. *Nat. Protoc.* **5**, 93–121 (2010).
65. C. Zuñiga, L. Zaramela, K. Zengler, Elucidation of complexity and prediction of interactions in microbial communities. *Microb. Biotechnol.* **10**, 1500–1522 (2017).
66. C. Zuñiga, C.-T. Li, G. Yu, M. M. Al-Bassam, T. Li, L. Jiang, L. S. Zaramela, M. Guarnieri, M. J. Betenbaugh, K. Zengler, Environmental stimuli drive a transition from cooperation to competition in synthetic phototrophic communities. *Nat Microbiol* **4**, 2184–2191 (2019).
67. M. K. Kim, D. S. Lun, Methods for integration of transcriptomic data in genome-scale metabolic models. *Comput. Struct. Biotechnol. J.* **11**, 59–65 (2014).
68. R. K. Kumar, N. K. Singh, S. Balakrishnan, C. W. Parker, K. Raman, K. Venkateswaran, Metabolic modeling of the International Space Station microbiome reveals key microbial interactions. *Microbiome* **10**, 102 (2022).
69. J. Qian, D. Hospodsky, N. Yamamoto, W. W. Nazaroff, J. Peccia, Size-resolved emission rates of airborne bacteria and fungi in an occupied classroom. *Indoor Air* **22**, 339–351 (2012).
70. W. G. D. Fernando, R. Ramarathnam, A. S. Krishnamoorthy, S. C. Savchuk, Identification and use of potential bacterial organic antifungal volatiles in biocontrol. *Soil Biol. Biochem.* **37**, 955–964 (2005).
71. N. Khan, P. Martínez-Hidalgo, T. A. Ice, M. Maymon, E. A. Humm, N. Nejat, E. R. Sanders, D. Kaplan, A. M. Hirsch, Antifungal Activity of Bacillus Species Against Fusarium and Analysis of the Potential Mechanisms Used in Biocontrol. *Front. Microbiol.* **9**, 2363 (2018).
72. J. P. Baptista, G. M. Teixeira, M. L. A. de Jesus, R. Bertê, A. Higashi, M. Mosela, D. V. da Silva, J. P. de Oliveira, D. S. Sanches, J. D. Brancher, M. I. Balbi-Peña, U. de Padua Pereira, A. G. de Oliveira, Antifungal activity and genomic characterization of the biocontrol agent Bacillus velezensis CMRP 4489. *Sci. Rep.* **12**, 17401 (2022).
73. R. I. Adams, D. S. Lymperopoulou, P. K. Misztal, R. De Cassia Pessotti, S. W. Behie, Y. Tian, A. H. Goldstein, S. E. Lindow, W. W. Nazaroff, J. W. Taylor, M. F. Traxler, T. D. Bruns, Microbes and associated soluble and volatile chemicals on periodically wet household surfaces. *Microbiome* **5**, 128 (2017).
74. D. Fira, I. Dimkić, T. Berić, J. Lozo, S. Stanković, Biological control of plant pathogens by Bacillus species. *J. Biotechnol.* **285**, 44–55 (2018).

75. R. Lahlali, S. Ezrari, N. Radouane, J. Kenfaoui, Q. Esmaeel, H. El Hamss, Z. Belabess, E. A. Barka, Biological Control of Plant Pathogens: A Global Perspective. *Microorganisms* **10** (2022).
76. W. Adi Wicaksono, T. Reisenhofer-Graber, S. Erschen, P. Kusstatscher, C. Berg, R. Krause, T. Cernava, G. Berg, Phyllosphere-associated microbiota in built environment: Do they have the potential to antagonize human pathogens? *J. Advert. Res.* **43**, 109–121 (2023).
77. A. K. Saxena, M. Kumar, H. Chakdar, N. Anuroopa, D. J. Bagyaraj, Bacillus species in soil as a natural resource for plant health and nutrition. *J. Appl. Microbiol.* **128**, 1583–1594 (2020).
78. J.-M. Liu, Y.-T. Liang, S.-S. Wang, N. Jin, J. Sun, C. Lu, Y.-F. Sun, S.-Y. Li, B. Fan, F.-Z. Wang, Antimicrobial activity and comparative metabolomic analysis of *Priestia megaterium* strains derived from potato and dendrobium. *Sci. Rep.* **13**, 5272 (2023).
79. P. Piewngam, S. Khongthong, N. Roekngam, Y. Theapparatt, S. Sunpaweravong, D. Faroongsarnng, M. Otto, Probiotic for pathogen-specific *Staphylococcus aureus* decolonisation in Thailand: a phase 2, double-blind, randomised, placebo-controlled trial. *Lancet Microbe* **4**, e75–e83 (2023).
80. J. Gagnaire, P. O. Verhoeven, F. Grattard, J. Rigai, F. Lucht, B. Pozzetto, P. Berthelot, E. Botelho-Nevers, Epidemiology and clinical relevance of *Staphylococcus aureus* intestinal carriage: a systematic review and meta-analysis. *Expert Rev. Anti. Infect. Ther.* **15**, 767–785 (2017).
81. L. Senn, O. Clerc, G. Zanetti, P. Basset, G. Prod'hom, N. C. Gordon, A. E. Sheppard, D. W. Crook, R. James, H. A. Thorpe, E. J. Feil, D. S. Blanc, The Stealthy Superbug: the Role of Asymptomatic Enteric Carriage in Maintaining a Long-Term Hospital Outbreak of ST228 Methicillin-Resistant *Staphylococcus aureus*. *MBio* **7**, e02039-15 (2016).
82. J. R. Price, M. Yokoyama, K. Cole, J. Sweetman, L. Behar, S. Stoneham, D. Cantillon, S. J. Waddell, J. Hyde, R. Alam, D. Crook, J. Paul, M. J. Llewelyn, Undetected carriage explains apparent *Staphylococcus aureus* acquisition in a non-outbreak healthcare setting. *J. Infect.* **83**, 332–338 (2021).
83. P. Setlow, Germination of spores of *Bacillus* species: what we know and do not know. *J. Bacteriol.* **196**, 1297–1305 (2014).
84. E. Caselli, M. D'Accolti, A. Vandini, L. Lanzoni, M. T. Camerada, M. Coccagna, A. Branchini, P. Antonioli, P. G. Balboni, D. D. Luca, S. Mazzacane, Impact of a Probiotic-Based Cleaning Intervention on the Microbiota Ecosystem of the Hospital Surfaces: Focus on the Resistome Remodulation. *PLoS One* **11**, e0148857 (2016).
85. L. M. González, N. Mukhitov, C. A. Voigt, Resilient living materials built by printing bacterial spores. *Nat. Chem. Biol.* **16**, 126–133 (2020).

86. M. Nodehi, T. Ozbakkaloglu, A. Gholampour, A systematic review of bacteria-based self-healing concrete: Biomineralization, mechanical, and durability properties. *Journal of Building Engineering* **49**, 104038 (2022).
87. E. Birch, B. Bridgens, M. Zhang, M. Dade-Robertson, Bacterial Spore-Based Hygromorphs: A Novel Active Material with Potential for Architectural Applications. *Sustain. Sci. Pract. Policy* **13**, 4030 (2021).
88. S. Lax, C. R. Nagler, J. A. Gilbert, Our interface with the built environment: immunity and the indoor microbiota. *Trends Immunol.* **36**, 121–123 (2015).
89. S. Lax, J. A. Gilbert, Hospital-associated microbiota and implications for nosocomial infections. *Trends Mol. Med.* **21**, 427–432 (2015).
90. M. D’Accolti, I. Soffritti, L. Lanzoni, M. Bisi, A. Volta, S. Mazzacane, E. Caselli, Effective elimination of Staphylococcal contamination from hospital surfaces by a bacteriophage-probiotic sanitation strategy: a monocentric study. *Microb. Biotechnol.* **12**, 742–751 (2019).
91. I. Soffritti, M. D’Accolti, C. Cason, L. Lanzoni, M. Bisi, A. Volta, G. Campisciano, S. Mazzacane, F. Bini, E. Mazziga, P. Toscani, E. Caselli, M. Comar, Introduction of Probiotic-Based Sanitation in the Emergency Ward of a Children’s Hospital During the COVID-19 Pandemic. *Infect. Drug Resist.* **15**, 1399–1410 (2022).
92. A. K. Fahimipour, E. M. Hartmann, A. Siemens, J. Kline, D. A. Levin, H. Wilson, C. M. Betancourt-Román, G. Z. Brown, M. Fretz, D. Northcutt, K. N. Siemens, C. Huttenhower, J. L. Green, K. Van Den Wymelenberg, Daylight exposure modulates bacterial communities associated with household dust. *Microbiome* **6**, 175 (2018).
93. G. R. Young, A. Sherry, D. L. Smith, Built environment microbiomes transition from outdoor to human-associated communities after construction and commissioning. *Sci. Rep.* **13**, 15854 (2023).
94. S. Li, Z. Yang, D. Hu, L. Cao, Q. He, Understanding building-occupant-microbiome interactions toward healthy built environments: A review. *Front. Environ. Sci. Eng. China* **15**, 65 (2021).
95. M. Kokubo, S. Fujiyoshi, D. Ogura, M. Nakajima, A. Fujieda, J. Noda, F. Maruyama, Relationship between the Microbiome and Indoor Temperature/Humidity in a Traditional Japanese House with a Thatched Roof in Kyoto, Japan. *Diversity* **13**, 475 (2021).
96. J. A. Gilbert, B. Stephens, Microbiology of the built environment. *Nat. Rev. Microbiol.* **16**, 661–670 (2018).
97. T. Islam, M. F. Rabbee, J. Choi, K.-H. Baek, Biosynthesis, Molecular Regulation, and Application of Bacilysin Produced by Bacillus Species. *Metabolites* **12** (2022).

98. W. Stone, J. Tolmay, K. Tucker, G. M. Wolfaardt, Disinfectant, Soap or Probiotic Cleaning? Surface Microbiome Diversity and Biofilm Competitive Exclusion. *Microorganisms* **8** (2020).
99. J. Kramer, Ö. Özkaya, R. Kümmerli, Bacterial siderophores in community and host interactions. *Nat. Rev. Microbiol.*, 1–12 (2019).
100. K. T. Schiessl, E. M.-L. Janssen, S. M. Kraemer, K. McNeill, M. Ackermann, Magnitude and Mechanism of Siderophore-Mediated Competition at Low Iron Solubility in the *Pseudomonas aeruginosa* Pyochelin System. *Front. Microbiol.* **8**, 1964 (2017).
101. G. T. Rocha, P. R. M. Queiroz, P. Grynberg, R. C. Togawa, A. D. C. de Lima Ferreira, I. N. do Nascimento, A. C. M. M. Gomes, R. Monnerat, Biocontrol potential of bacteria belonging to the *Bacillus subtilis* group against pests and diseases of agricultural interest through genome exploration. *Antonie Van Leeuwenhoek* **116**, 599–614 (2023).
102. J. Hu, W. Shuai, J. T. Sumner, A. A. Moghadam, E. M. Hartmann, Clinically relevant pathogens on surfaces display differences in survival and transcriptomic response in relation to probiotic and traditional cleaning strategies. *NPJ Biofilms Microbiomes* **8**, 72 (2022).
103. G. Christie, P. Setlow, *Bacillus* spore germination: Knowns, unknowns and what we need to learn. *Cell. Signal.* **74**, 109729 (2020).
104. E. A. Dertz, J. Xu, A. Stintzi, K. N. Raymond, Bacillibactin-mediated iron transport in *Bacillus subtilis*. *J. Am. Chem. Soc.* **128**, 22–23 (2006).
105. X. Chen, Y. Lu, M. Shan, H. Zhao, Z. Lu, Y. Lu, A mini-review: mechanism of antimicrobial action and application of surfactin. *World J. Microbiol. Biotechnol.* **38**, 143 (2022).
106. Q. Gu, Y. Yang, Q. Yuan, G. Shi, L. Wu, Z. Lou, R. Huo, H. Wu, R. Borriss, X. Gao, Bacillomycin D Produced by *Bacillus amyloliquefaciens* Is Involved in the Antagonistic Interaction with the Plant-Pathogenic Fungus *Fusarium graminearum*. *Appl. Environ. Microbiol.* **83** (2017).
107. L. Zhang, C. Sun, Fengycins, Cyclic Lipopeptides from Marine *Bacillus subtilis* Strains, Kill the Plant-Pathogenic Fungus *Magnaporthe grisea* by Inducing Reactive Oxygen Species Production and Chromatin Condensation. *Appl. Environ. Microbiol.* **84** (2018).
108. R. Beckett, Probiotic design. *J. Archit.* **26**, 6–31 (2021).
109. E. Caselli, L. Arnoldo, C. Rognoni, M. D’Accolti, I. Soffritti, L. Lanzoni, M. Bisi, A. Volta, R. Tarricone, S. Brusaferrò, S. Mazzacane, Impact of a probiotic-based hospital sanitation on antimicrobial resistance and HAI-associated antimicrobial consumption and costs: a multicenter study. *Infect. Drug Resist.* **12**, 501–510 (2019).

110. M. D'Accolti, I. Soffritti, S. Mazzacane, E. Caselli, Fighting AMR in the Healthcare Environment: Microbiome-Based Sanitation Approaches and Monitoring Tools. *Int. J. Mol. Sci.* **20** (2019).
111. E. Caselli, M. D'Accolti, I. Soffritti, L. Lanzoni, M. Bisi, A. Volta, F. Berloco, S. Mazzacane, "An Innovative Strategy for the Effective Reduction of MDR Pathogens from the Nosocomial Environment" in *Advances in Microbiology, Infectious Diseases and Public Health: Volume 13*, G. Donelli, Ed. (Springer International Publishing, Cham, 2019), pp. 79–91.
112. B. Hota, Contamination, disinfection, and cross-colonization: are hospital surfaces reservoirs for nosocomial infection? *Clin. Infect. Dis.* **39**, 1182–1189 (2004).
113. S. J. Dancer, Importance of the environment in meticillin-resistant *Staphylococcus aureus* acquisition: the case for hospital cleaning. *Lancet Infect. Dis.* **8**, 101–113 (2008).
114. S. J. Dancer, The role of environmental cleaning in the control of hospital-acquired infection. *J. Hosp. Infect.* **73**, 378–385 (2009).
115. A. E. Aiello, E. Larson, Antibacterial cleaning and hygiene products as an emerging risk factor for antibiotic resistance in the community. *Lancet Infect. Dis.* **3**, 501–506 (2003).
116. G. Rosenberg, N. Steinberg, Y. Oppenheimer-Shaanan, T. Olender, S. Doron, J. Ben-Ari, A. Sirota-Madi, Z. Bloom-Ackermann, I. Kolodkin-Gal, Not so simple, not so subtle: the interspecies competition between *Bacillus simplex* and *Bacillus subtilis* and its impact on the evolution of biofilms. *NPJ Biofilms Microbiomes* **2**, 15027 (2016).
117. A. Soni, I. Oey, P. Silcock, P. Bremer, *Bacillus* spores in the food industry: A review on resistance and response to novel inactivation technologies: *Bacillus* spores in response to technologies.... *Compr. Rev. Food Sci. Food Saf.* **15**, 1139–1148 (2016).
118. A. I. Delbrück, Y. Zhang, R. Heydenreich, A. Mathys, *Bacillus* spore germination at moderate high pressure: A review on underlying mechanisms, influencing factors, and its comparison with nutrient germination. *Compr. Rev. Food Sci. Food Saf.* **20**, 4159–4181 (2021).
119. A. Soni, I. Oey, P. Silcock, P. J. Bremer, Impact of temperature, nutrients, pH and cold storage on the germination, growth and resistance of *Bacillus cereus* spores in egg white. *Food Res. Int.* **106**, 394–403 (2018).
120. Y. Zhang, A. Mathys, Superdormant spores as a hurdle for gentle germination-inactivation based spore control strategies. *Front. Microbiol.* **9**, 3163 (2018).
121. S. Ghosh, M. Scotland, P. Setlow, Levels of germination proteins in dormant and superdormant spores of *Bacillus subtilis*. *J. Bacteriol.* **194**, 2221–2227 (2012).
122. Y. Lequette, E. Garénaux, G. Tauveron, S. Dumez, S. Perchat, C. Slomianny, D. Lereclus, Y. Guérardel, C. Faille, Role played by exosporium glycoproteins in the surface

- properties of *Bacillus cereus* spores and in their adhesion to stainless steel. *Appl. Environ. Microbiol.* **77**, 4905–4911 (2011).
123. C. Faille, C. Jullien, F. Fontaine, M.-N. Bellon-Fontaine, C. Slomianny, T. Benezech, Adhesion of *Bacillus* spores and *Escherichia coli* cells to inert surfaces: role of surface hydrophobicity. *Can. J. Microbiol.* **48**, 728–738 (2002).
 124. U. Rönner, U. Husmark, A. Henriksson, Adhesion of bacillus spores in relation to hydrophobicity. *J. Appl. Bacteriol.* **69**, 550–556 (1990).
 125. H. J. Busscher, A. H. Weerkamp, Specific and non-specific interactions in bacterial adhesion to solid substrata. *FEMS Microbiol. Lett.* **46**, 165–173 (1987).
 126. B. Dréno, T. Zuberbier, C. Gelmetti, G. Gontijo, M. Marinovich, Safety review of phenoxyethanol when used as a preservative in cosmetics. *J. Eur. Acad. Dermatol. Venereol.* **33 Suppl 7**, 15–24 (2019).
 127. I. Lowe, J. Southern, The antimicrobial activity of phenoxyethanol in vaccines. *Lett. Appl. Microbiol.* **18**, 115–116 (1994).
 128. Z.-L. Liu, X. Chen, Water-content-dependent morphologies and mechanical properties of *Bacillus subtilis* spores' cortex peptidoglycan. *ACS Biomater. Sci. Eng.* **8**, 5094–5100 (2022).
 129. A. J. Westphal, P. B. Price, T. J. Leighton, K. E. Wheeler, Kinetics of size changes of individual *Bacillus thuringiensis* spores in response to changes in relative humidity. *Proc. Natl. Acad. Sci. U. S. A.* **100**, 3461–3466 (2003).
 130. K. Nagler, P. Setlow, Y.-Q. Li, R. Moeller, High salinity alters the germination behavior of *Bacillus subtilis* spores with nutrient and nonnutrient germinants. *Appl. Environ. Microbiol.* **80**, 1314–1321 (2014).
 131. C. Jin, A. Sengupta, Microbes in porous environments: from active interactions to emergent feedback. *Biophys. Rev.* **16**, 173–188 (2024).
 132. C. Bressuire-Isoard, V. Broussolle, F. Carlin, Sporulation environment influences spore properties in *Bacillus*: evidence and insights on underlying molecular and physiological mechanisms. *FEMS Microbiol. Rev.* **42**, 614–626 (2018).
 133. A. Sturm, J. Dworkin, Phenotypic diversity as a mechanism to exit cellular dormancy. *Curr. Biol.* **25**, 2272–2277 (2015).
 134. S. D. Bhandari, T. Gallegos-Peretz, T. Wheat, G. Jaudzems, N. Kouznetsova, K. Petrova, D. Shah, D. Hengst, E. Vacha, W. Lu, J. C. Moore, P. Metra, Z. Xie, Amino acid fingerprinting of authentic nonfat dry milk and skim milk powder and effects of spiking with selected potential adulterants. *Foods* **11**, 2868 (2022).

135. N. Gopal, C. Hill, P. R. Ross, T. P. Beresford, M. A. Fenelon, P. D. Cotter, The prevalence and control of *Bacillus* and related spore-forming bacteria in the dairy industry. *Front. Microbiol.* **6**, 1418 (2015).
136. FoodData Central. <https://fdc.nal.usda.gov/fdc-app.html#/food-details/171269/nutrients>.
137. S. Lu, X. Liao, L. Zhang, Y. Fang, M. Xiang, X. Guo, Nutrient L-Alanine-Induced Germination of *Bacillus* Improves Proliferation of Spores and Exerts Probiotic Effects in vitro and in vivo. *Front. Microbiol.* **12**, 796158 (2021).
138. A. Théâtre, C. Cano-Prieto, M. Bartolini, Y. Laurin, M. Deleu, J. Niehren, T. Fida, S. Gerbinet, M. Alanjary, M. H. Medema, A. Léonard, L. Lins, A. Arabolaza, H. Gramajo, H. Gross, P. Jacques, The Surfactin-Like Lipopeptides From *Bacillus* spp.: Natural Biodiversity and Synthetic Biology for a Broader Application Range. *Front Bioeng Biotechnol* **9**, 623701 (2021).
139. Z. Cui, L. Hu, L. Zeng, W. Meng, D. Guo, L. Sun, Isolation and characterization of *Priestia megaterium* KD7 for the biological control of pear fire blight. *Front. Microbiol.* **14**, 1099664 (2023).
140. E. Heuser, K. Becker, E. A. Idelevich, Evaluation of an automated system for the counting of microbial colonies. *Microbiol. Spectr.* **11**, e0067323 (2023).
141. A. U. M. Khan, A. Torelli, I. Wolf, N. Gretz, AutoCellSeg: robust automatic colony forming unit (CFU)/cell analysis using adaptive image segmentation and easy-to-use post-editing techniques. *Sci. Rep.* **8**, 7302 (2018).
142. A. P. Kourtis, K. Hatfield, J. Baggs, Y. Mu, I. See, E. Epton, J. Nadle, M. A. Kainer, G. Dumyati, S. Petit, S. M. Ray, Emerging Infections Program MRSA author group, D. Ham, C. Capers, H. Ewing, N. Coffin, L. C. McDonald, J. Jernigan, D. Cardo, Vital Signs: Epidemiology and Recent Trends in Methicillin-Resistant and in Methicillin-Susceptible *Staphylococcus aureus* Bloodstream Infections - United States. *MMWR Morb. Mortal. Wkly. Rep.* **68**, 214–219 (2019).
143. S. Xiao, R. M. Jones, P. Zhao, Y. Li, The dynamic fomite transmission of Methicillin-resistant *Staphylococcus aureus* in hospitals and the possible improved intervention methods. *Build. Environ.* **161**, 106246 (2019).
144. S. Caulier, C. Nannan, A. Gillis, F. Licciardi, C. Bragard, J. Mahillon, Overview of the antimicrobial compounds produced by members of the *Bacillus subtilis* group. *Front. Microbiol.* **10**, 302 (2019).
145. P. Nonejuie, R. M. Trial, G. L. Newton, A. Lamsa, V. Ranmali Perera, J. Aguilar, W.-T. Liu, P. C. Dorrestein, J. Pogliano, K. Pogliano, Application of bacterial cytological profiling to crude natural product extracts reveals the antibacterial arsenal of *Bacillus subtilis*. *J. Antibiot. (Tokyo)* **69**, 353–361 (2016).

146. D. J. Gonzalez, N. M. Haste, A. Hollands, T. C. Fleming, M. Hamby, K. Pogliano, V. Nizet, P. C. Dorrestein, Microbial competition between *Bacillus subtilis* and *Staphylococcus aureus* monitored by imaging mass spectrometry. *Microbiology* **157**, 2485–2492 (2011).
147. R. Leistner, B. Kohlmorgen, A. Brodzinski, F. Schwab, E. Lemke, G. Zakonsky, P. Gastmeier, Environmental cleaning to prevent hospital-acquired infections on non-intensive care units: a pragmatic, single-centre, cluster randomized controlled, crossover trial comparing soap-based, disinfection and probiotic cleaning. *EClinicalMedicine* **59**, 101958 (2023).
148. T. Ramos, S. Dedesko, J. A. Siegel, J. A. Gilbert, B. Stephens, Spatial and temporal variations in indoor environmental conditions, human occupancy, and operational characteristics in a new hospital building. *PLoS One* **10**, e0118207 (2015).
149. A. M. Ramos, A. L. Frantz, Probiotic-based sanitation in the built environment—an alternative to chemical disinfectants. *Applied Microbiology* **3**, 536–548 (2023).
150. S. A. Kishilova, Prospects for the use of probiotic organisms to develop alternative strategies for disinfection and prevention of infectious diseases. *FOOD METAENGINEERING* **1** (2023).
151. J. Jeżewska-Frańkowiak, K. Seroczyńska, J. Banaszczyk, G. Jędrzejczak, A. Żylicz-Stachula, P. M. Skowron, The promises and risks of probiotic *Bacillus* species. *Acta Biochim. Pol.* **65**, 509–519 (2018).
152. B. Stephens, P. Azimi, M. S. Thoemmes, M. Heidarinejad, J. G. Allen, J. A. Gilbert, Microbial Exchange via Fomites and Implications for Human Health. *Curr Pollut Rep* **5**, 198–213 (2019).
153. A. Kramer, I. Schwebke, G. Kampf, How long do nosocomial pathogens persist on inanimate surfaces? A systematic review. *BMC Infect. Dis.* **6**, 130 (2006).
154. K. R. Bright, C. P. Gerba, P. A. Rusin, Rapid reduction of *Staphylococcus aureus* populations on stainless steel surfaces by zeolite ceramic coatings containing silver and zinc ions. *J. Hosp. Infect.* **52**, 307–309 (2002).
155. J. H. Wagenvoort, W. Sluijsmans, R. J. Penders, Better environmental survival of outbreak vs. sporadic MRSA isolates. *J. Hosp. Infect.* **45**, 231–234 (2000).
156. V. O. Baede, M. Tavakol, M. C. Vos, G. M. Knight, W. J. B. van Wamel, MACOTRA study group, Dehydration tolerance in epidemic versus nonepidemic MRSA demonstrated by isothermal microcalorimetry. *Microbiol. Spectr.* **10**, e0061522 (2022).
157. N. E. Klepeis, W. C. Nelson, W. R. Ott, J. P. Robinson, A. M. Tsang, P. Switzer, J. V. Behar, S. C. Hern, W. H. Engelmann, The National Human Activity Pattern Survey (NHAPS): a resource for assessing exposure to environmental pollutants. *J. Expo. Anal. Environ. Epidemiol.* **11**, 231–252 (2001).

158. M. Schaffner, P. A. Rühls, F. Coulter, S. Kilcher, A. R. Studart, 3D printing of bacteria into functional complex materials. *Sci. Adv.* **3**, eaao6804 (2017).
159. A. M. Duraj-Thatte, A. Manjula-Basavanna, J. Rutledge, J. Xia, S. Hassan, A. Sourlis, A. G. Rubio, A. Lasha, M. Zenkl, A. Kan, D. A. Weitz, Y. S. Zhang, N. S. Joshi, Programmable microbial ink for 3D printing of living materials produced from genetically engineered protein nanofibers. *Nat. Commun.* **12**, 6600 (2021).
160. B. A. E. Lehner, D. T. Schmieden, A. S. Meyer, A straightforward approach for 3D bacterial printing. *ACS Synth. Biol.* **6**, 1124–1130 (2017).
161. D. Datta, E. L. Weiss, D. Wangpraseurt, E. Hild, S. Chen, J. W. Golden, S. S. Golden, J. K. Pokorski, Phenotypically complex living materials containing engineered cyanobacteria. *Nat. Commun.* **14**, 4742 (2023).
162. H. S. Kim, M. H. Noh, E. M. White, M. V. Kandefer, A. F. Wright, D. Datta, H. G. Lim, E. Smiggs, J. J. Locklin, M. A. Rahman, A. M. Feist, J. K. Pokorski, Biocomposite thermoplastic polyurethanes containing evolved bacterial spores as living fillers to facilitate polymer disintegration. *Nat. Commun.* **15**, 3338 (2024).
163. S.-Y. Kwak, J. P. Giraldo, T. T. S. Lew, M. H. Wong, P. Liu, Y. J. Yang, V. B. Koman, M. K. McGee, B. D. Olsen, M. S. Strano, Polymethacrylamide and carbon composites that grow, strengthen, and self-repair using ambient carbon dioxide fixation. *Adv. Mater.* **30**, e1804037 (2018).
164. W.-I. Cho, M.-S. Chung, Bacillus spores: a review of their properties and inactivation processing technologies. *Food Sci. Biotechnol.* **29**, 1447–1461 (2020).
165. A. Spök, G. Arvanitakis, G. McClung, Status of microbial based cleaning products in statutory regulations and ecolabelling in Europe, the USA, and Canada. *Food Chem. Toxicol.* **116**, 10–19 (2018).
166. V. Kunamineni, M. Meena, D. Shirish V., Bacteria based self healing concrete – A review. *Constr. Build. Mater.* **152**, 1008–1014 (2017).
167. W. L. Nicholson, P. Setlow, C. R. Harwood, S. M. Cutting, Molecular biological methods for Bacillus. (1990).
168. Z. R. Harrold, M. R. Hertel, D. Gorman-Lewis, Optimizing Bacillus subtilis spore isolation and quantifying spore harvest purity. *J. Microbiol. Methods* **87**, 325–329 (2011).
169. P. Setlow, Observations on research with spores of Bacillales and Clostridiales species. *J. Appl. Microbiol.* **126**, 348–358 (2019).
170. A. Landajuela, M. Braun, C. D. A. Rodrigues, E. Karatekin, Detection of membrane fission in single Bacillus subtilis cells during endospore formation with high temporal resolution. *STAR Protoc.* **5**, 102965 (2024).

171. M. R. Binelli, A. Kan, L. E. A. Rozas, G. Pisaturo, N. Prakash, A. R. Studart, Complex living materials made by light-based printing of genetically programmed bacteria. *Adv. Mater.* **35**, e2207483 (2023).
172. S. You, Y. Xiang, H. H. Hwang, D. B. Berry, W. Kiratitanaporn, J. Guan, E. Yao, M. Tang, Z. Zhong, X. Ma, D. Wangpraseurt, Y. Sun, T.-Y. Lu, S. Chen, High cell density and high-resolution 3D bioprinting for fabricating vascularized tissues. *Sci. Adv.* **9**, eade7923 (2023).